NASA Contractor Report 3781

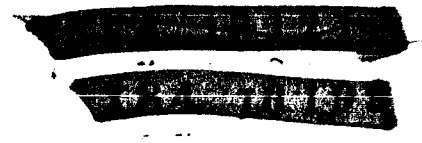

Development of Selected Advanced Aerodynamics and Active Control Concepts for Commercial Transport Aircraft

A. B. Taylor

CONTRACT NAS1-15327
FEBRUARY 1984

NASA

NASA Contractor Report 3781

Development of Selected Advanced Aerodynamics and Active Control Concepts for Commercial Transport Aircraft

A. B. Taylor
McDonnell Douglas Corporation
Long Beach, California

Prepared for
Langley Research Center
under Contract NAS1-15327

National Aeronautics
and Space Administration

**Scientific and Technical
Information Office**

1984

FOREWORD

This document is the summary report of the work carried out by Douglas Aircraft Company under Contract NAS1-15327, which was part of the NASA Energy Efficient Transport (EET) project. The EET is one of several projects contained in the Aircraft Energy Efficiency (ACEE) activity. Douglas-sponsored work was done in association with EET, and appropriate summaries of the results are included in the report.

The NASA EET Project Manager was Mr. R. V. Hood of Langley Research Center. The Technical Monitor was Mr. T. G. Gainer; Mr. D. W. Bartlett was coordinator of aerodynamics research. The on-site NASA representative was Mr. J. R. Tulinius. Many of the wind tunnel programs were conducted at Ames Research Center and some at Langley Research Center, and acknowledgment is given to the Directors and staffs for their assistance. Acknowledgment is also given to the Director and staff of Dryden Flight Test Center for their assistance during the flight evaluation activity.

The key Douglas program personnel were:

M. Klotzsche	ACEE Project Manager
A. B. Taylor	EET Project Manager
J. E. Donelson	Long Duct Nacelle Aerodynamic Development Task
W. A. Shirley	Active Control Transport Development Task
D. K. Steckel, J. A. Dahlin, P. A. Henne	High-Aspect-Ratio Supercritical Wing – Cruise Speed Task
W. R. Oliver, J. B. Allen	High-Aspect-Ratio Supercritical Wing – High Lift Task
Dr. C. A. Shollenberger	Winglet Model Testing – Preflight Evaluation Task
P. T. Sumida	Winglet Flight Evaluation Task
J. T. Callaghan	Winglet Model Testing – Postflight Evaluation Task
D. S. Retrum, N. S. Vrabel	Program Financial and Schedule Control Task

Throughout the program, notable contributions were received from the following Douglas personnel:

J. G. Callaghan	Aerodynamics
J. T. Callaghan	Aerodynamics
J. D. Cadwell, J. C. Strong	Aerodynamics (Wind Tunnel Testing)

CONTENTS

CONTENTS (Continued) Page

ILLUSTRATIONS

ILLUSTRATIONS (Continued)

INTRODUCTION

In 1977, Douglas was awarded the first of three contracts in the NASA Energy Efficient Transport (EET) project. This project was one of several in the Aircraft Energy Efficiency (ACEE) activity initiated by NASA in 1976. The ACEE work was conducted to develop near-term technology, accelerate advanced technology to a state of readiness, and explore and research high-risk areas for potential application to transport aircraft. The specific purpose of the EET project was to expedite research in aerodynamics and active controls as applied to commercial aircraft.

The three contracts awarded to Douglas were:

- Selected Winglet and Mixed-Flow Long-Duct Nacelle Development for DC-10 Derivative Aircraft (Reference 1).
- Selected Advanced Aerodynamic and Active Control Concepts Development (Reference 2).
- Development of Selected Advanced Aerodynamics and Active Controls Concepts for Commercial Transport Aircraft (the subject of this summary report).

Each contract was supplemented by Douglas-funded work and drew upon Douglas transport configuration and engineering studies so that a realistic background was available. The first contract addressed concepts which might be applicable in the near term to derivatives of the DC-10 transport, or by analogy to similar aircraft. The second contract was aimed principally at far-term applications. The investigations in aerodynamics concentrated on the design and experimental evaluation of high-aspect-ratio supercritical wings aimed at high performance levels. In active controls, the primary effort was design and experimental investigations of the aircraft systems required to augment the stability of an aircraft designed with relaxed static stability, and of the criteria to define configuration limits. The present contract was structured to advance the more promising concepts of the first two investigations to as near readiness for commercial application as possible.

As a result of the groundwork laid in the studies of References 1 and 2, the following categories of work were prepared for the present contract:

- Long-duct nacelle aerodynamic development for DC-10 derivatives.
- Long-duct nacelle development for DC-10 derivatives (including the possibility of flight evaluation).
- Active control transport development.
- High-aspect-ratio supercritical wing aerodynamic development.
- Winglet development for DC-10 derivatives.

At a later stage, the long-duct nacelle work was limited to aerodynamic wind tunnel development. The winglet development task was consequently expanded to include flight development, which itself was followed by further model test investigations.

In this report, the categories of work are discussed in their actual sequence. References to the more detailed reports are contained in each section.

SYMBOLS

A7	Control law identifier
A8	Control law identifier
ACEE	Aircraft Energy Efficiency program
ATMR	Advanced Technology Medium Range Transport Technology
BWL	basic winglet
C_D	drag coefficient
C_L	lift coefficient
$C_{L_{MAX}}$	maximum lift coefficient
DLE	drooped leading edge
EET	Energy Efficient Transport project, a number of tasks sponsored by NASA under the ACEE program to expedite development in aerodynamics and active controls
EXT	extended
FCK	fixed camber Krueger flap
g	acceleration due to gravity
GLA	gust load alleviation
H_1, H_2	horizontal tail configurations
HASCW	high-aspect-ratio supercritical wing
L/D	lift-to-drag ratio
LDN	long-duct nacelle
LE	leading edge
M	Mach number
MLC	maneuver load control
NAE	National Aeronautical Establishment, Ottawa
P_1 through P_5	nacelle-pylon configurations
RSWL	reduced-span winglet
s	mathematical operator used in Laplacian transforms (used in synthesis of control laws)
SYM	symbol

V_2	takeoff safety speed
V_{MIN}	Federal Aviation Administration certified stall speed
VCK	variable-camber Krueger flap
VORT	vortilet
W_1	HASCW high-speed wind tunnel model
WL	winglet
w/o	without

LONG-DUCT NACELLE AERODYNAMIC DEVELOPMENT

The long-duct nacelle (LDN) concept, applied to a turbofan engine installation, encloses the fan flow in a duct so that it is internally mixed with the core flow exhausting through a common nozzle. In this way, an increase in propulsive efficiency is sought that is substantially greater than any aircraft performance losses due to the weight increase in the duct and to any drag increase. In such an installation, the risk of interference drag must be addressed because of the presence of the large-diameter duct close to the wing.

The earlier EET work, summarized in Reference 1, showed that the LDN had a very low interference drag, which could be reduced to an insignificant level by adding a small fairing to the current DC-10 pylon shape. The test data also showed that the pressure distributions in the wing-pylon-nacelle channel obtained with a flow-through and a powered nacelle were the same; hence, power effects could be considered negligible.

After this wind tunnel program was completed, concurrent Douglas work on mixer models showed that the internal flow required a lower Mach number at the mixing plane and an increased mixing length. The most expeditious way of satisfying this requirement was to extend the nacelle afterbody rearwards. In this way, a larger diameter at the internal mixing plane and a longer nozzle could be obtained.

The revised LDN shape was 54 cm (21.5 in.) full-scale, or 8 percent longer than the baseline reported in Reference 1. Figure 1 shows the model dimensions. A flow-through wind tunnel model was used, since the baseline tests had shown that pressure distributions in the critical inboard channel between nacelle, pylon, and wing could be properly represented. The production (symmetrical section) DC-10 pylon shape was used.

The test was conducted in the Calspan 8-foot transonic wind tunnel. The model used was a 4.7-percent scale semispan configuration representative of a DC-10 derivative powered by GE CF6-50 engines. The model was mounted off the floor with a splitter plate to remove the boundary layer (Figure 2).

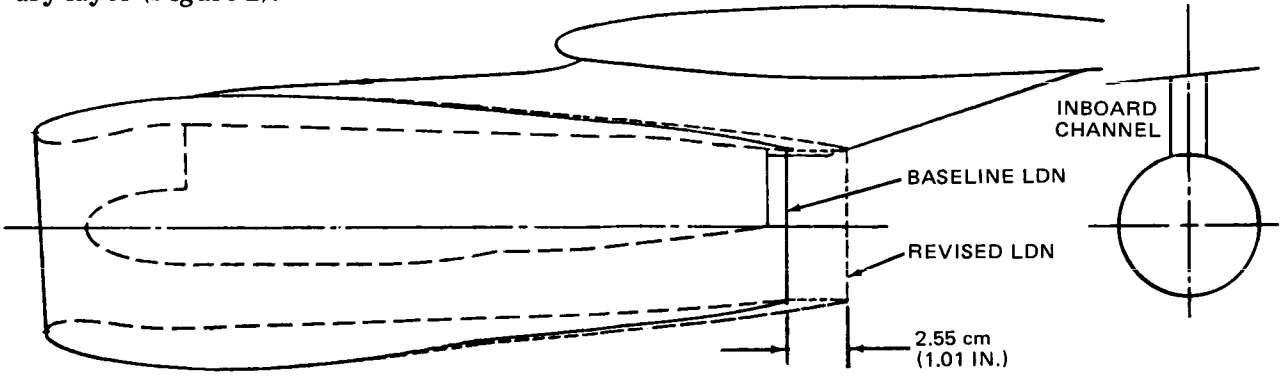

FIGURE 1. COMPARISON OF BASELINE AND REVISED LDN MODEL

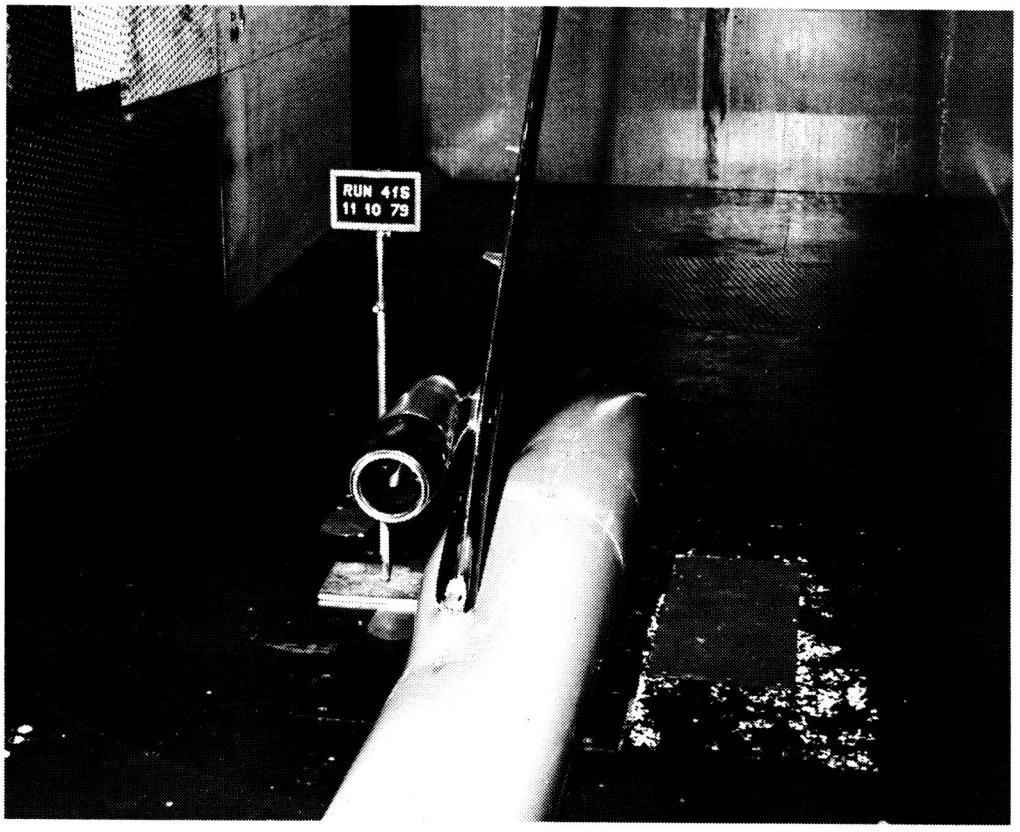

FIGURE 2. LDN MODEL

The primary objectives of the program were to:

- Evaluate the effect of the revised shape on the wing-pylon-nacelle channel velocities, and hence to estimate the potential for increased drag relative to the baseline.
- Compare the channel flow characteristics of the baseline with those obtained in the tests presented in Reference 1.

The program is fully reported in Reference 3.

Results

Data were obtained at Mach numbers up to the DC-10-30 typical cruise condition of 0.82 and 0.5 lift coefficient. The channel pressures measured for the baseline LDN were in good agreement with the results in Reference 1. At 0.6 Mach number, the channel flow of both configurations was subcritical, with the suction peak slightly higher across the channel for the revised LDN.

The channel flow became critical (local Mach number of 1) at a free-stream Mach number that was 0.04 to 0.05 lower for the revised LDN than for the baseline. Figure 3 compares the channel

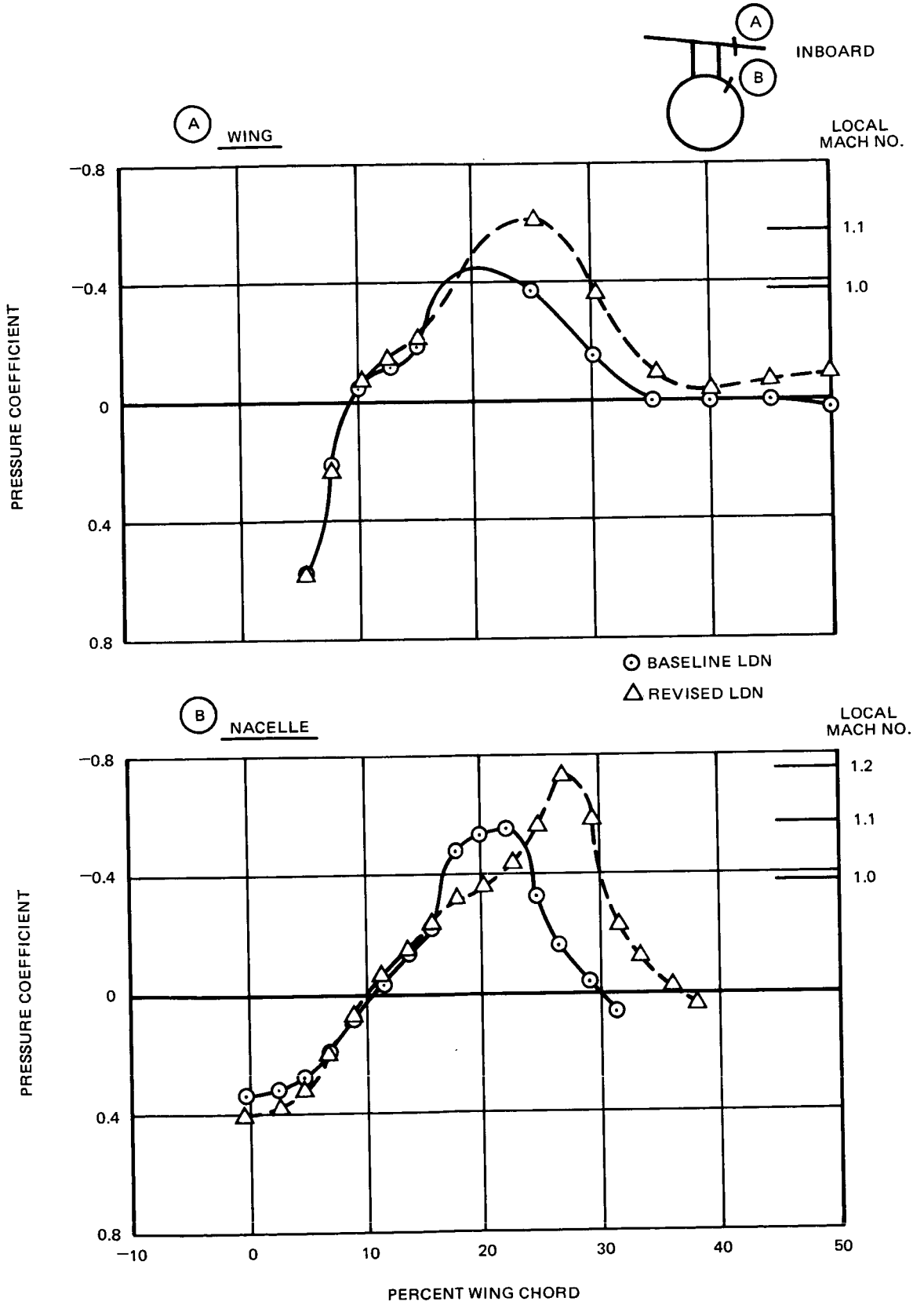

FIGURE 3. EFFECT OF LDN INSTALLATION ON INBOARD CHANNEL PRESSURES

pressure distributions for both LDN configurations at 0.82 Mach number and 0.5 lift coefficient. The peak local Mach number is 1.2 for the revised LDN, compared with 1.1 for the baseline, and the peak occurs further aft. The peak channel Mach number is below the 1.3 to 1.4 levels which have been previously demonstrated to cause shock-induced nacelle flow separation with its attendant drag penalty.

Boundary layer analyses using the measured pressure distributions showed that the flow on the revised LDN afterbody was attached. Lift curve slopes for both LDN configurations were found to be the same. The incremental drag for the revised LDN was two to four counts higher than for the baseline LDN (three counts is approximately equal to 1 percent of the airplane drag). The estimated drag increment was somewhat lower. No evidence is available to explain the difference between measured and estimated drag. However, based on past experience by Douglas with this facility, it is probable that this installation cannot accurately determine such small drag increments. The higher channel velocities are of sufficient magnitude to be a concern, and suggest that treatment is required to lower the peak suction pressures. This treatment could consist of a revision to the shape of the nacelle afterbody or to the pylon, as shown in Figure 4.

For an LDN having the derivative CF6-80 engine, which is also suitable for the DC-10 aircraft, the geometry provisions for an improved internal mixer can be accommodated in the baseline LDN shape. The results reported in Reference 1 are therefore applicable in this case.

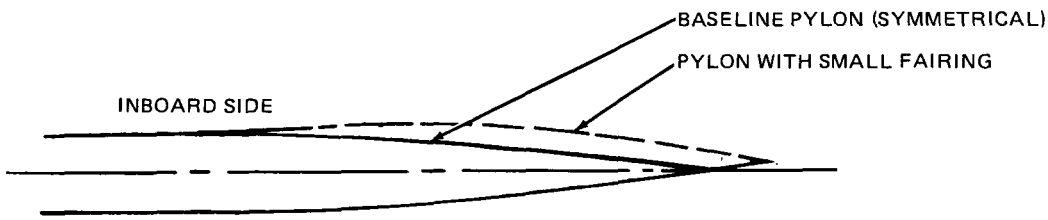

FIGURE 4. PYLON SECTIONS SHOWING BASELINE AND FAIRED SHAPES

Conclusions from the Long-Duct Nacelle Task

The primary conclusions of the program are:

1. The revised LDN had an appreciable effect on the channel pressure distributions, resulting in an increased peak channel Mach number of approximately 0.10 at typical cruise conditions. However, the pressure recovery on the nacelle afterbody was about the same as for the baseline.
2. The incremental drag for the revised LDN was measured as two to four counts (three counts is approximately equal to 1 percent of the airplane drag), compared with the estimated increment of one count. However, this result may not be representative of the true incremental drag since previous tests in this facility have not been very successful in determining small drag increments due to configuration changes.
3. The measured drag increment and the increased channel velocities for the revised LDN are of sufficient concern to warrant consideration of pylon or nacelle changes designed to reduce the impact of the revised nacelle shape on the channel velocities and its potential attendant drag increase. If needed, the pylon might be modified as shown in the successful EET tests of Reference 1.

EXPERIMENTAL INVESTIGATION OF ELASTIC MODE CONTROL ON A MODEL OF A TRANSPORT AIRCRAFT

The use of active controls to improve aircraft efficiency has been receiving increased attention in recent years. There is now confidence that reduced drag and lower structural weight can be realized by using control surfaces for static stabilization and elastic mode suppression. Once the aircraft control surfaces are designed for multiple use and high response, as they must be for stability augmentation and wing load alleviation, it becomes possible to extend the concept to flutter margin augmentation, which offers additional weight savings for many aircraft. Such augmentation could offer additional opportunities with other advanced developments such as winglets and high-aspect-ratio supercritical wings. These developments may introduce additional flutter considerations and require the designer to add either heavy structural reinforcement or an augmentation system to stabilize the flutter modes.

The study was designed to investigate the use of active controls to suppress flutter and alleviate gust loads on a derivative of the DC-10 transport. The primary objectives of the investigation were to:

- Confirm the effectiveness of active controls to suppress critical flutter modes at speeds above the passive flutter speed.
- Assess the accuracy of analysis methods applied to active control functions of flutter suppression and gust load alleviation.

The program involved the testing of both a semispan and a full-span flutter model. Several control laws based on classical methods were investigated. Laws developed by the NASA Langley Research Center, based on aerodynamic energy and optimal control methods, were also investigated, and references to this work are included in this report. The EET program is reported in Reference 4.

Program Approach

The experimental investigation of an elastic mode control (EMC) system used an aeroelastic flutter model of the DC-10 derivative aircraft. This derivative had a 4.3 m (14 foot) longer wing span and an 8.1 m (26.7 foot) larger fuselage than the existing DC-10-30 transport aircraft. In addition, the outboard aileron was extended in span and operated throughout the entire flight regime. Previously, this derivative aircraft had been designed with active control surfaces for maneuver load control (MLC) and gust load alleviation (GLA). The objective in applying EMC was to employ simple control laws, generally similar in nature to those shown effective in previous applications and studies of MLC and GLA for transport aircraft.

The components of the active system for the test program were developed and tested prior to installation. The aeroelastic wind tunnel model was vibration-tested in a manner similar to full-scale aircraft ground vibration testing. The model, a 4.5-percent representation of the derivative aircraft, was tested first in a semispan configuration (Figure 5) in the Douglas-Long Beach low-speed wind tunnel, and then in the complete model configuration (Figure 6) in the Northrop 7- by 10-foot low-speed wind tunnel. These tests measured flutter and gust characteristics with the active control system on and off. The tests results were then compared to predictions for evaluation.

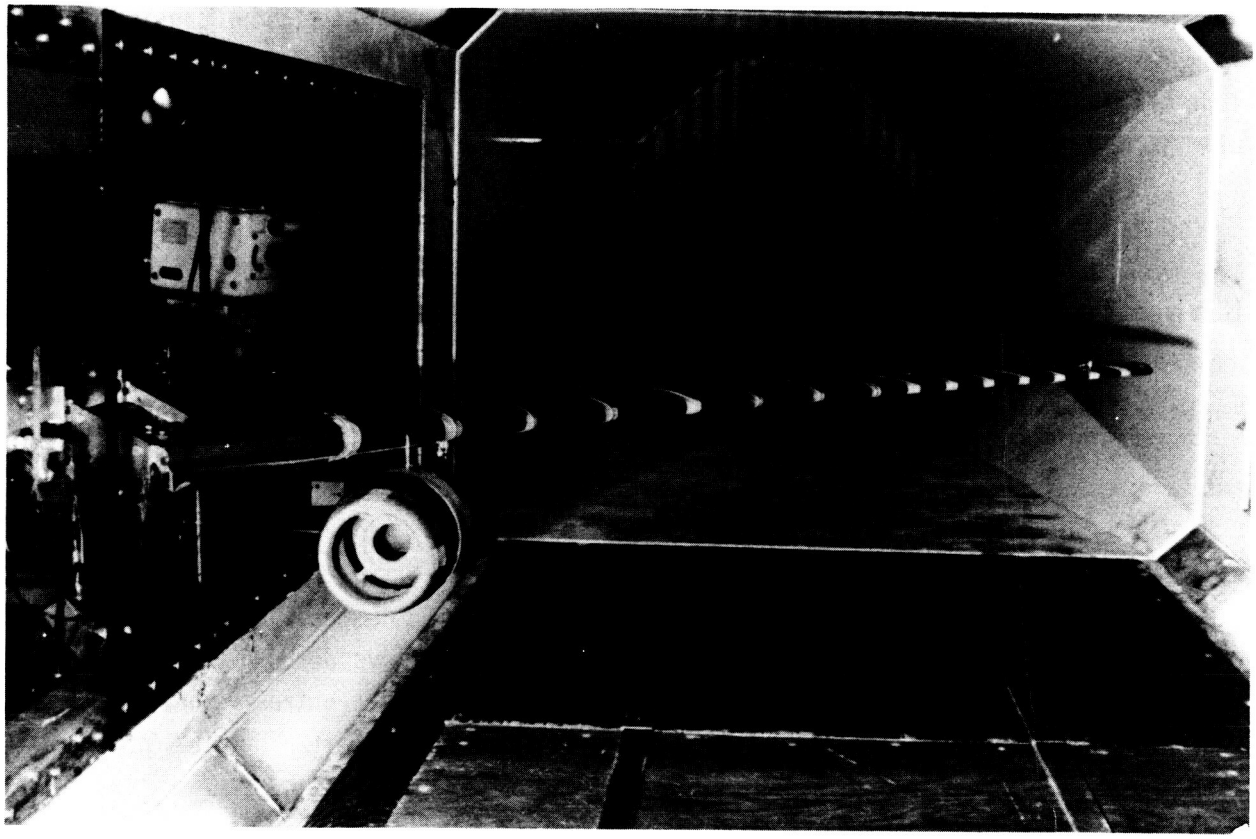

FIGURE 5. SEMISPAN ACTIVE CONTROL MODEL

Control laws were developed for several critical flight conditions and configurations. The wing sensor used was a single vertical accelerometer near each wing tip. Modeling for the semispan control law used primarily representations of the aileron actuator, the dynamics of the aircraft wing, and a flutter-gust filter. For the full-span models, additional filtering and adjustment capability was added. The control laws were designed to suppress the critical 12-Hz primary flutter mode. For the full-span flutter model, it was predicted that a secondary 22-Hz mode would also be present near the critical speed. One full-span control law (A7) was adjusted with reduced gain to avoid stimulating the higher frequency mode. The other (A8) was designed with a notch filter to suppress this mode. The semispan control law is shown in the upper part of Figure 7. The full-span laws are shown in the lower part of the figure. Since the aileron control

L011770

FIGURE 6. FULL-SPAN ACTIVE MODEL CONTROL

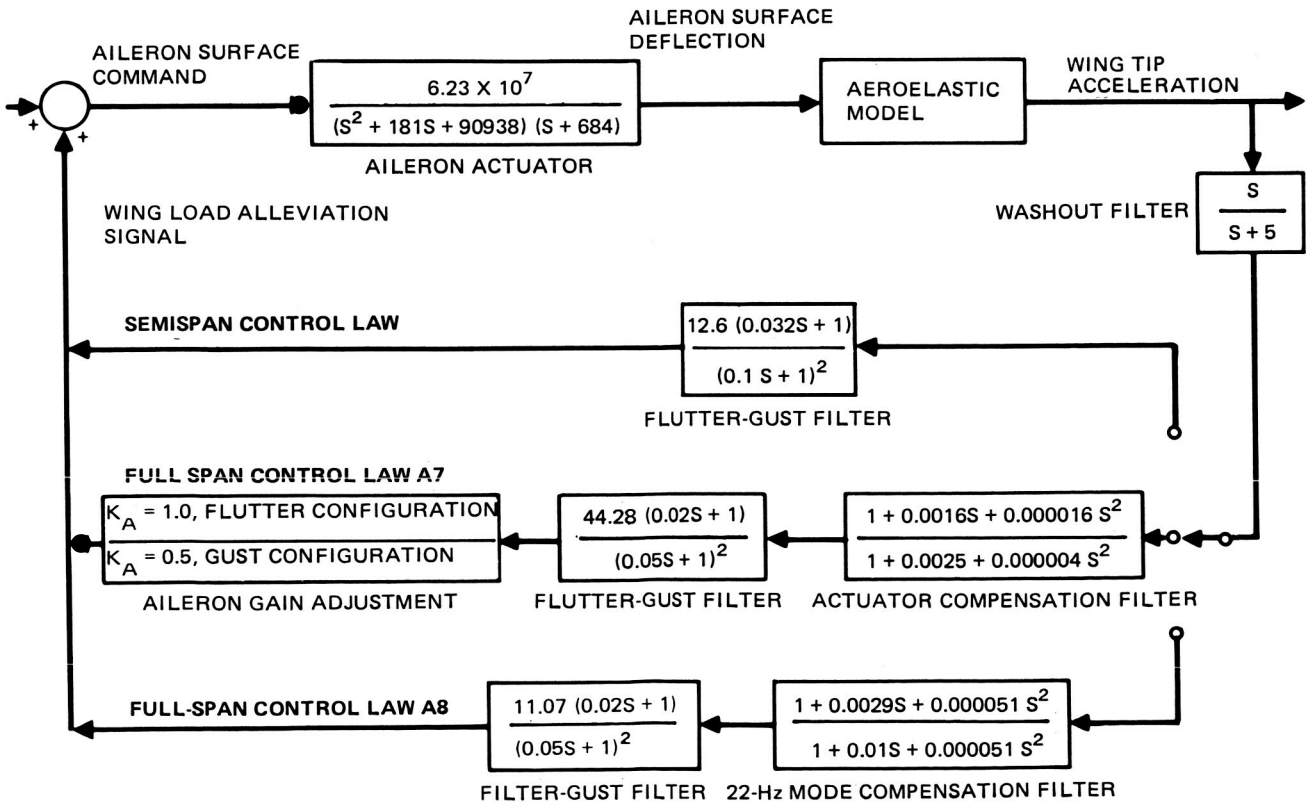

FIGURE 7. BLOCK DIAGRAM OF AILERON CONTROL LAWS

law, in providing gust load alleviation, can destabilize the short-period mode and introduce a poorly damped filter mode, an elevator control law, not shown in the figure, was designed to add damping to the low frequency modes. An additional accelerometer, mounted at the model center of gravity, provided the sensor for the elevator control law.

The control laws developed by NASA personnel for the semispan model are described in References 5, 6, and 7. The last two references also discuss the test results using these laws.

A gust environment was generated in the wind tunnel by installing a banner across the stilling chamber upstream of the test chamber. The spectrum of this turbulence was measured with hot-wire instrumentation, and was input to the gust analysis.

Results

The semispan flutter results are compared with predictions in Figure 8, and the agreement is shown to be good. This figure shows the flutter damping characteristics with zero fuel, which is near the most critical condition. The variation of flutter speed with fuel condition is shown in Figure 9. At the flutter-critical condition having 10 percent fuel, the increase in flutter speed due to the active control system is 13 percent.

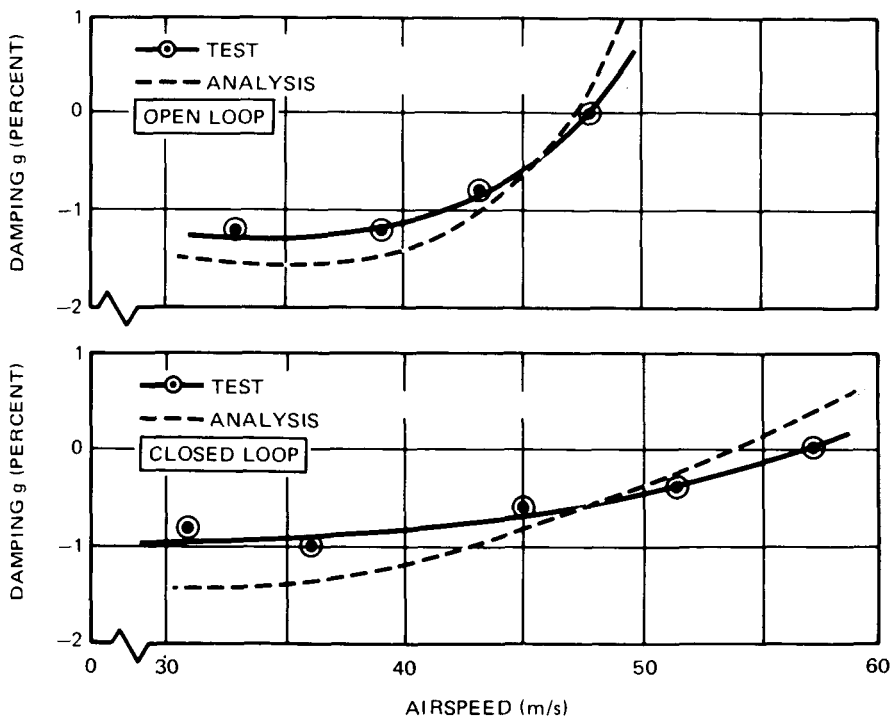

FIGURE 8. OPEN AND CLOSED-LOOP SEMISPAN FLUTTER CHARACTERISTICS FOR THE ZERO FUEL CONFIGURATION

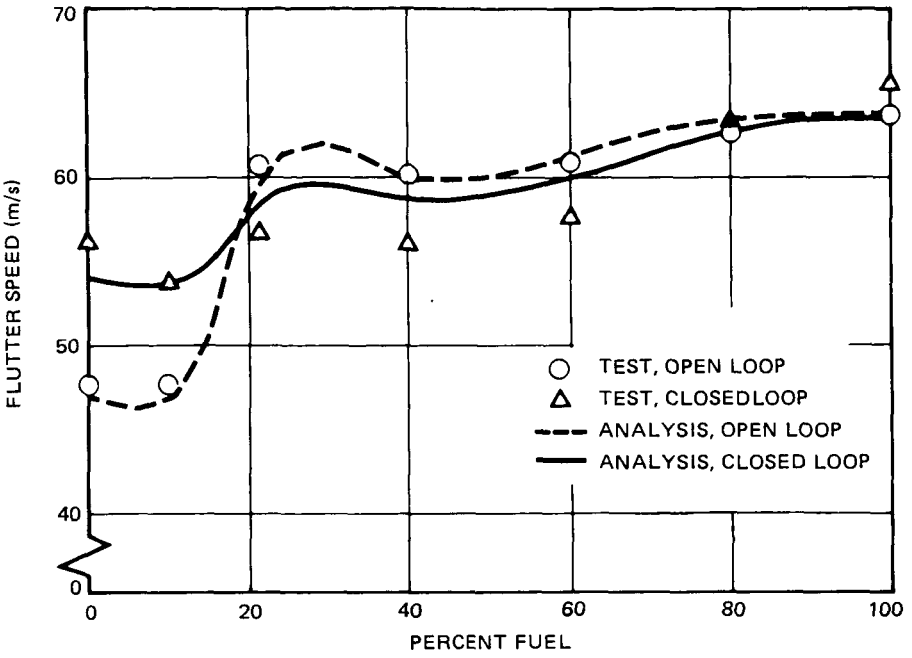

FIGURE 9. SEMISPAN MODEL FLUTTER SPEED VERSUS PERCENT FUEL

Measurements to provide data for estimating the response of the wing to a turbulent gust field were made in the presence of the banner gust generator. The power spectral density test results are compared in Figure 10 with analyses based upon a two-dimensional representation of the turbulence. The figure, presenting open-loop and closed-loop cases, shows reasonable agreement between test and analytical results. The active control system, or closed loop, was effective in reducing the load due to the first wing bending mode (the mode generating the highest loads). The midspan root-mean-square bending moment was reduced by 22 to 40 percent, depending upon speed.

Most flutter testing of the full-span model was conducted using a reduced gain adjustment of the A7 control law. The gain reduction of one-half was made to avoid a predicted instability at 40 Hz without complications which might result from the use of a notch filter. Damping versus speed is shown in Figure 11 and compared with analysis and open-loop test results. The critical 12-Hz mode was entirely suppressed as predicted, and agreement with prediction was good. There was no evidence of the next critical flutter mode (22.2 Hz) until flutter onset was imminent. An increase in overall flutter margin of 17 percent was obtained.

Analysis had predicted that the flutter speed of the higher frequency mode would decrease with increasing gain. Results of testing with variable gain did not confirm this. Use of the alternative control law, employing a notch filter to suppress the higher frequency mode, was not as effective as predicted by analysis.

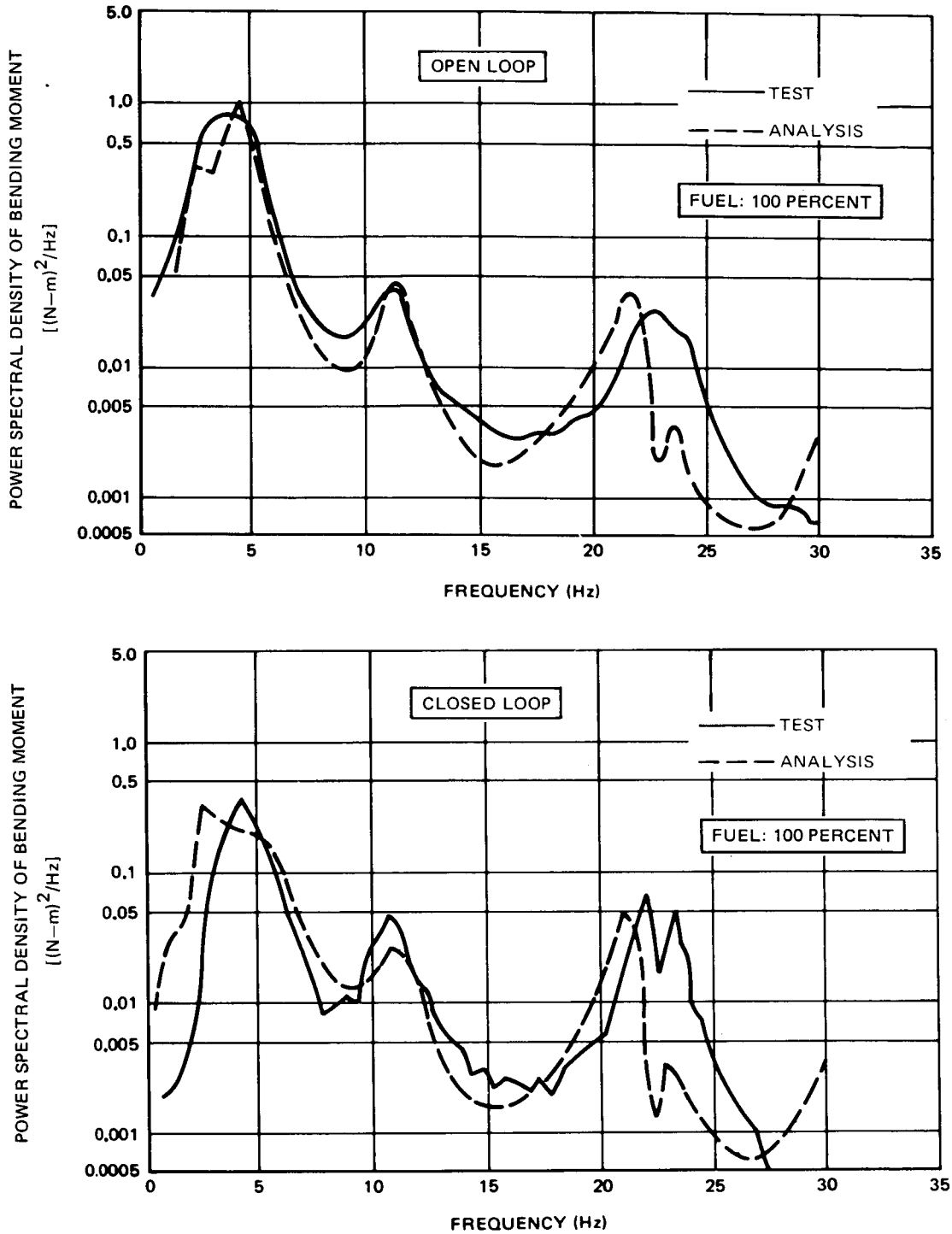

FIGURE 10. SEMISPAN POWER SPECTRAL DENSITY OF MIDSPAN BENDING MOMENT

The full-span model turbulence testing showed that the active system was capable of reducing the bending moment in the elastic mode frequency range (frequencies greater than 3.5 Hz). Figure 12 shows the midspan bending moment power spectral density due to turbulence. These data for the quoted frequencies correlated well with analytical predictions. A significant reduction in bending moment was exhibited at low fuel states. The measured data also appear to show

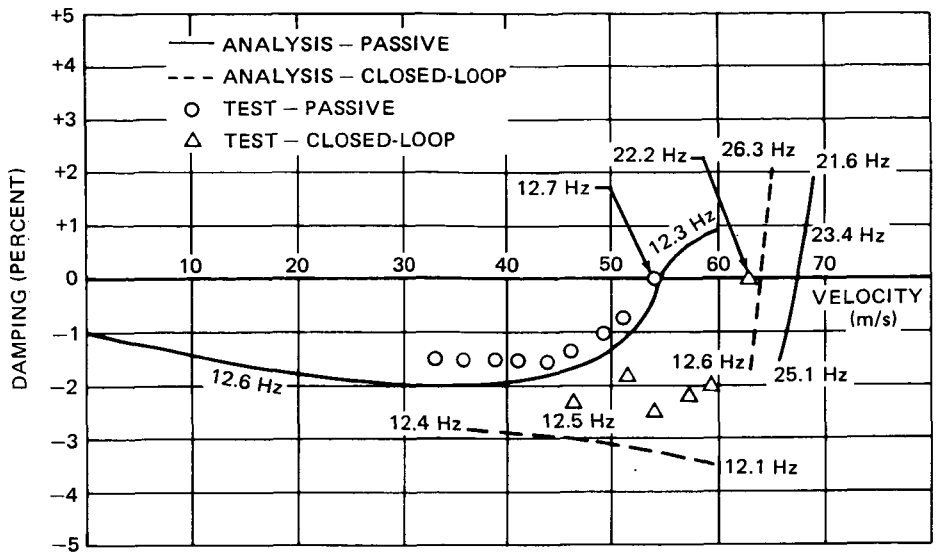

FIGURE 11. FLUTTER DAMPING VERSUS VELOCITY FOR THE FULL-SPAN MODEL

that the active system increases the model loads for the rigid-body short-period mode. This increase in load is considered to be due to the use of improper model constraints in the analysis; on-line video observations showed the model resting against its installation stops in the presence of turbulence, a condition likely to affect the short-period rigid-body mode. Further, it was evident that the turbulence field was nonhomogeneous, which was not accounted for in the analysis.

Conclusions from the Elastic Mode Control Investigation

The following primary conclusions were obtained:

1. A simple control system and control law were shown to increase the flutter speed of the first critical flutter mode. On the full-span model, a second flutter mode became unstable at speeds above the passive flutter speed, and attempts to control this mode were unsuccessful.
2. The active system was generally effective in achieving significant reductions in gust loads caused by turbulence induced in the tunnel. For the full-span model, however, problems with predicting the effects of the model support system and difficulties in predicting the turbulence field limited the value of the test results, particularly for the rigid-body modes. However, a substantial reduction in mid-span flexible wing bending moment was indicated by use of the active system.
3. For the flutter tests, agreement between prediction and test results was generally good. For the gust load alleviation tests, the relative change in model response agreed with analysis for the semispan model, but not for the full-span model.

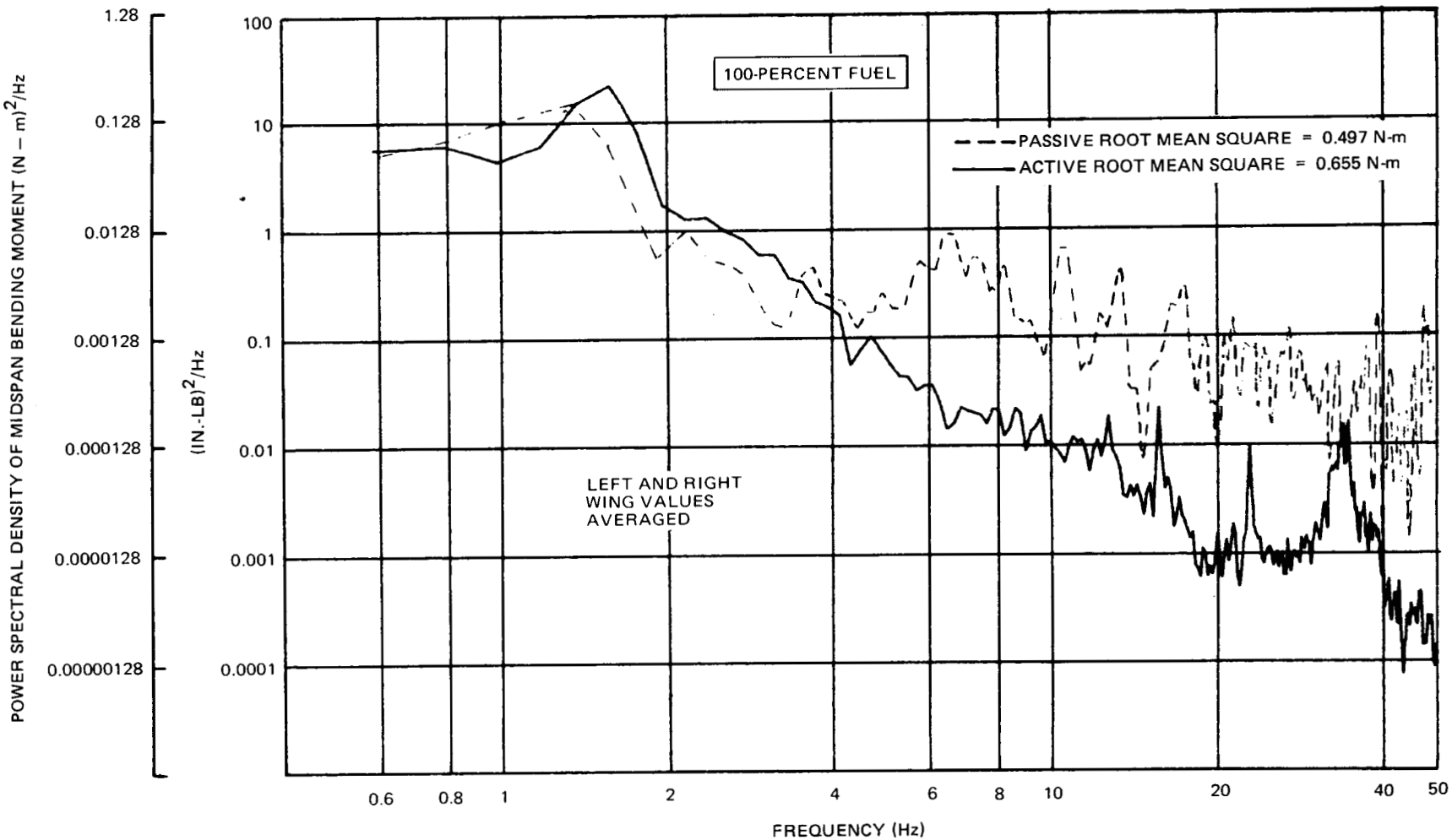

FIGURE 12. FULL-SPAN POWER SPECTRAL DENSITY OF MIDSPAN BENDING MOMENT

HIGH-ASPECT-RATIO SUPERCRITICAL WING TECHNOLOGY

Research on supercritical wings has shown the performance potential from the use of this technology. However, the potential can be realized only if the airplane meets current operational, social, and economic needs. In an era of rising inflation, concern over the price and availability of fuel, and increasingly stringent noise regulations, Douglas concluded that advanced technology would have to be used in a new transport aircraft for it to compete in the marketplace. A new design would also have to be more fuel-efficient to improve the level of comfort or significantly increase speed. In addition, greater low-speed aerodynamic efficiency must supplement advanced engine technology to meet new noise requirements.

Preliminary systems studies showed that the supercritical technology advantage could best be applied by increasing wing thickness and aspect ratio. In order to develop the technology further, a detailed study of the thick, high-aspect-ratio supercritical wing was included in the EET project. Little data had previously been gathered on such wings aimed at advanced performance, integrated with transport configurations, particularly in the high-lift regime.

Initial work under the EET project developed the geometry and performance data base for an efficient high-aspect-ratio supercritical wing (HASCW). This development was conducted using Douglas studies for a 200-plus-passenger medium-range transport with a wide body, called the DC-X-200. The cruise speed development is reported in Reference 8 and the high lift in Reference 9. Summaries of this work are contained in Reference 2.

In the work conducted under this contract, the characteristics established in the initial phase were utilized to develop a more optimum wing configuration. The development was extended to the more timely application of a smaller aircraft design. This design, entitled the Advanced Technology Medium Range (ATMR) transport, was sized for 170 to 180 passengers, and employed a narrow-body configuration (Figure 13). The cruise speed work, in addition to basic wing-body development, addressed the effects of nacelle-pylon location, horizontal tail configuration, and boundary layer transition on lift curve slope. The high-lift development was aimed at obtaining improvement in performance from the level of Reference 9. Also, further investigation was needed to alleviate the pitch-up encountered during the earlier work.

After this work was successfully completed, as reported in References 10 and 11, application studies revealed that mechanical and structural problems may arise with the relatively thin flap regions characteristic of supercritical airfoils. In addition, it was suspected that the benefits of supercritical airfoils could be eroded by the effects of large, adverse pressure gradients near the trailing edge. Based on some encouraging work performed by Douglas, under Company sponsorship, the EET work was continued, studying airfoils with improved geometry in the flap region and improvements in sectional drag characteristics.

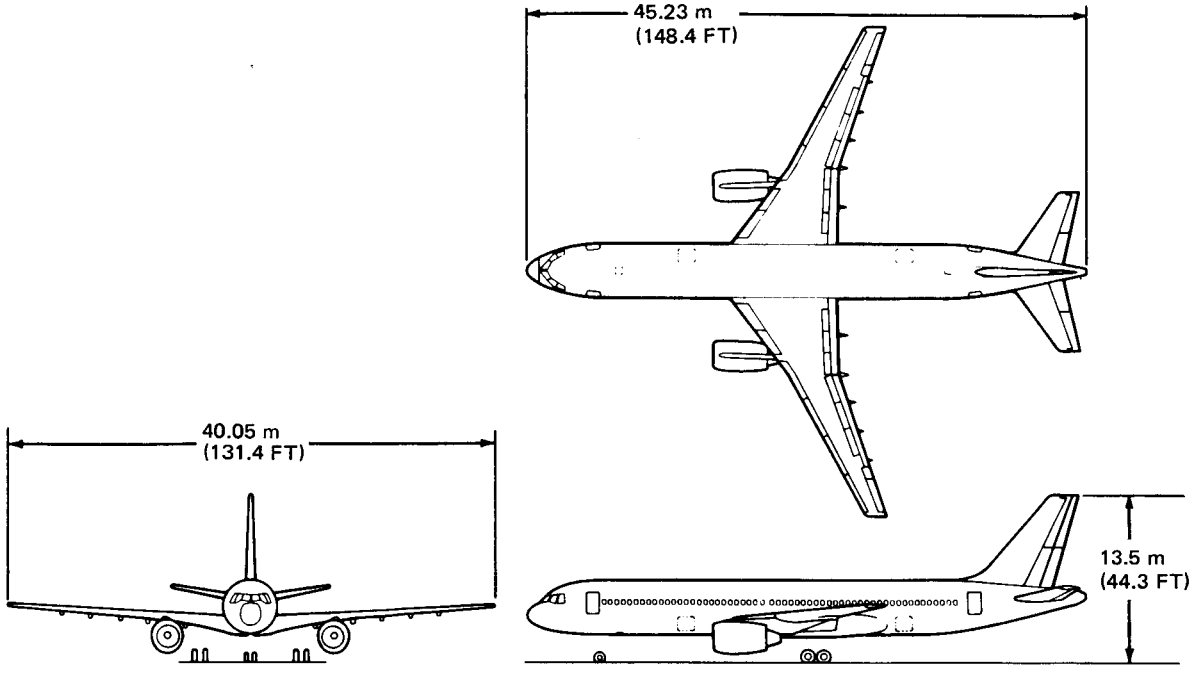

FIGURE 13. ATMR – GENERAL ARRANGEMENT

HIGH-ASPECT-RATIO SUPERCRITICAL WING AERODYNAMIC DEVELOPMENT – CRUISE SPEED

Three-Dimensional Wing Configuration

The initial EET phase (Reference 8) utilized a number of wing designs of alternative planform, twist, leading edge radius, and camber. The drag results showed that the wings exceeded the performance target for drag rise, but generally suffered from excessive drag creep. Some improvement in buffet boundary was also desired.

The ATMR nominal design Mach number was 0.8 and the design C_L was 0.55. The previous DC-X-200 wing configurations had a drag divergence Mach number capability in excess of 0.8. For the ATMR, this capability, in conjunction with the significant favorable effect of a narrower fuselage, enabled the wing sweep to be reduced (Figure 14). In terms of high-speed drag, buffet, and pitching moment characteristics, the W_8 wing from Reference 7 had the best overall aerodynamic characteristics, and so airfoil sections from this wing were used as a starting point. The final wing configuration was designated W_1, and was estimated to have better performance in the high-speed cruise and buffet regimes as well as the low-speed, high-lift regime.

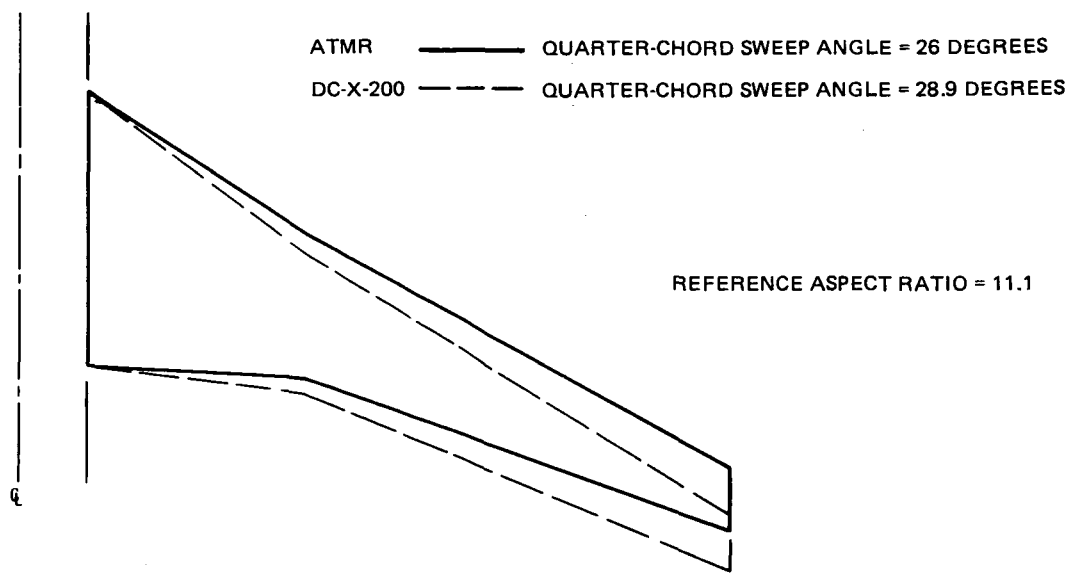

FIGURE 14. ATMR WING PLANFORM

Three-Dimensional Test Results

Two tests were conducted in the NASA Ames Research Center 11-foot transonic wind tunnel. A sting-mounted, 5.59-percent scale model of the ATMR aircraft was used (Figure 15).

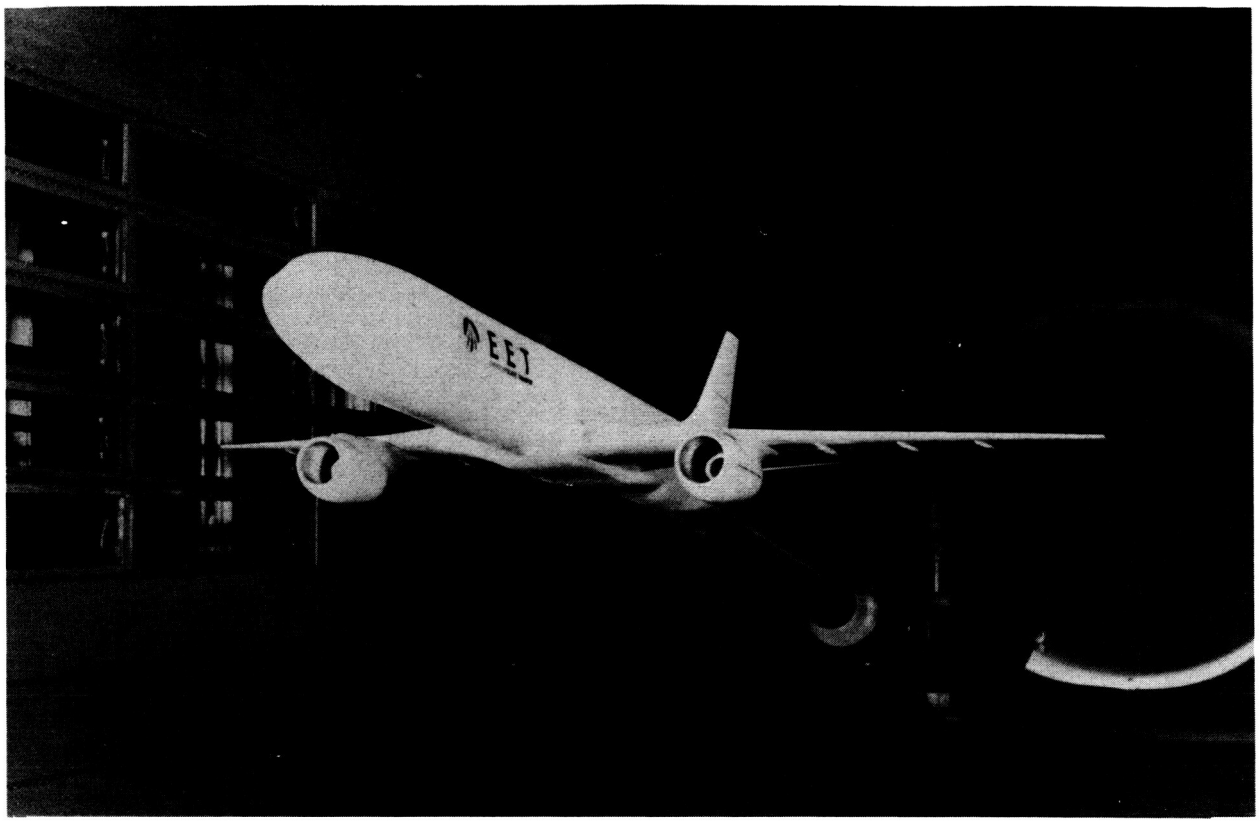

FIGURE 15. HIGH-SPEED HASCW MODEL

Wing-Body Drag Characteristics – The basic wing body drag divergence characteristics are compared with the earlier EET data in Figure 16, matched at lower Mach number to compare drag rise and creep. These results were as good as or slightly better than predicted. A substantial reduction in premature drag creep is shown. This improvement is due in part to a reduction in the upper surface velocities, and correspondingly the shock strengths, as shown in the pressure distributions in Figure 17.

Nacelle-Pylon Drag Characteristics – Five positions of a common nacelle, using symmetrical pylons, were tested. The configurations were selected to assess the effect of longitudinal, vertical, and spanwise nacelle position on drag. The configurations are shown in Figure 18, P_1 through P_4 being located at 39-percent semispan and P_5 at 33-percent semispan. Pylons P_1 through P_4 were aligned with flap linkage positions and so terminated in a fairing. Due to its repositioning, pylon P_5 was shaped without a flap linkage fairing. Figure 19 presents the drag increment. Near the design lift coefficient, the P_1 drag increment is very close to the calculated parasite drag level for the isolated nacelle and pylon, but at low lift coefficients there is a substantial interference penalty. This interference can be attributed to supersonic velocity regions and strong shocks on the wing lower surface near the wing-pylon intersection. As the nacelle is moved closer to the wing leading edge, using pylons P_2 and P_3, interference drag penalties are shown at the design lift coefficient. For the furthest-aft location, the penalty at design lift coefficient is approximately 5 percent of aircraft drag.

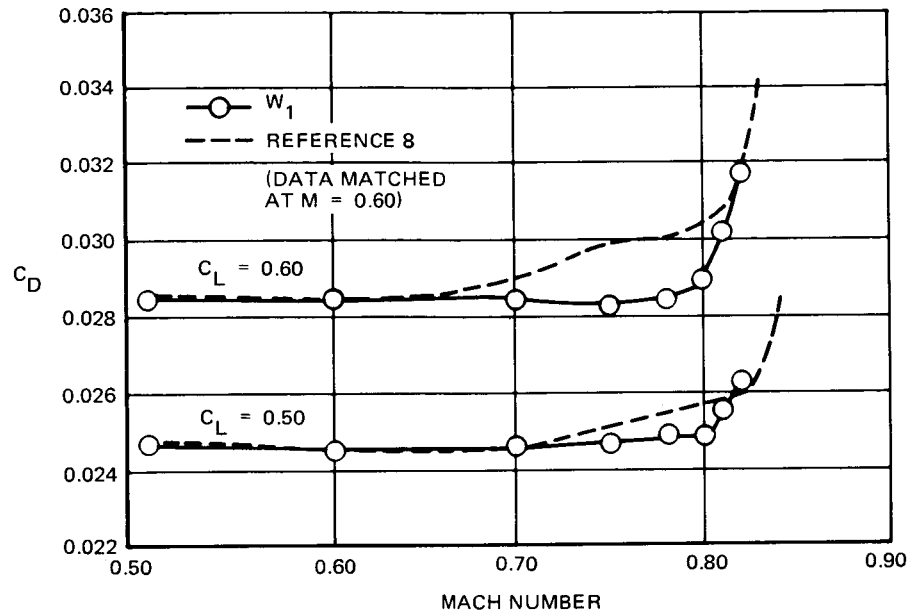

FIGURE 16. CLEAN WING DRAG-RISE CHARACTERISTICS

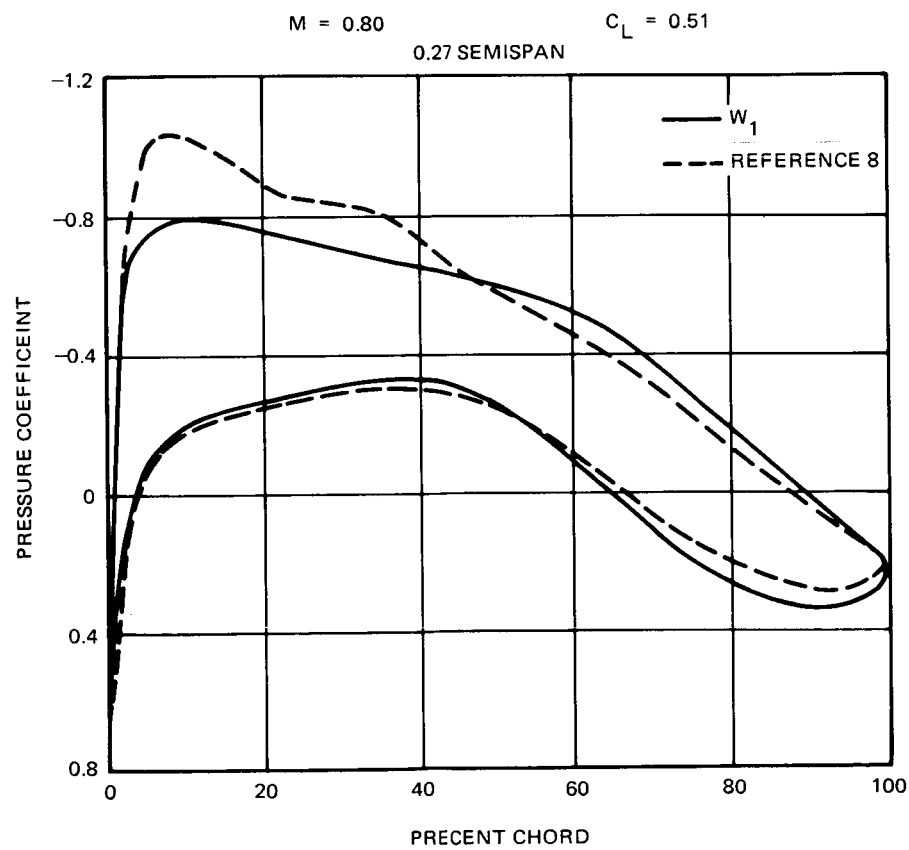

FIGURE 17. COMPARISON OF WING SECTIONAL PRESSURE DISTRIBUTIONS

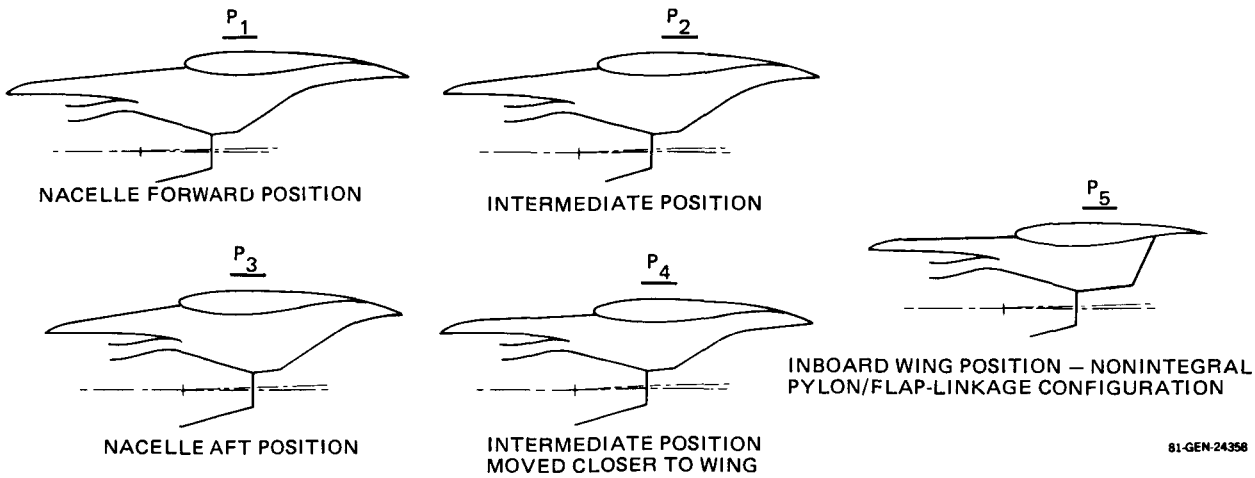

FIGURE 18. NACELLE POSITIONS TESTED

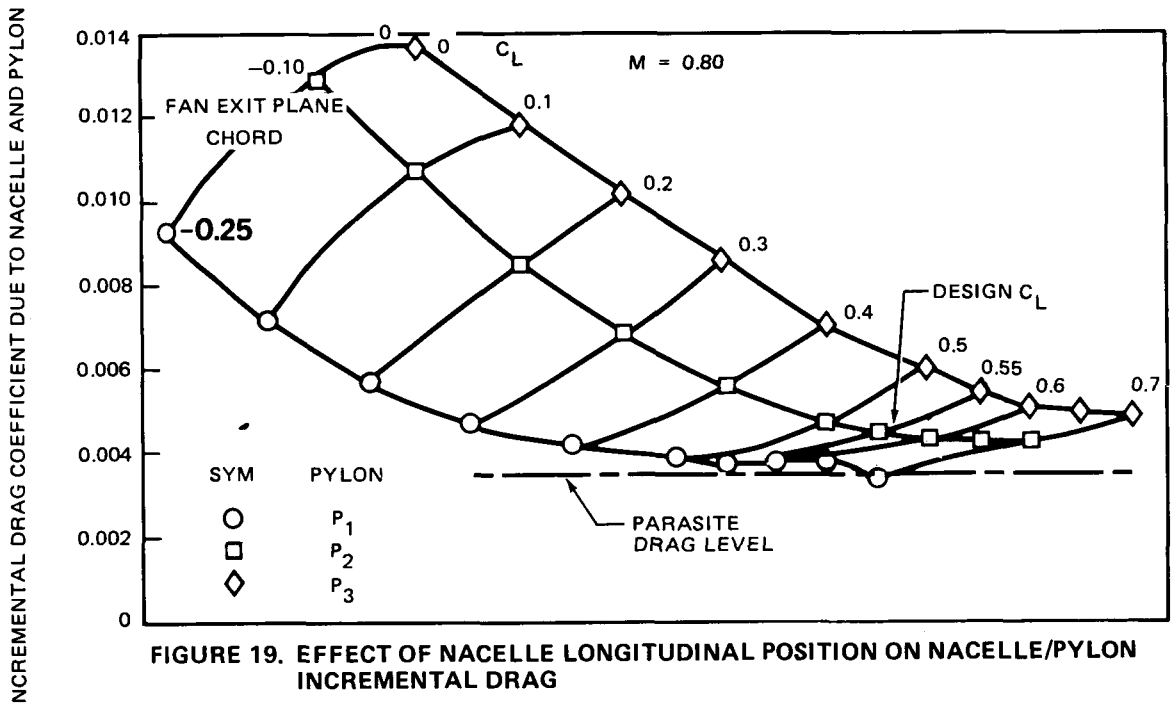

FIGURE 19. EFFECT OF NACELLE LONGITUDINAL POSITION ON NACELLE/PYLON INCREMENTAL DRAG

The nacelle was brought slightly closer to the wing by the use of pylon P_4, causing only a small increase in drag. The nacelle spanwise position was changed by using pylon P_5 to move the nacelle inboard, and a small drag reduction resulted.

Buffet Boundary – Buffet levels were evaluated using the lift curve break criterion. In Figure 20, the lift coefficient boundary is compared with the best performing wing from Reference 8. The level is slightly better than was obtained in the Reference 8 tests and is more than required for the aircraft design.

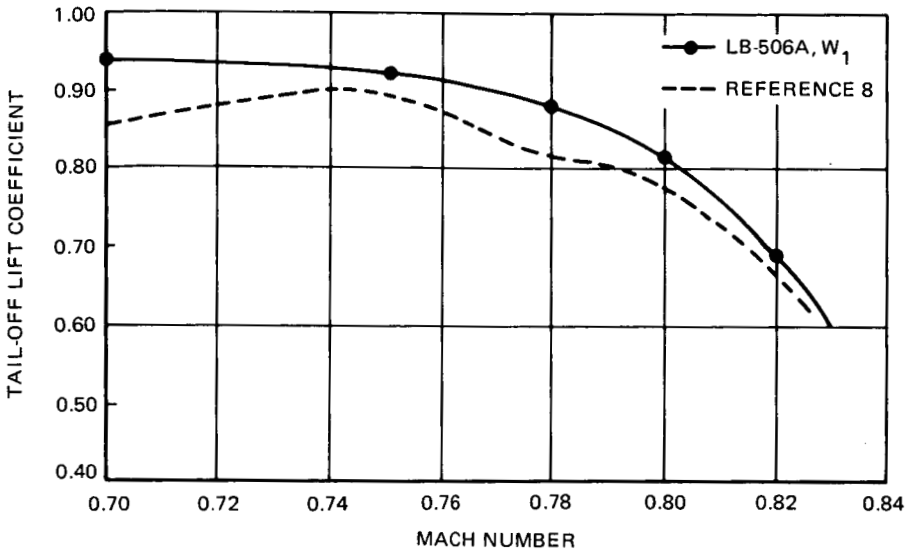

FIGURE 20. BUFFET ONSET BOUNDARY

Pitch Characteristics – At high lift coefficient, tail-on pitch-up was observed. During the second test, the effect of configuration modification was measured. These modifications changed the horizontal tail and the nacelle pylon position, and examined the effect of Reynolds number.

Figure 21 shows the planforms of the baseline H_1 and alternate horizontal tails H_2. The H_2 tail tip was approximately directly aft of the wing trailing-edge break and trace of the baseline nacelle. A significant reduction in the high-speed pitch-up tendency with the H_2 tail is shown in Figure 22. A further modification, locating the nacelle at 33-percent semispan, resulted in a

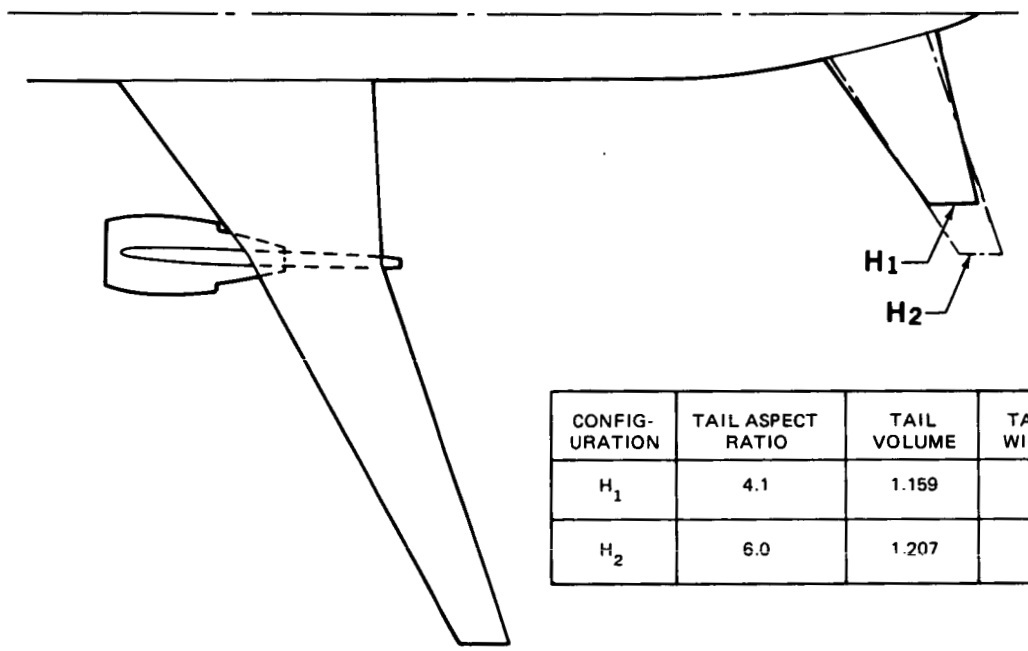

CONFIG-URATION	TAIL ASPECT RATIO	TAIL VOLUME	TAIL SPAN WING SPAN
H_1	4.1	1.159	0.297
H_2	6.0	1.207	0.380

FIGURE 21. TAIL CONFIGURATIONS TESTED

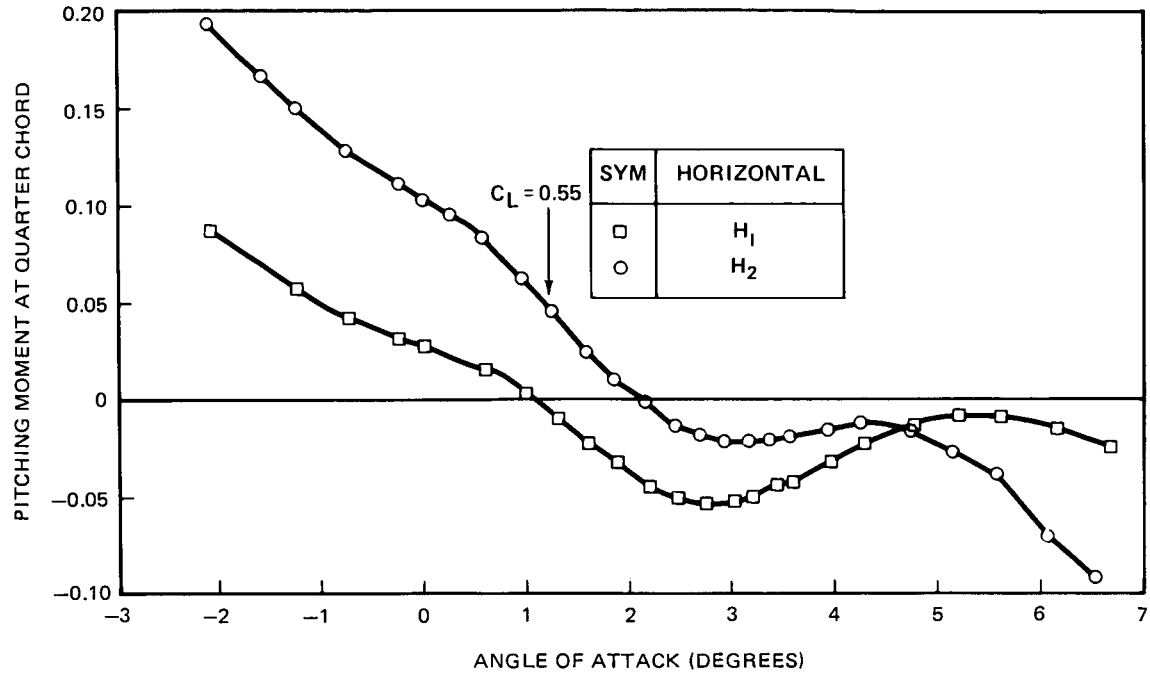

FIGURE 22. EFFECT OF HORIZONTAL TAIL CONFIGURATION ON PITCHING MOMENT

significant degradation of the pitch characteristics, even with the H_2 tail. Test data showed that as the Reynolds number was reduced by one-half, the pitch-up became much more severe. These results emphasize the value of high Reynolds number testing, and give rise to speculation that with a Reynolds number approaching that of flight, the configuration pitch characteristics might be quite acceptable.

Comparisons of Data with Estimates – The test data were compared with the predictions made by the theoretical methods used in the configuration design. Very good correlation was obtained.

Two-Dimensional Test Configurations

Two advanced two-dimensional airfoils were designed using variations in trailing edge camber and thickness distributions. The first section, developed with improved geometry in the flap region, had performance characteristics estimated to be equal to a baseline outboard panel airfoil section of the three-dimensional EET wing previously described. A 30-percent increase in thickness in the vicinity of the flap spar was provided at approximately 80-percent chord. The airfoil was derived from the EET baseline by modifying the lower surface only, and it had the same base thickness. This airfoil is denoted as the thick aftersection airfoil.

The second airfoil, also based on Douglas research, was aimed at improvements in sectional drag characteristics with little change in airfoil dimensions which affect the geometry

characteristics of the primary structure. The design was created by modifying the aft upper-surface pressure gradient to be more favorable for boundary layer growth.

In addition to these concepts, the DC-10 winglet development program (described later in this report) had identified an advantage for an outerwing section modification to effectively increase camber and therefore increase loading on the winglet. This modification was translated to the use of lower-surface trailing-edge wedges applied to a conventional airfoil section. Investigations of this concept were therefore added to the program to extend the data base for winglet technology.

Two-Dimensional Test Results

The models were tested in the National Aeronautical Establishment (NAE) 15- by 60-inch blowdown tunnel in Ottawa, Canada. All had a 10-inch chord and spanned the 15-inch width of the tunnel.

Thick Aftersection Airfoil Results – The measured upper-surface pressure distributions on the airfoil section indicated that shock strengths were reduced from the baseline. The drag characteristics were superior at mid- to high-section lift coefficients at the higher Mach number (0.74) tested. No significant differences in moment characteristics were encountered at low-section lift coefficients, and only small changes were found at higher coefficients.

Although this airfoil was designed to have the same performance as the baseline, a drag reduction was obtained (Figure 23). This result verifies the trend of the design concept of the thickness and camber treatment of the aft airfoil region.

The addition of a small lower-surface trailing-edge wedge caused a modest increase in drag at low Mach number due to the additional base thickness. The increase in aft camber increased lift for a fixed angle of incidence and provided a more negative pitching moment.

Modified Upper-Surface Airfoil Results – The measured change in upper-surface trailing-edge region pressure was approximately twice the expected value. A stronger shock was evident. The results indicated that too much lift was eliminated in the design of the aft 25-percent of the upper surface. A small drag reduction was measured in the low- to mid-section lift-coefficient range. However, at the design condition, little or no improvement in performance was measured. No significant difference in lift characteristics was evident. The nose-down pitching moment was reduced from the baseline level. The measured moment change was a further indication of a larger than estimated reduction in aft loading. The measured drag-rise characteristics showed that the design objective was not obtained. However, when the lower surface trailing-edge wedge was applied (as previously to the thick aftersection airfoil), a

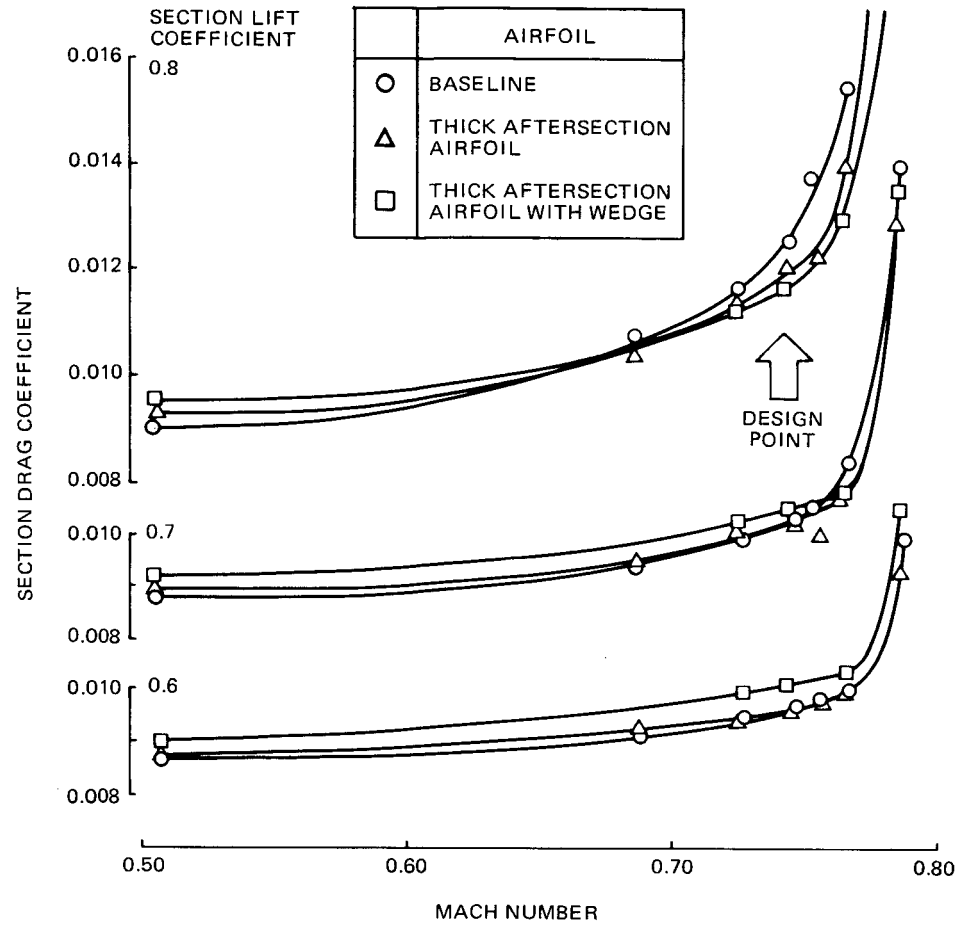

FIGURE 23. DRAG RISE PERFORMANCE OF THICK AFTERSECTION AIRFOIL WITH AND WITHOUT WEDGE

marked performance improvement was obtained (Figure 24). The drag reduction was again due to additional aft loading.

Effect of Aft Camber on the Conventional Airfoil – The applied aft camber caused additional aft loading on the airfoil. The drag characteristics were similar to the previous tests, where a modest increase in drag at the low- to mid-section lift-coefficient range was evident. However, significant improvements were measured in the higher range of lift coefficients. The power of the applied camber was substantial, obtaining a drag reduction of 25 counts at the high-lift coefficient condition and higher Mach number. The drag reduction was due primarily to a reduction in compressibility drag. It would therefore appear that the trailing-edge camber is an effective device applied to a conventional airfoil.

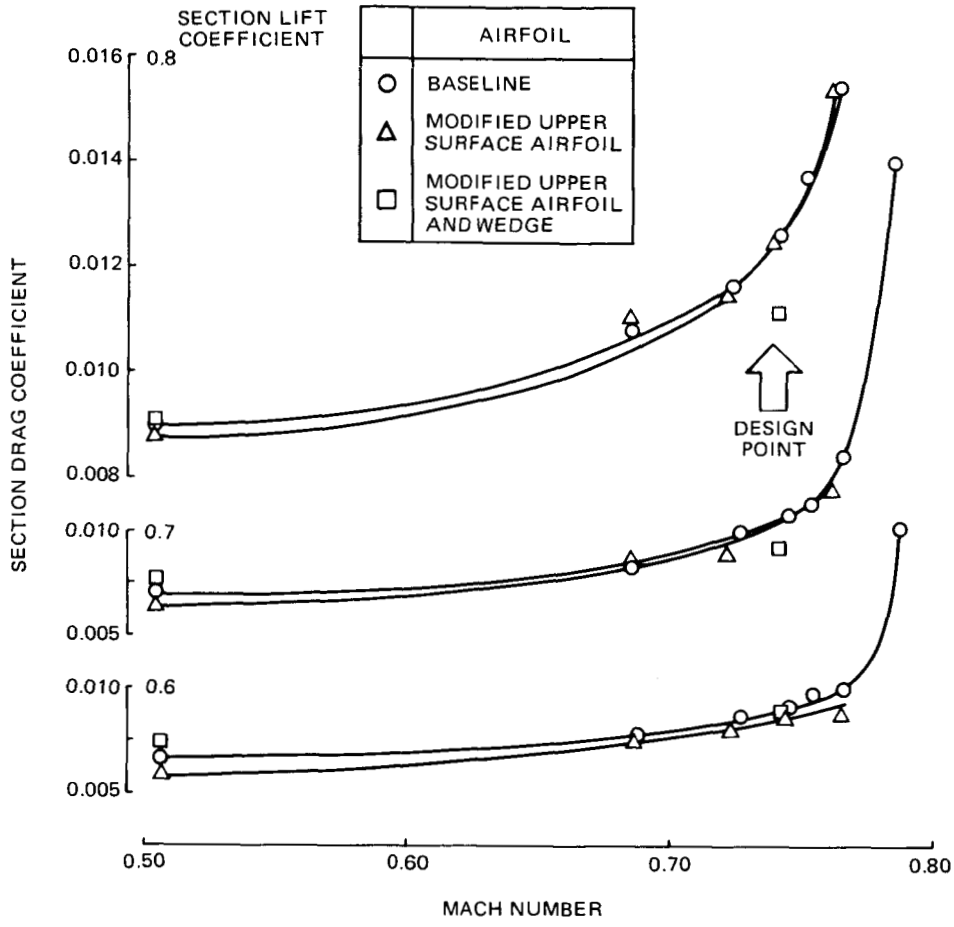

FIGURE 24. DRAG RISE PERFORMANCE OF MODIFIED UPPER SURFACE AIRFOIL WITH AND WITHOUT WEDGE

Conclusions from the Three-Dimensional Tests

The following principal conclusions were drawn:

1. The high-speed drag characteristics were as good as or slightly better than predicted and the level of premature drag creep was substantially reduced from earlier EET designs.
2. Variations in the longitudinal position of the nacelle were found to have the largest impact on the nacelle-pylon drag increment. Substantial interference penalties were measured for nacelle positions further aft than the baseline position.
3. The complete configuration buffet boundary characteristics were good.
4. The tail-on pitch characteristics were favorably affected by an increase in span of the horizontal tail to the trace of the wing nacelle position. As test Reynolds number was increased, a considerable improvement in the pitch-up was obtained.

Conclusions from the Two-Dimensional Tests

The following primary conclusions were made:

1. The design of the baseline airfoil with a thicker aftersection, offering more structural depth for flaps, was shown to be conservative. Transonic performance was better than expected. The effect of a small trailing-edge wedge was beneficial at the design point.
2. The second airfoil, having a modified upper surface near the trailing edge, failed to obtain better performance than the baseline. However, the effect of a small trailing-edge wedge was substantial.
3. The addition of trailing-edge cambers to the conventional section resulted in a marked reduction in compressibility drag.

HIGH-ASPECT-RATIO SUPERCRITICAL WING AERODYNAMIC DEVELOPMENT – HIGH LIFT

Test Configurations

Tests were conducted on both the wide-body DC-X-200 configuration used in the work of Reference 9 and the narrow-body ATMR configuration previously described for the high-speed development. The wide-body and narrow-body models are illustrated in Figures 25 and 26, respectively. The former was a 4.7-percent representation of the DC-X-200, and the latter a 5.59-percent model of the ATMR.

The major components evaluated during the study are illustrated in Figure 27. The leading-edge devices included variable-camber Kruegers (VCK), fixed-camber Kruegers (FCK), and slats. The trailing-edge devices included single-segment flaps, two-segment flaps, and flaperons.

The wide-body model was tested in the NASA Langley Research Center V/STOL facility and in the NASA Ames Research Center 12-foot wind tunnel. The narrow-body model was tested only in the Ames 12-foot tunnel.

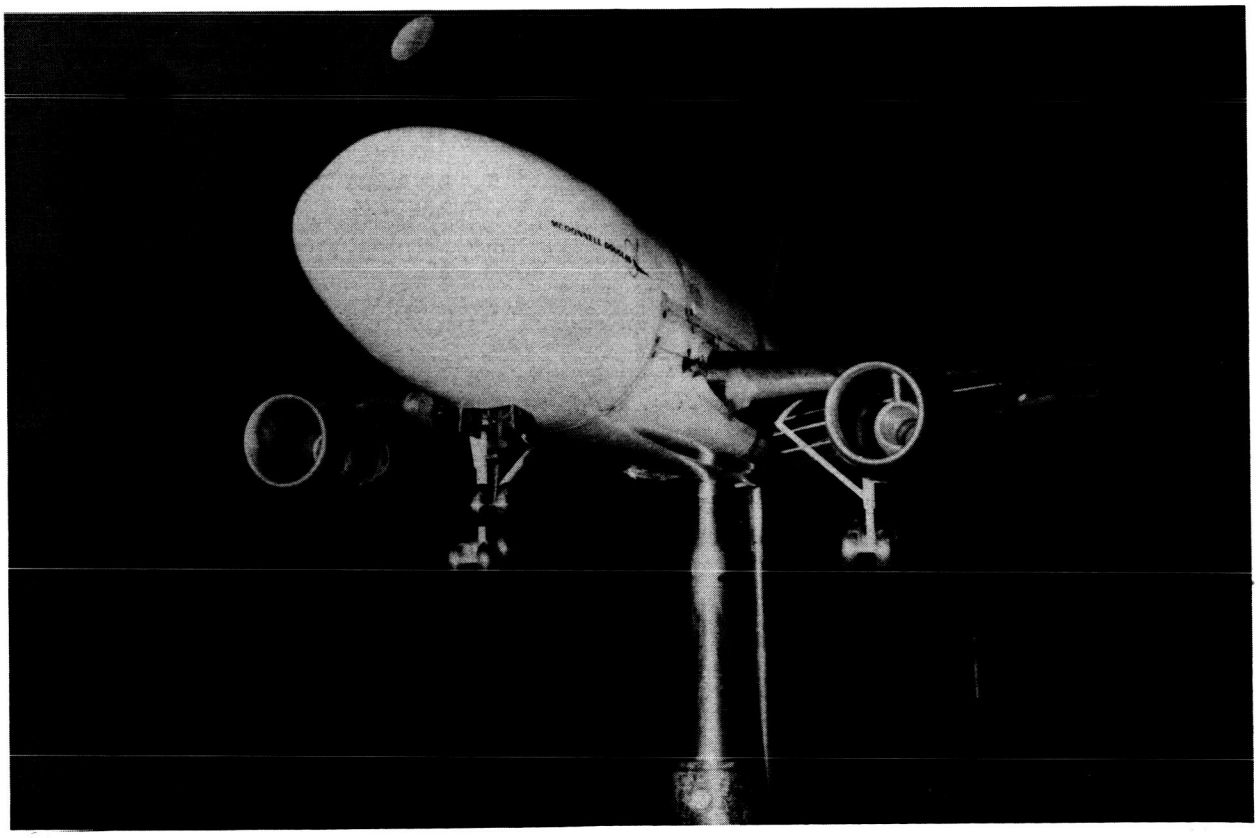

FIGURE 25. WIDE-BODY HASCW HIGH-LIFT MODEL

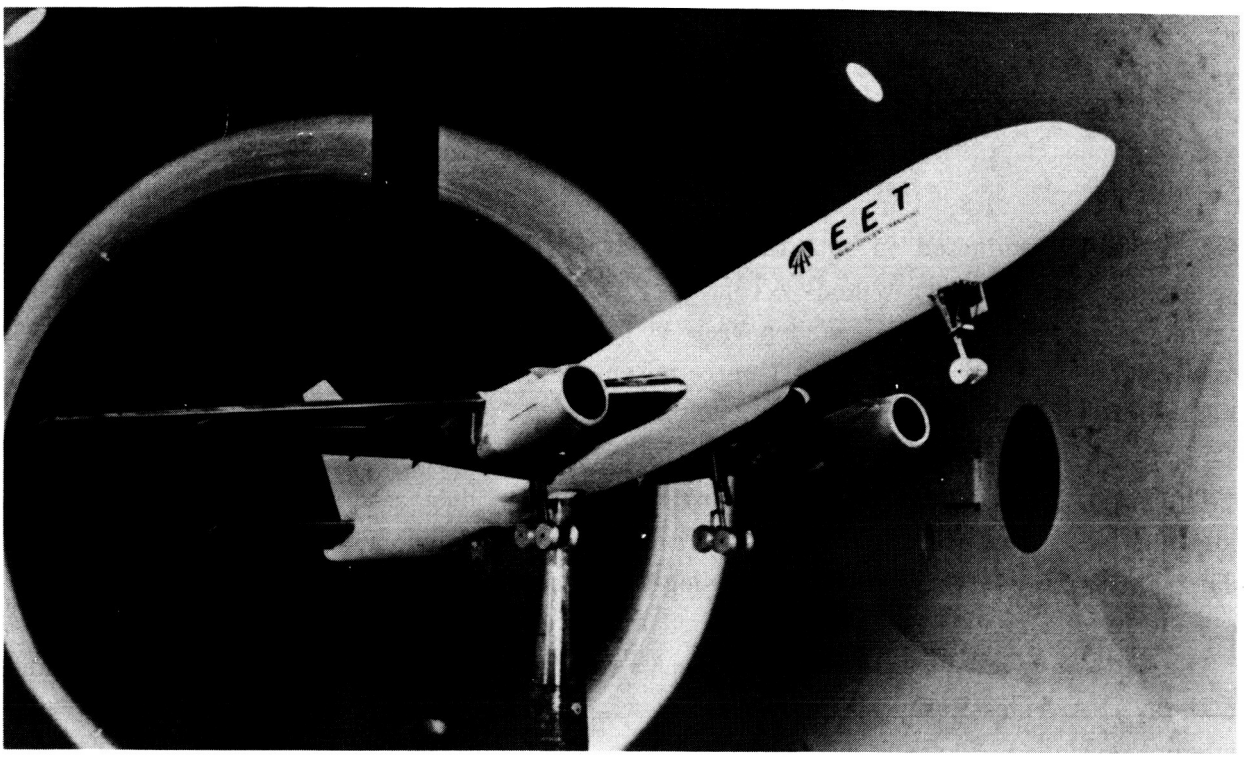

FIGURE 26. NARROW-BODY HIGH-LIFT MODEL

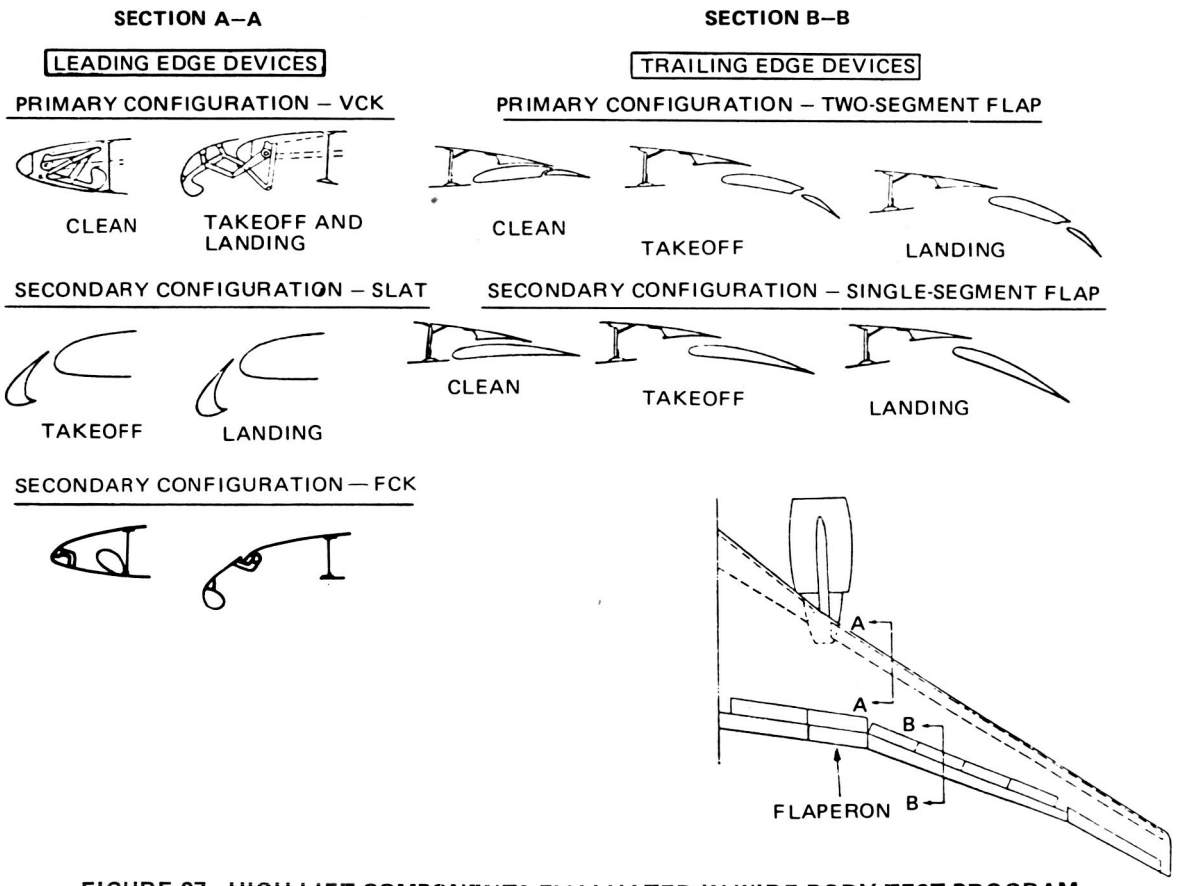

FIGURE 27. HIGH-LIFT COMPONENTS EVALUATED IN WIDE-BODY TEST PROGRAM

Results of the Wide-Body Tests

Reduced VCK Deflection – The results of Reference 9 showed that the maximum lift coefficient with the slat leading edge was equivalent to that with the VCK. However, the lower pressure coefficients obtained for the VCK indicated that a reduction in deflection might result in increased maximum lift. In the first test at the Langley facility, increased maximum lift coefficient was not obtained with the low Reynolds number available; however, this result was confirmed with the higher Reynolds number experienced during the Ames tunnel test.

Sealed Slats – To improve the L/D envelope at takeoff conditions over the values of Reference 9, a sealed (i.e., zero gap) inboard and outboard slat configuration was tested. Analysis prior to the test indicated the possibility that to obtain good pitch characteristics, a retracted inboard slat (i.e., clean leading edge) might be required; this was confirmed by the results. Compared with the slotted landing slat used with takeoff flaps, the sealed slat resulted in a penalty in maximum lift coefficient. However, the sealed configuration was significantly superior in lift-to-drag ratio. The sealed slat resulted in superior pitch characteristics to the slotted slat configuration.

Fixed Camber Krueger – The full-span FCK produced lift and pitching moment characteristics equivalent to those of the full-span slat and full-span VCK configuration. The combination of FCK inboard with slat outboard improved the pitch characteristics. However. post-stall characteristics were unsatisfactory.

A short-chord FCK was found to be successful in improving pitching moment characteristics. This FCK and slat configuration resulted in only slightly lower maximum lift values and better pitching moment trends that did the full-span slat configuration.

Slat Trim Effects – The basic configuration of the slat was trimmed at the side of the fuselage and continuous over the pylon. Trim variations included a gap at the fuselage and undeflected slat over the pylon. Pitching moment characteristics showed a lower maximum lift coefficient and more adverse post-stall behavior than the short-chord FCK.

Results of the Narrow-Body Tests

Clean Wing Comparisons – Comparison of the wide-body and narrow-body models, tail-off, showed the narrow body to have a superior maximum lift coefficient and pitching moment. The pitch-down after stall was forceful, although nose-up moments were preset before the stall. Maximum lift coefficient and pitch characteristics were affected by changes in Reynolds number and Mach number.

Landing Configuration Characteristics – The primary landing configuration consisted of a two-segment flap deflected at 25 degrees/12 degrees, a slotted outboard slat deflected at 27 degrees, and a slotted slat or short-chord inboard FCK. The results of performance tests are shown in Figure 28. This figure also compares results of the wide-body tests. The FCK and slotted outboard slat did not attain the maximum lift coefficient value of the wide-body slat configuration, in part because the outboard slat was overdeflected. The FCK and slat configuration has a superior maximum lift coefficient to the all-slat configuration. Moreover, the all-slat configuration exhibited the most undesirable pitching moment trend.

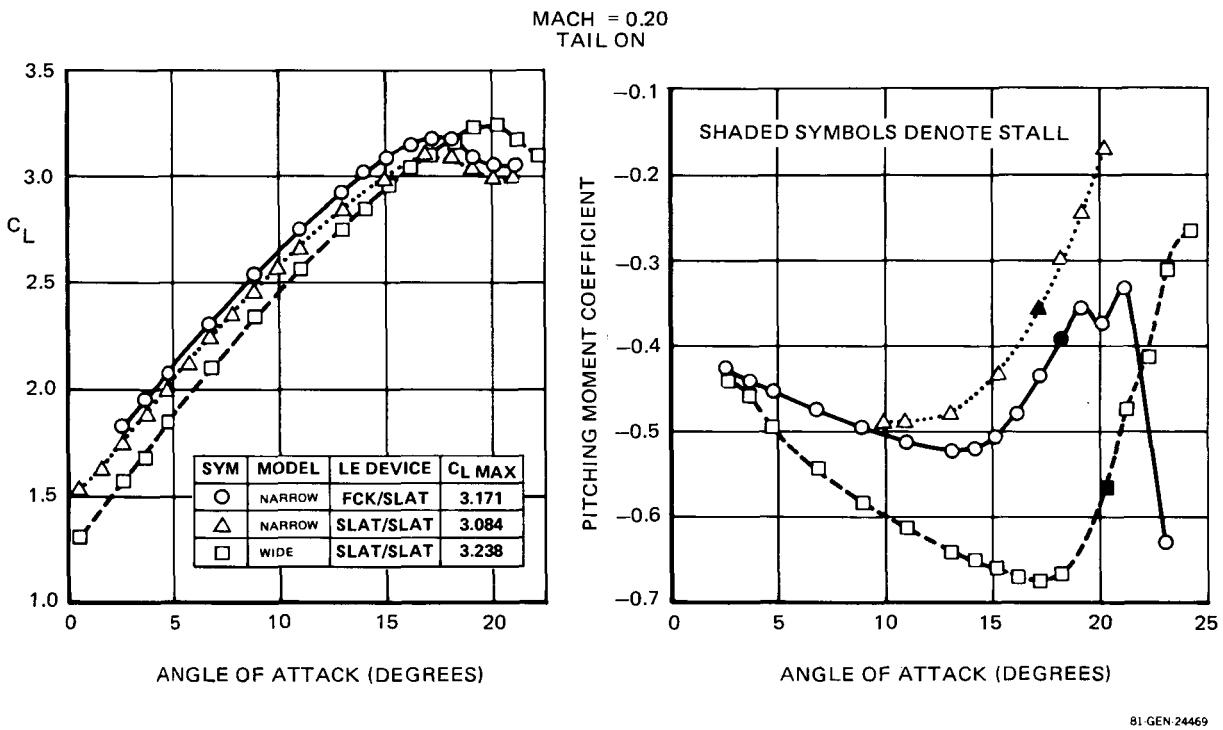

FIGURE 28. COMPARISON OF NARROW-BODY AND WIDE-BODY LANDING CONFIGURATION CHARACTERISTICS

The effect of Reynolds number on maximum lift coefficient is significant, as shown in Figure 29. Hence, the L/D ratio will increase, and pitching moment trends should improve. However, no extrapolation of this curve is recommended.

Takeoff Configuration Characteristics – Most of the testing in takeoff conditions was conducted with sealed (zero gap) slats, in view of the advantage of higher lift-to-drag values. The narrow-body model utilized an FCK inboard and sealed slat outboard. Compared with the previously described sealed slat for the wide-body model, a significantly higher maximum lift coefficient was obtained. A higher stall angle was also reached. Pitch characteristics were improved. These comparisons are shown in Figure 30. It should be noted that the wide-body results reflect a lower Reynolds number; about half the inferiority is due to this lower number.

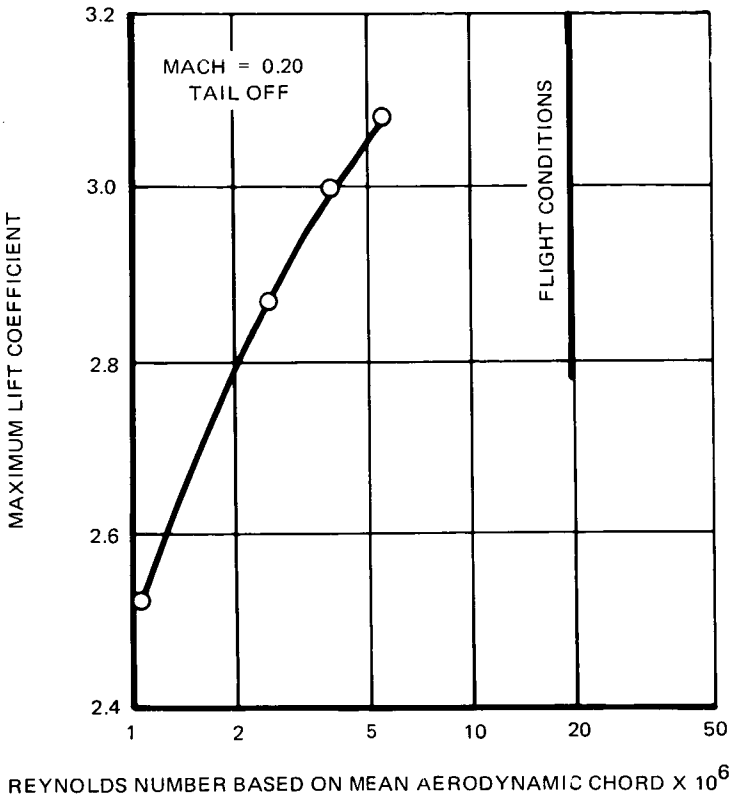

FIGURE 29. EFFECT OF REYNOLDS NUMBER ON NARROW-BODY LANDING CONFIGURATIONS $C_{L_{MAX}}$

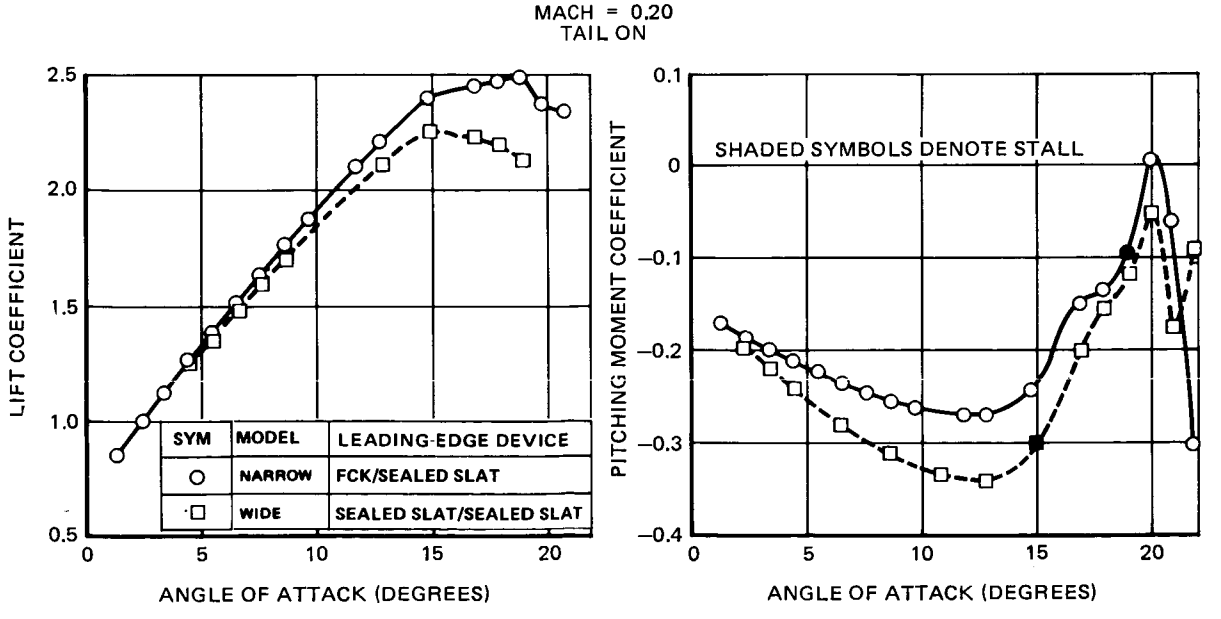

FIGURE 30. COMPARISON OF NARROW-BODY AND WIDE-BODY TAKEOFF CONFIGURATION CHARACTERISTICS

The superiority of the narrow-body configuration in lift-to-drag ratio is shown in Figure 31. Again, about half the improvement is due to Reynolds number effects. Reynolds number evaluations on the narrow-body model suggest that maximum lift coefficient will continue to increase as flight values are approached.

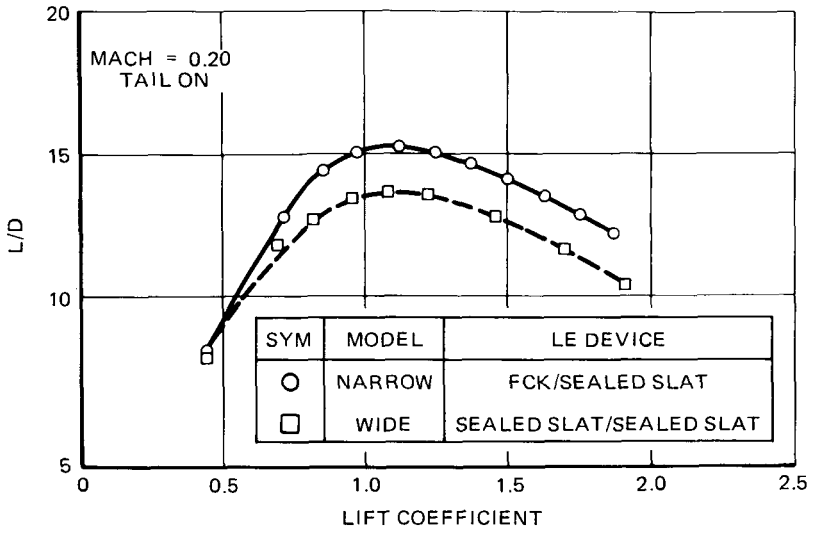

FIGURE 31. COMPARISON OF NARROW-BODY AND WIDE-BODY TAKEOFF LIFT-TO-DRAG RATIOS

Conclusions from the High-Lift Tests

The following primary conclusions were drawn from the wide-body data:

1. In the takeoff flap configuration, a sealed outboard slat, with a clean leading edge inboard, provided significant improvement in lift-to-drag and pitching moments compared to the basic slat configuration, but suffered a penalty in maximum lift coefficient.

2. An inboard FCK (especially a short-chord FCK), used in conjunction with a outboard slat, provided the best improvement in stalling behavior, with only a relatively small loss in maximum lift coefficient.

The following primary conclusions were drawn from the narrow-body data:

1. The clean wing achieved superior lift and pitching moment characteristics to the wide-body wing.

2. Superior maximum lift coefficient and pitching moments were obtained for the configurations with an inboard FCK; the L/D values for the inboard sealed slat and FCK configurations were equivalent.

3. Strong Reynolds number effects were evident in the measured maximum lift coefficient characteristics, even at the highest test Reynolds number.

WINGLET TECHNOLOGY DEVELOPMENT FOR DC-10 DERIVATIVES

The winglet concept, developed by Dr. R. T. Whitcomb (Reference 12), employs an airfoil surface mounted almost vertically at an airplane's wing tip. It is intended to reduce lift-induced drag, which accounts for as much as 40 percent of the total drag at cruise speed. Historically, one of the primary ways of reducing this drag has been to increase the wing span, but this results in a heavier wing structure and so dilutes the performance gain. The concept of the winglet is to achieve the same drag reduction as with the wing-tip extension but with less penalty on the wing bending moment.

A substantial amount of wind tunnel and flight testing has been conducted on winglets since the original Whitcomb experiments for NASA. Significant performance gains have been demonstrated for large first-generation jet transport aircraft and for other smaller aircraft. However, application of the winglet to a representative second-generation jet transport, such as the DC-10, was recognized as needing further investigation, primarily due to the differences in wing design.

Second-generation wings tend to be less tip-loaded and therefore do not offer the potential for induced-drag reduction provided by a wing-tip device. Also, they incorporate advanced high-lift devices, resulting in significantly higher lift coefficients in the low-speed regime. Such high loadings afford greater potential for low-speed drag reduction but introduce the possibility of adverse viscous effects on winglet performance. The distinction of high loading also separates the typical large transport application from some current production corporate aircraft.

Under the EET project, investigations were conducted to build the technology for the DC-10-type aircraft. Results of the initial EET high-speed wind tunnel test (Reference 13) were used to develop a satisfactory configuration (Figure 32) and identify the cruise performance benefit. The second phase, conducted under the present contract, was intended to further the technology to where the need for full-scale evaluation (or readiness for application) could be identified. The second EET phase consisted of the following studies:

- High-speed stability and control wind tunnel tests.
- Low-speed wind tunnel tests to determine effects on both performance and stability and control characteristics.
- Low-speed flutter tests of a dynamic wind tunnel model to determine data on flutter speeds, damping, and frequency characteristics that could be correlated with analytical predictions.
- Investigation of the effect of these results, together with those of related Douglas studies, on the most significant performance characteristics of a typical DC-10.

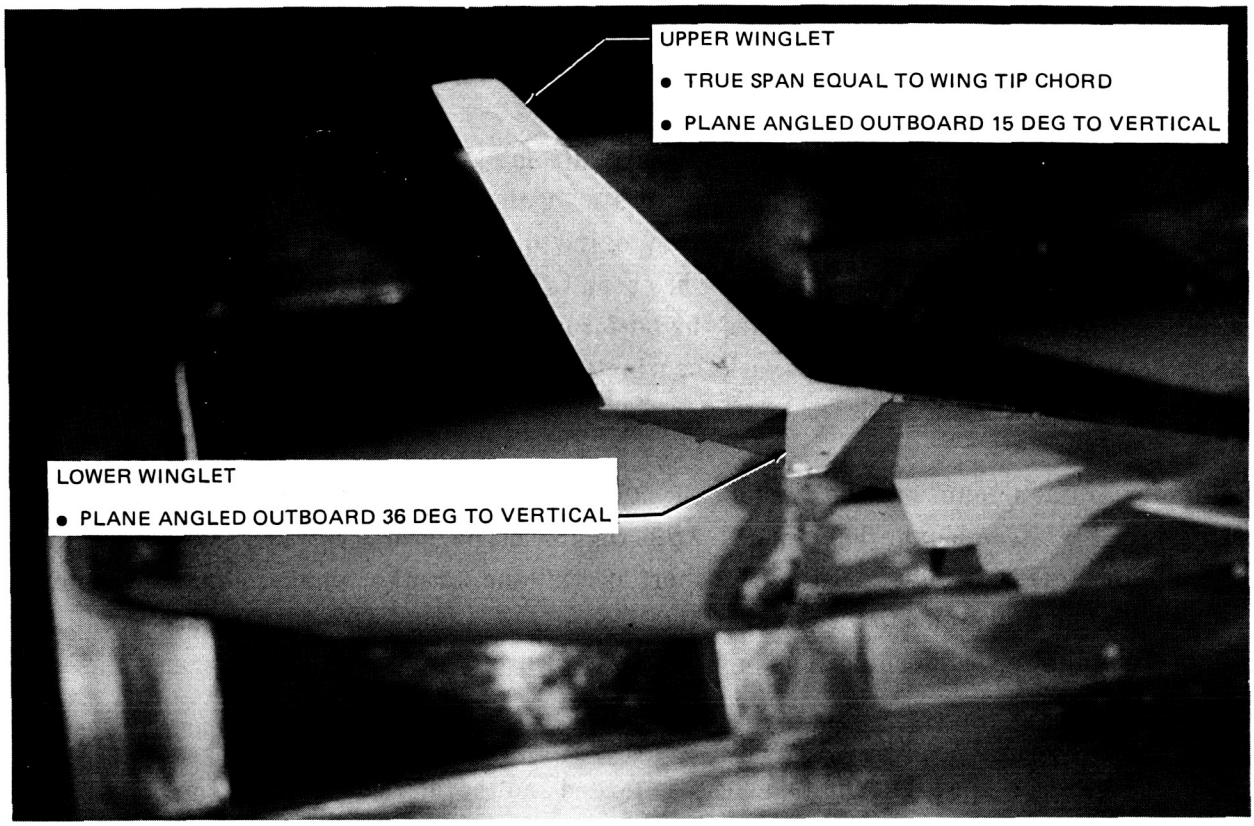

FIGURE 32. WINGLET MODEL UNDER DEVELOPMENT

The results of the second phase, as of the first, were generally promising. However, problem areas were revealed from these wind tunnel tests which required further assessment. It was therefore decided that the next logical step in development was full-scale flight evaluation.

The objectives of this third phase were to determine through flight evaluation:

- The effects of winglets on performance and flying qualities.
- The effects of winglets on aircraft flutter.
- The effects of winglets on flight loads. (This portion of the program was sponsored by Douglas.)

The flight testing was structured so that key data comparisons between the baseline aircraft without winglets and the winglet-configured aircraft were obtained from back-to-back test phases. In addition to the basic winglet (BWL) derived from the wind tunnel tests, a reduced-span winglet (RSWL) was tested so that the effects of upper winglet span could be studied. The program was conducted on a DC-10 Series 10 aircraft supplied by Douglas. The test aircraft is shown in Figure 33 in the BWL configuration and in Figure 34 in the RSWL configuration. The aircraft was leased from Continental Airlines and was returned to airline service after the program.

FIGURE 33. TEST AIRCRAFT WITH BASIC WINGLET

FIGURE 34. TEST AIRCRAFT WITH REDUCED-SPAN WINGLET

The third phase results showed that significant drag reduction could be achieved with winglets with no adverse effects on flying qualities. There was some configuration development during the flight test program. This development raised some unresolved issues which required further investigation to obtain the maximum benefit from winglets. A fourth phase was therefore instituted. The primary objectives of this phase were to investigate, through wind tunnel testing:

- The effect of a small deflection, or "droop," of the outboard aileron on high-speed stability and control characteristics. This droop resulted in an additional cruise drag reduction for winglets during the flight evaluation.
- The feasibility of simpler winglet leading-edge devices while maintaining the low-speed drag reduction achieved with a Krueger device in flight.
- Exploration of the potential for further cruise drag reduction through modifications of the winglet and the wing trailing edge.

The second, third, and fourth phases are summarized in the following sections. The second phase is fully reported in Reference 14 and the third in Reference 15. The third phase is summarized in Reference 16.

WINGLET MODEL TESTING AND ANALYSIS – PREFLIGHT EVALUATION

High-Speed Stability and Control Wind Tunnel Test

Configuration and Results – The winglet configuration, closely representing the configuration used in first phase tests (see Figure 32), was tested on a 3.25-percent full-span model of the DC-10 Series 30 aircraft. The test was conducted to evaluate the effect of winglets on the aircraft stability characteristics, outboard aileron effectiveness, and buffet boundary. The NASA Ames Research Center 11-foot wind tunnel was used for the test.

The test showed that winglets produced a small increase in longitudinal, directional, and lateral stability derivatives at cruise speeds. The longitudinal increase was equivalent to 2-percent aft shift in the center of gravity. For a typical cruise condition, the dutch-roll mode had a slightly shorter period, slightly shorter time to one-half amplitude, and produced virtually no change in damping ratio. The spiral mode was slightly less stable, the time to half amplitude increasing 15 percent. The trend of the stability data closely approximated that of the baseline aircraft without winglets. It is considered that winglets had a negligible effect on the high-speed stability characteristics.

Aileron data were measured for the potential evaluation of a DC-10 derivative which might employ these controls at high speed for active control load alleviation. (In the current DC-10, the outboard ailerons are locked faired at high speed.) The wind tunnel tests showed no change in outboard aileron effectiveness with winglets up to Mach numbers of 0.85. In the next regime up to Mach 0.92, a definite improvement in effectiveness was measured. At Mach 0.95, effectiveness was degraded for 5 degrees trailing edge up, but improved for 15 degrees.

Winglets caused no change in the flow mechanism which causes buffet onset. They had no discernible effect on cruise buffet characteristics.

Low-Speed Performance and Stability and Control Wind Tunnel Test

Configuration and Results – The winglet configuration employed in the stability and control tests was incorporated into a 4.7-percent full-span model of the DC-10-30 for low-speed testing. At a late stage in the program, a reduced-span upper winglet was also tested. The model configurations are shown in Figure 35. The NASA Ames Research Center 12-foot wind tunnel was used. The tests were conducted to determine the effects of winglets on high-lift performance, investigate the need for winglet leading-edge protection against flow separation, and identify stability and control characteristics.

DIMENSIONS IN CENTIMETERS (INCHES) MODEL SCALE

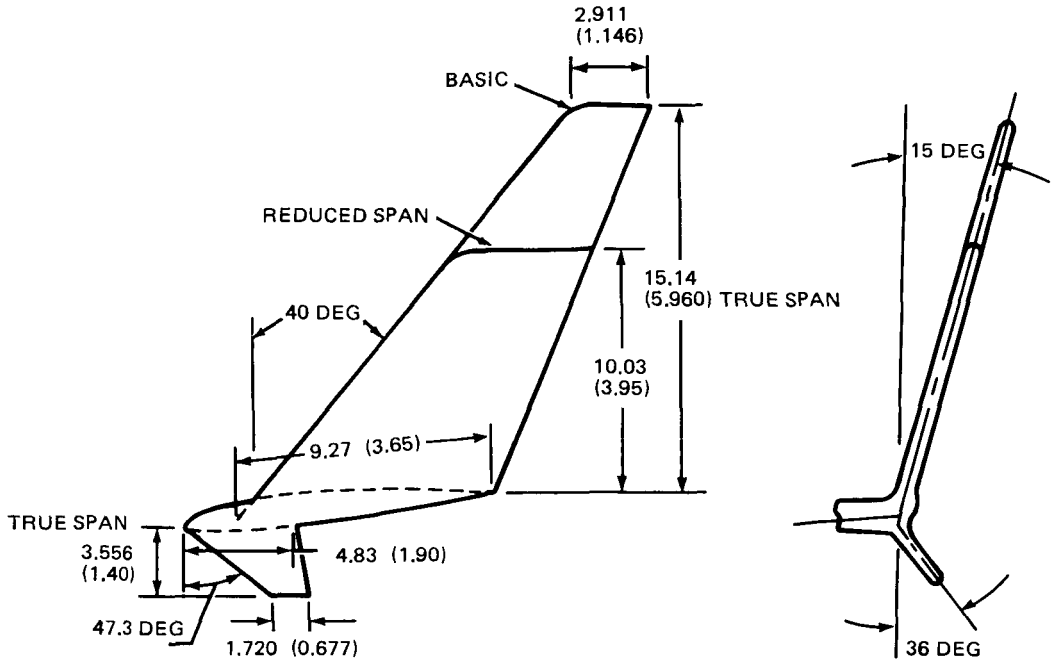

FIGURE 35. DC-10 SERIES 30 LOW-SPEED WIND TUNNEL MODEL DIMENSIONS

The winglet leading-edge protection was proposed after initial analyses had identified the likelihood of winglet flow separation, with attendant risk of wing flow degradation, at high aircraft lift coefficients. After preliminary feasibility studies to show how such a device might be articulated in the real aircraft, a slat was selected as a representative device. It should be noted that in the subsequent flight evaluation phase, this slat was changed to a Krueger flap. In the postflight investigation, after more detailed installation studies, a drooped leading-edge flap was recommended.

Flow visualization results showed a progression of flow quality on the winglet from well-behaved attached flow at low angles of attack to degraded and separated flow at high angles. Generally, the upper winglet slat delayed the onset of flow separation to higher angles of attack. Prior to separation, the flow became spanwise, originating from the winglet trailing edge and spreading outboard with increasing angle of attack. Even when the winglet flow was completely separated, the wing tip flow remained well-behaved. The impact of the winglet on the aircraft lift characteristics was found to be negligible.

The drag characteristics of the aircraft were significantly improved by winglets, as shown in Figure 36. The figure also includes a flow quality indication, based on the flow visualization results. These data are for a takeoff condition with 15-degree flaps, and in this case, the drag reduction with the winglet slat retracted was more than with the slat open. The maximum

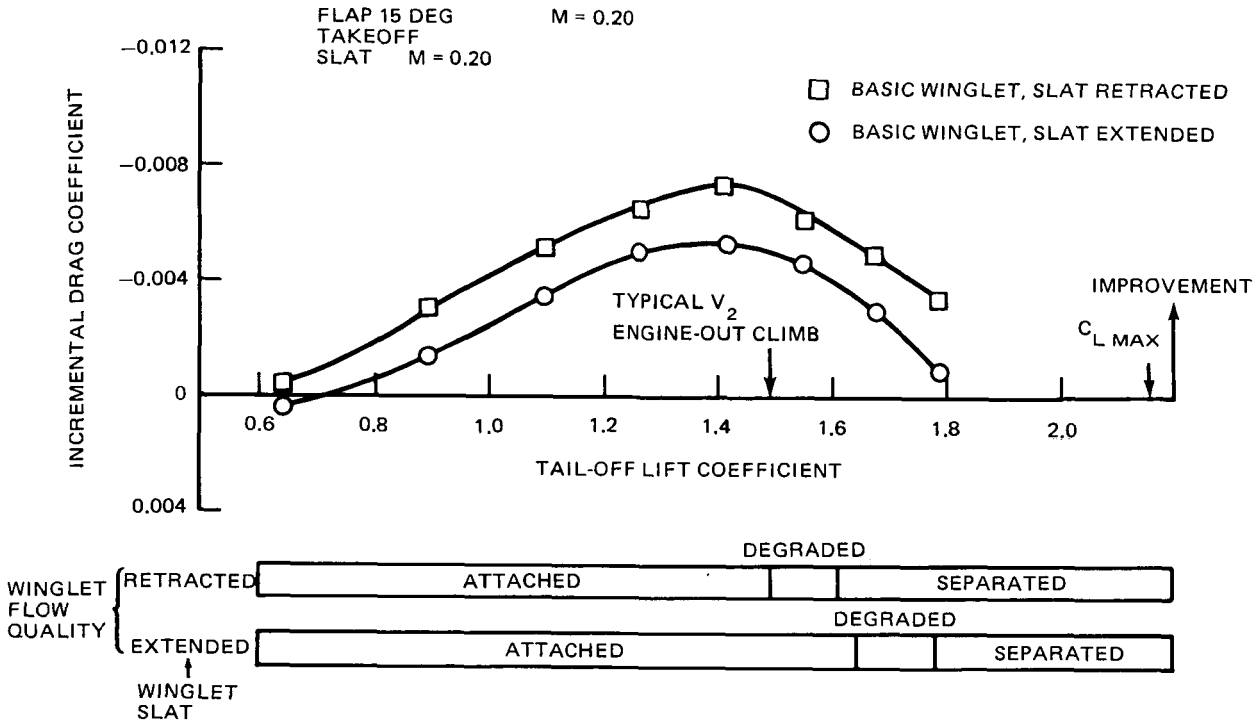

FIGURE 36. BASIC WINGLET DRAG IMPROVEMENT FOR TAKEOFF CONFIGURATION

reduction was near the takeoff safety speed, V_2, and thereafter declined due to flow separation. Such a separation near an important operating regime gives rise to concern of low-speed buffet. The reduced-span winglet results indicated a drag reduction approximately in proportion to the upper winglet spans.

Pressure measurements indicated that the winglet flow separated before the wing stall, and that the winglet separation originated at the tip and progressed to the root.

Investigations made of the effect of ice buildup on the winglet leading edge showed a minimal impact. Based on these results, it was considered that the provision of ice protection on the leading edge would be an unnecessary complication for a production aircraft.

The impact of winglets on stability and control characteristics was very small. Changes in stall characteristics were insignificant. Winglets provided small increases in lateral and directional stability, with the increases in side force, yawing moment, and rolling moment diminishing with increasing angle of attack. The effect on lateral-directional coefficients was negligible. These data suggested that there would be no effect on flying qualities.

An increase in aileron effectiveness due to the winglets was noted up to nearly 12 degrees angle of attack for deflections in both directions. Above 12 degrees, a small loss in effectiveness was found for 20 degrees trailing edge down and a small increase for trailing edge up.

Configuration and Results – The flutter behavior with winglets was investigated with a simple cantilevered dynamic model. A 4.5-percent low-speed flutter model of the DC-10 Series 30 aircraft was employed. The winglet configuration was identical to that tested in the preceding aerodynamic tests of this phase. Provision was made to replace the aerodynamic surface with a mass, so as to determine the contributing effects of mass and aerodynamics. The wind tunnel test was conducted in the Northrop 7- by 10-foot subsonic tunnel.

Initial analysis showed that two significant flutter modes would result from the winglet installation. The 3-Hz inner panel torsion mode, which is critical for the baseline configuration, was degraded by a small to moderate amount. The 4-Hz outer panel mode, present on the baseline aircraft but not critical, was degraded by a large amount and became critical with the winglet at fuel quantities greater than 60 percent. The winglet results are shown in Figure 37. The figure also shows some test points made by tuning (softening) the pylon so that the inner panel mode (Mode 1) was stabilized. As in the other cases, the correlation between analysis and test was excellent. The analysis utilized production methodology, using unsteady aerodynamics generated by the doublet lattice method.

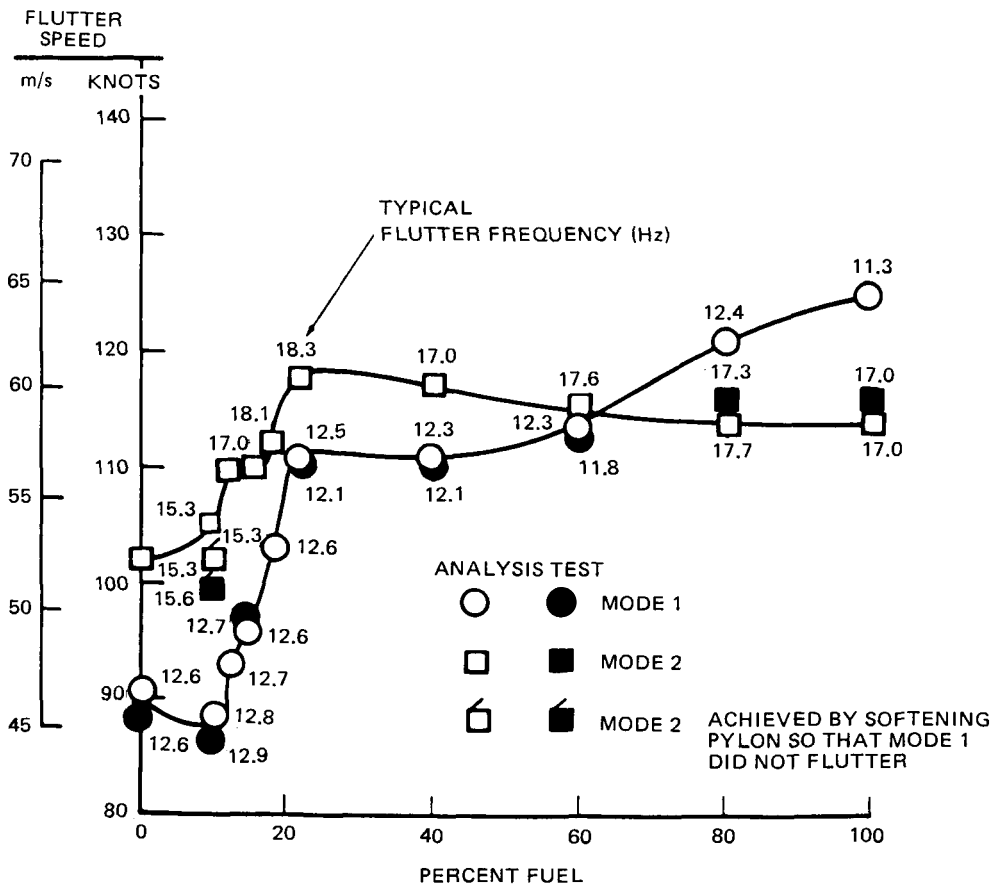

FIGURE 37. EFFECT OF FUEL STATE ON FLUTTER SPEED FOR WINGLET AIRCRAFT

It was found that, for the higher frequency mode, the mass and inertia effect and the aerodynamic effect were detrimental, and each was roughly of equal magnitude.

Configuration Integration Effects

Structural and Applications Studies (Basic Winglet) – Preliminary studies were made considering a derivative of the baseline DC-10 Series 30 aircraft. This baseline aircraft had a 259,000-kg (572,000 lb) gross weight, and was powered by General Electric CF6-50C1 engines. No technology improvements other than winglets were considered. For these studies, the basic winglet, as tested in the first phase and early in the second phase, was used.

The installation of the winglets was estimated to add 1,374 kg (3,030 lb) to the baseline operational empty weight. The wing structural strengthening included in this figure was sufficient to enable the baseline flutter speed to be maintained. At a typical range of 7,400 km (4,000 n mi), the fuel saving was 2.9 percent.

Structural and Applications Studies (Reduced Span Winglet) – In conjunction with the contract work, Douglas studies investigated applications for the winglet in greater detail. These structural studies found that more severe penalties than previously estimated would occur with winglets on a derivative of the Series 30; however, the fuel burn saving would still be economically attractive if other improvements were to be included at the time of the redesign.

Although retrofits were considered infeasible for the Series 30, it appeared that such a concept may be feasible for the smaller wing span Series 10 if a smaller winglet were to be used. Such a design would sacrifice aerodynamic benefit in favor of reducing the incremental wing loads. The reduced-span winglet could also be considered for new production derivatives. Initial studies identified a suitable reduced-span upper winglet having a span 62 percent of the basic design.

Compared with a derivative of the Series 10 with the basic winglet, which was estimated to save 3.5 percent of fuel burned over the baseline, the reduced-span winglet version was estimated to save 3 percent. These estimates included the weight effects.

Conclusions from the Winglet Preflight Investigation

The following conclusions were reached from the preflight high-speed stability and control wind tunnel tests:

1. Winglets had a negligible effect on the high-speed stability characteristics of the aircraft.

2. Winglets caused essentially no change in aileron effectiveness up to Mach 0.82 and an improvement at higher Mach numbers up to 0.95. (This result will be of use should high-speed use of the outboard aileron be considered for active controls.)

3. There was no impact on cruise buffet characteristics.

The following principal conclusions were arrived at from the preflight low-speed performance and stability and control wind tunnel test:

1. The basic and reduced-span winglets had negligible effects on the aircraft lift characteristics.

2. Significant drag reductions were achieved. Generally, a winglet of reduced span resulted in a lower drag reduction proportional to its span.

3. The upper winglet encountered flow separation before the wing stalled.

4. A winglet leading-edge slat delayed flow separation on the upper winglet, and such a device should be considered for flight use.

5. No adverse effect on stability, control, or flying qualities resulted from the addition of winglets.

The preflight flutter investigations led to the following principal conclusions:

1. The winglets had generally detrimental effects on the flutter characteristics.

2. The mass and inertia effects and the aerodynamic effects of the winglet are both detrimental and roughly of equal magnitude in the higher frequency wing flutter mode.

3. Production flutter methods using unsteady aerodynamics generated by the doublet lattice method can be used accurately for prediction of effects on subsonic flutter speeds.

The following conclusions were reached from a study of the integrated effects of the preflight analytical and experimental investigations:

1. A winglet reduced in span from the basic winglet would result in reduced structural penalty, thereby making it possible to consider applications retrofitting to active DC-10 Series 10 aircraft.

2. The reduced-span winglet, as installed, was estimated to save 3 percent of fuel burned.

WINGLET FLIGHT EVALUATION

Winglet Design Configuration

The planned configurations of the basic winglet (BWL) and the reduced-span winglet (RSWL) are shown in Figure 38. The BWL configuration was directly related to the original Whitcomb designs. The specific design for the DC-10 was developed in the initial EET wind tunnel test (Reference 13). Minor changes were made chiefly as the result of subsequent tests (Reference 14). Based on the results of the low-speed wind tunnel test, the flight test design included as a contingency a bolt-on Krueger flap leading-edge device for the upper winglet and a provision to move the lower winglet forward or remove it altogether. As is described in the section on results, further configuration alterations were investigated during the flight program.

The structure designed for the tests consisted of an upper winglet, a lower winglet, and a wing box extension attached to the test aircraft wing box at the outer fuel-closure bulkhead (Figure 39). In addition, the wing box upper skin panels were strengthened. The winglet assemblies were installed in the open, using simple hoist equipment.

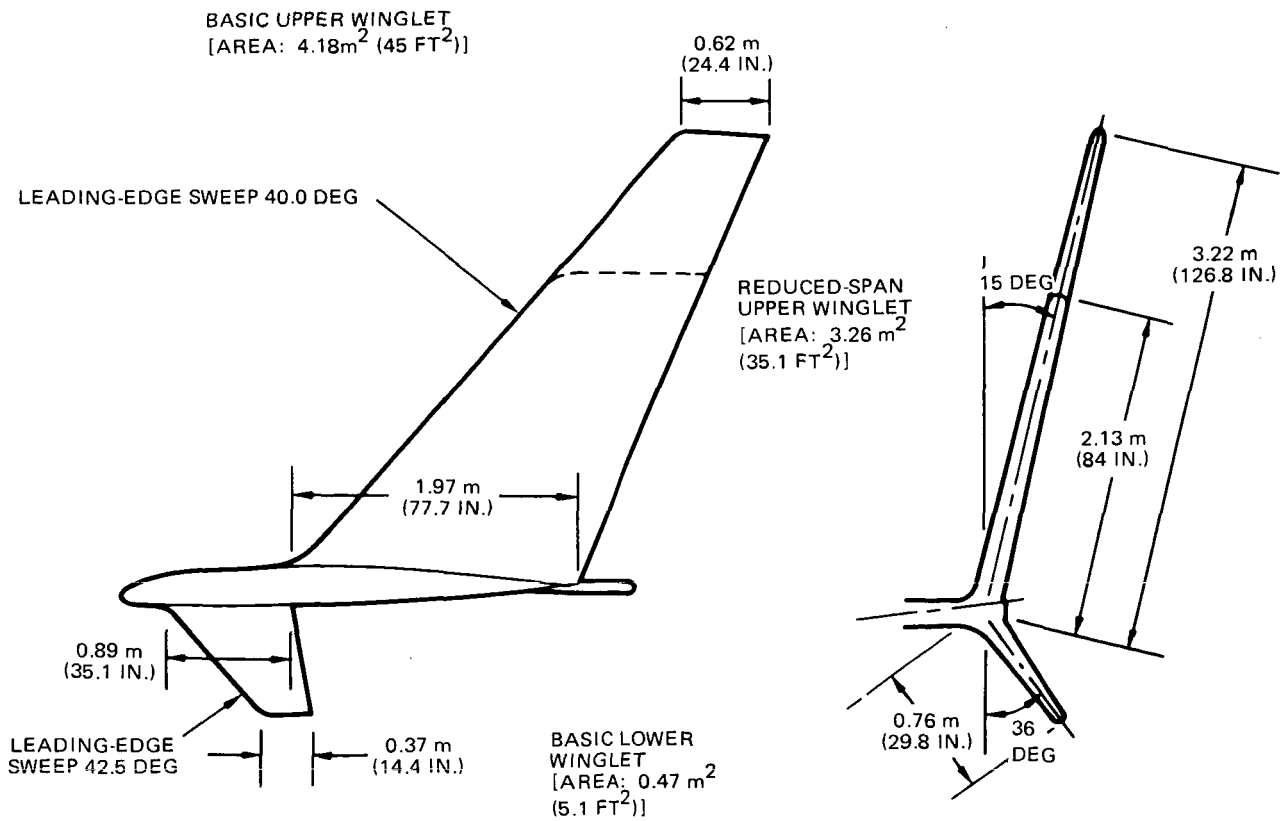

FIGURE 38. PLANNED FLIGHT TEST WINGLET GEOMETRY

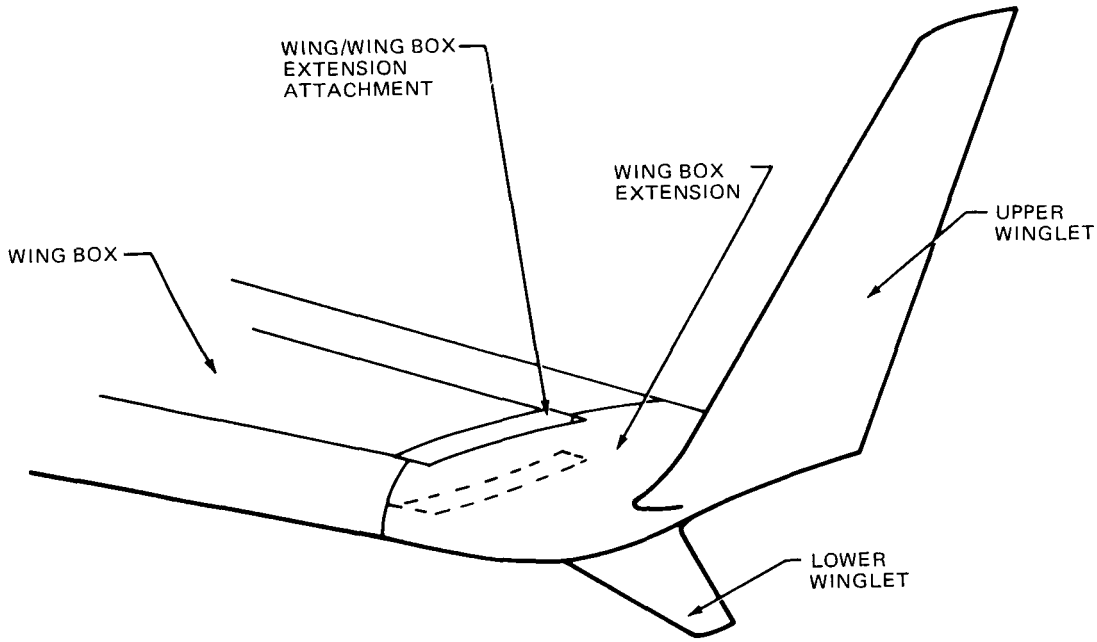

FIGURE 39. WINGLET INSTALLATION COMPONENTS

Design Analyses

Winglet loads were estimated with a combination of theoretical and wind tunnel data. The resulting forces and moments were then applied to existing aeroelastic models of the wing structure to estimate external loads. In addition, the influence of the winglet on the wing spanwise lift distribution was estimated.

It was determined that the test objectives could be met with aircraft loadings and operational conditions lower than the maximum certified. These limitations minimized the modifications to the wing structure that were to remain with the aircraft on its return to airline service. Normal criteria were used in the winglet design, thus providing substantial margins of safety in the new structure.

Flutter analyses, based on the work of the second program, were made to establish the basis for the tests. The critical flutter mode for the basic DC-10 Series 10 without winglets is a symmetric 3-Hz mode. The winglets were estimated to reduce the flutter speed of this mode. In addition, the winglets introduced a 4-Hz flutter mode. Because of these adverse effects, mass balance was installed in each wing tip to ensure adequate flutter margins for flight testing.

Flight Program Approach

To ensure accuracy in comparison and correlation, back-to-back testing of the baseline and winglet aircraft was conducted in all key areas. The important areas for comparison were performance, stability and control, and loads. The program began with tests of the baseline aircraft, continued with BWL configuration tests, and was completed with RSWL testing. The flight test program is summarized in Figure 40.

	BASELINE	WINGLET	
		BWL	RSWL
PERFORMANCE			
CRUISE	X	X	X
LOW SPEED	X	X	X
STABILITY AND CONTROL	X STEADY SIDESLIP ONLY	X	X STEADY SIDESLIP ONLY
DIAGNOSTIC DATA			
FLOW VISUALIZATION (TUFTS)		X	X
WING DEFLECTION MEASUREMENT (CAMERA)	X	X	X
PRESSURE MEASUREMENTS (WING)	X	X	X
PRESSURE MEASUREMENTS (UPPER WINGLET)		X	X
STRUCTURAL AERODYNAMIC DAMPING		X	X ENVELOPE EXPANSION CHECK ONLY
LOADS MEASUREMENT (DOUGLAS)			
ADDITIONAL PRESSURE MEASUREMENT		X	X
STRAIN GAUGES	X	X	X

FIGURE 40. FLIGHT TEST PROGRAM

Aerodynamics evaluations were made in the following areas:

- Drag improvement at cruise and low speed
- High-speed buffet boundary
- Low-speed stall speeds and characteristics
- High- and low-speed stability and control characteristics.

Structural and aerodynamic damping (flutter) tests were conducted with the BWL at the minimum fuel state for performance testing and at the flutter-critical state. Specific measurements of frequency and damping were made using accelerometers.

Loads measurement testing was performed to determine the impact of the winglet on wing loads, and the winglet load itself. In addition, the flight loads were monitored for potentially critical maneuvers.

The flight instrumentation consisted of the existing (production) air data computer (ADC), an additional flight test ADC and inertial navigation system, onboard monitoring equipment including a computer, pressure orifices and strain gauges, accelerometers, and visual aids. Owing to the back-to-back nature of the performance test, thrust-instrumented and calibrated engines were not required. However, air data and engine parameters were carefully measured.

Flight Test Program

The baseline flight test program was conducted from Long Beach, and was primarily devoted to establishing the basis for cruise and low-speed performance.

The BWL test phase began with a general handling and envelope expansion flight. The envelope expansion and structural and aerodynamic damping tests were conducted in operations from Edwards Air Force Base. Chase plane support of this phase was provided by the NASA Dryden Flight Research Center. The subsequent test program was conducted from the Douglas test facility at Yuma, Arizona. During the first flight, low-speed buffet was encountered. As a result, development activity was introduced into the program aimed at identifying and resolving the problem.

Upon completion of the BWL phase, the upper winglet span was reduced for the RSWL testing. Owing to the results and quantity of data obtained in the preceding phase, the previously planned envelope expansion test was eliminated. For the same reason, other changes in the original plans were made. In particular, a test was added to measure the effect of drooping the outboard ailerons.

BWL Test Configurations

All the configurations tested in the BWL phase, including those added in the development activity, are described in Figure 41. In this figure, Configuration 1 is the original BWL, Configuration 2 is Configuration 1 with the Krueger flap fitted, and Configuration 3 is Configuration 2 with the lower winglet removed. A description of the remaining configurations in Figure 41 follows:

- Configurations 4 and 5: Configuration 3 with Vortilet No. 1, Krueger flap angle adjustments being applied in the latter case. The term "vortilet" was coined to describe an upper winglet dorsal fin originating near the wing-tip leading edge and extending to a point on the winglet leading edge.
- Configurations 6 and 8: Configuration 3 with the Krueger flap extended to the winglet root.
- Configuration 7: Configuration 8 with the lower winglet installed.

CONFIG NO.	1	2	3	4, 5	6, 8	7	9	10	11	12
PHYSICAL APPEARANCE			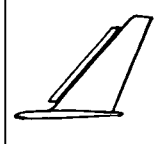	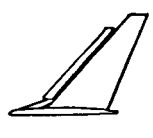	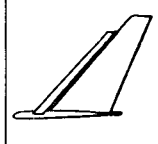	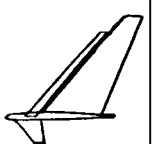				
DESCRIPTION	BASIC UPPER AND LOWER WINGLET AS ORIGINALLY DESIGNED	CONFIGURATION NUMBER 1 WITH KRUEGER FLAP ATTACHED TO UPPER WINGLET WITH 50-DEGREE DEFLECTION	CONFIGURATION NUMBER 2 WITH LOWER WINGLET REMOVED	CONFIGURATION NUMBER 3 WITH VORTILET 1 INSTALLED. VORTILET STARTED AT AFT END OF WING TIP LIGHT AND ENDED AT LOWER END OF KRUEGER FLAP KRUEGER FLAP DEFLECTION CONFIG NO. LH RH 4 50 50 5 45 40	BASIC UPPER WINGLET WITH KRUEGER FLAP EXTENDED TO WING TIP KRUEGER FLAP DEFLECTION CONFIG NO. LH RH 6 45 40 8 40 40	BASIC UPPER WINGLET WITH KRUEGER FLAP EXTENDED TO WING TIP AND DEFLECTED 40 DEGREES BASIC LOWER WINGLET INSTALLED	BASIC UPPER WINGLET WITHOUT LOWER WINGLET OR LEADING EDGE DEVICE	LARGE VORTILET 2 INSTALLED WHICH EXTENDED FROM AFT EDGE OF WING TIP LIGHT TO UPPER WINGLET LEADING EDGE AT ABOUT 37 PERCENT SPAN. MODIFIED (DROOPED LEADING EDGE) AIRFOIL ABOVE VORTILET 2. BASIC LOWER WINGLET INSTALLED	CONFIGURATION NUMBER 10 WITHOUT LOWER WINGLET	CONFIGURATION NUMBER 10 WITH MODIFIED AIRFOIL REMOVED AND KRUEGER FLAP INSTALLED ABOVE VORTILET 2

FIGURE 41. CONFIGURATION IDENTIFICATION FOR BASIC WINGLET FLIGHT PROGRAM

- Configuration 9: Configuration 1 without the lower winglet.
- Configuration 10: Configuration 1 with Vortilet No. 2 and a modified upper winglet airfoil (Mod 6). Vortilet No. 2 extends to a point on the upper winglet further outboard on its span than on Vortilet No. 1.
- Configuration 11: Configuration 10 without the lower winglet.
- Configuration 12: Configuration 10 with Mod 6 removed and the Krueger flap installed above the vortilet.

As the program progressed, it became clear that the eventual configuration should attempt to balance or resolve two aspects of the original BWL which were in apparent conflict — that the lower winglet was beneficial in improving cruise performance and that the lower winglet adversely contributed to a low-speed buffet problem.

BWL Results

Flutter — Frequency and damping data from the Configuration 1 critical condition flutter tests are shown in Figures 42 and 43 for the 3-Hz and 4.5-Hz modes, respectively. The frequency and damping of both modes are relatively constant over the test speed range. The predicted subcritical frequencies closely matched the measured frequencies.

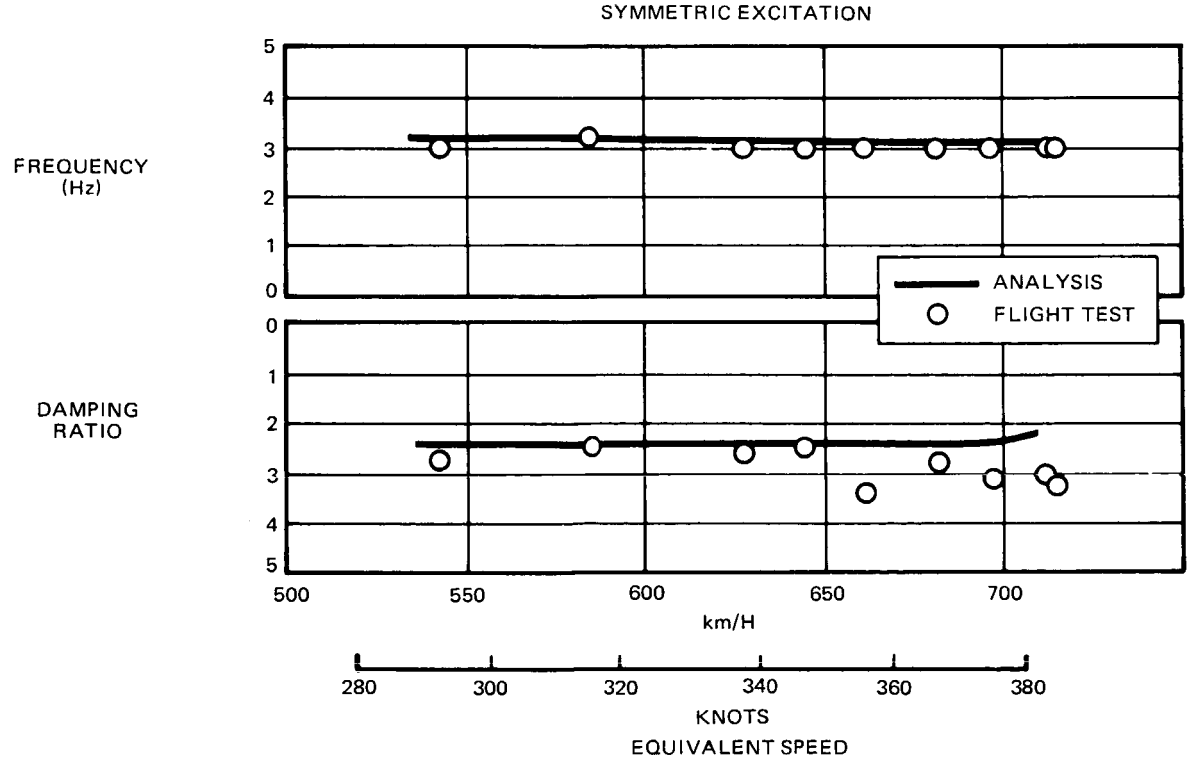

FIGURE 42. FREQUENCY AND DAMPING CHARACTERISTICS – 3 Hz MODE

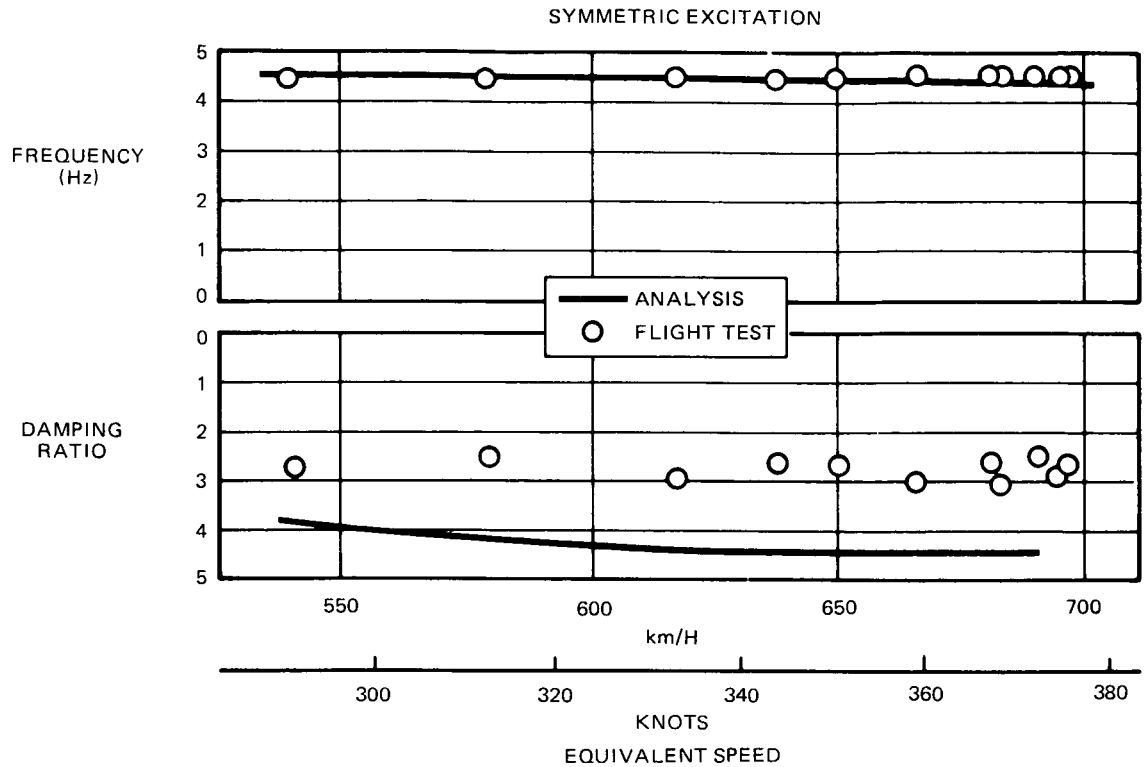

FIGURE 43. FREQUENCY AND DAMPING CHARACTERISTICS – 4.5 Hz MODE

Low-Speed Buffet – During the flight test with Configuration 1, winglet flow separation and consequently objectionable buffeting occurred during the critical takeoff conditions of 1.2 V_{MIN}. The buffet was characterized by a strong vertical bounce component that would make the configuration uncertifiable, according to the pilot. The flow separation patterns observed were similar to those obtained in the wind tunnel tests, except that the separation occurred at higher lift coefficients in the wind tunnel (speeds less than 1.2 V_{MIN}). As a result of these findings, an extensive effort was undertaken to find a configuration with acceptable buffet characteristics.

Figure 44 provides a summary and evaluation of the configurations with the buffet and flow separation observed. The figure includes the pilot's comments on the buffet levels for the speed condition corresponding to an all-engine takeoff (1.35 V_{MIN}) and an engine-out takeoff (1.2 V_{MIN}). The figure indicates the flow visualization observed on the suction side of the upper and lower winglets, the peak-to-peak acceleration measured at the pilot's seat, and the presence of the objectionable vertical bounce component in the buffet.

To eliminate the buffet problem, an investigation was conducted of configuration modifications intended to relieve the loading at the leading edge and at the winglet root. From the first results, it was also clear that separated flow from the lower winglet was migrating into the root section of the upper winglet. One attempt at preventing this migration involved the vortilet (Configuration 6), but this was not entirely successful. Recognizing the importance of the root

FLAP – 15 DEGREES SLAT – TAKEOFF

CONFIGURATION NUMBER / CONFIGURATION DESCRIPTION	1 BASIC UPPER AND LOWER WL	2 UPPER AND LOWER WL WITH FCK	3 UPPER WL WITH FCK	4 UPPER WL AND FCK AND VORTI	6 UPPER WL AND FCK EXT	7 UPPER AND LOWER WL AND FCK EXT	9 UPPER WL ONLY	10 VORT 2 WITH MOD 6 AND LOWER WL	11 VORT 2 WITH MOD 6 W/O LOWER WL	12 VORT 2 WITH FCK AND LOWER WL
BUFFET AT 1.35 V_{MIN}	LIGHT	LIGHT	VERY LIGHT	VERY LIGHT	NONE	PERCEPTIBLE	PERCEPTIBLE	LIGHT	LIGHT	LIGHT
BUFFET AT 1.20 V_{MIN}	MODERATE	MODERATE	MODERATE	MODERATE	LIGHT	MODERATE	LIGHT	MODERATE	MODERATE	MODERATE
VERTICAL BOUNCE AT 1.20 V_{MIN}	YES	YES	YES	YES	BARELY	YES	JUST BARELY	BARELY	BARELY	NO (LATERAL COMPONENT)
WING FLOW VISUALIZATION	SEPARATED	SEPARATED	SEPARATED	ATTACHED	ATTACHED	SEPARATED	ATTACHED	ATTACHED	ATTACHED	ATTACHED
WINGLET FLOW VISUALIZATION AT 1.2 V_{MIN}					 INTERMITTENT SEPARATION	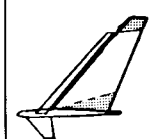 NO CHASE	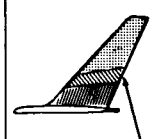 INTERMITTENT SEPARATION	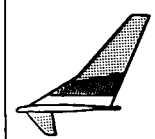	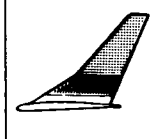	 NO CHASE
PILOT SEAT ACCELERATION AT 1.2 V_{MIN} (PEAK TO PEAK)	0.080	0.200	0.175	0.170	0.045	0.150	0.060	INSTRUMENTATION INOPERATIVE	INSTRUMENTATION INOPERATIVE	0.125

ATTACHED STREAMWISE FLOW
SEPARATED FLOW
SPANWISE FLOW
INTERMITTENT SEPARATION

FLOW VISUALIZATION SHOWN ON THE INBOARD SURFACE OF UPPER WINGLET AND OUTBOARD SURFACE OF LOWER WINGLET

FIGURE 44. SUMMARY OF BWL LOW-SPEED BUFFET CHARACTERISTICS

region, it was decided to remove the vortilet and extend the leading-edge device down to the wing. This resulted in an acceptable configuration (No. 6). The flow was basically attached except for the small region at the tip which was not protected since the Krueger was not full span. The buffet intensity was significantly reduced, with the vertical bounce component barely perceptible. It was clear that the Krueger flap allowed the winglet to continue to load up as the airplane lift increased to the V_2 condition.

Because of the importance of the lower winglet to cruise performance, it was reinstalled and the resulting configuration (No. 7) tested. Apparently, the problem of the migration of the separated flow on the lower winglet into the upper winglet root region reoccurred because this configuration proved unacceptable. Configuration 9, having no Krueger flap or lower winglet, had acceptable buffet characteristics but exhibited substantial flow separation and therefore a reduced level of drag improvement.

None of the remaining development configurations had acceptable buffet characteristics.

Low-Speed Drag – Figure 45 illustrates the flight-tested low-speed drag improvement for the BWL with extended Krueger leading-edge flap on and lower winglet removed (Configuration 6). The data are relative to the baseline levels, and are also compared with wind tunnel results. At the lift coefficient representative of engine-out climb speed (V_2), the winglet drag improvement is 5.7 percent for both flap deflections, equaling or exceeding pretest estimates based on wind tunnel data.

Cruise Performance

Figure 46 summarizes the cruise drag improvement for the BWL, given as the percent drag improvement over to the baseline airplane. The improvement is shown with and without the lower winglet installed. Also shown is the wind tunnel prediction based on Reference 13, but adjusted for wing aeroelastic effects. With the lower winglet installed, the figure shows that the flight-measured level is about 0.4 percent less than the prediction at the highest lift coefficient of DC-10 Series 10 operation ($C_L = 0.5$). At lower lift coefficients, the discrepancy was greater, suggesting a significant parasite drag penalty at zero lift. At $C_L = 0.47$, a typical cruise number, the measured improvement is 2.5 percent, 75 percent of the predicted improvement of 3.4 percent. The compressible and incompressible data are in good agreement. It should be noted that correlation between flight and wind tunnel results in the fourth phase (discussed later) was much better than with the second phase results.

It was evident, as shown in Figure 46, that the removal of the lower winglet resulted in a significant compressibility penalty, 1 percent at typical cruise C_L. The effect measured in the wind tunnel was 0.5 percent at compressible and incompressible Mach numbers.

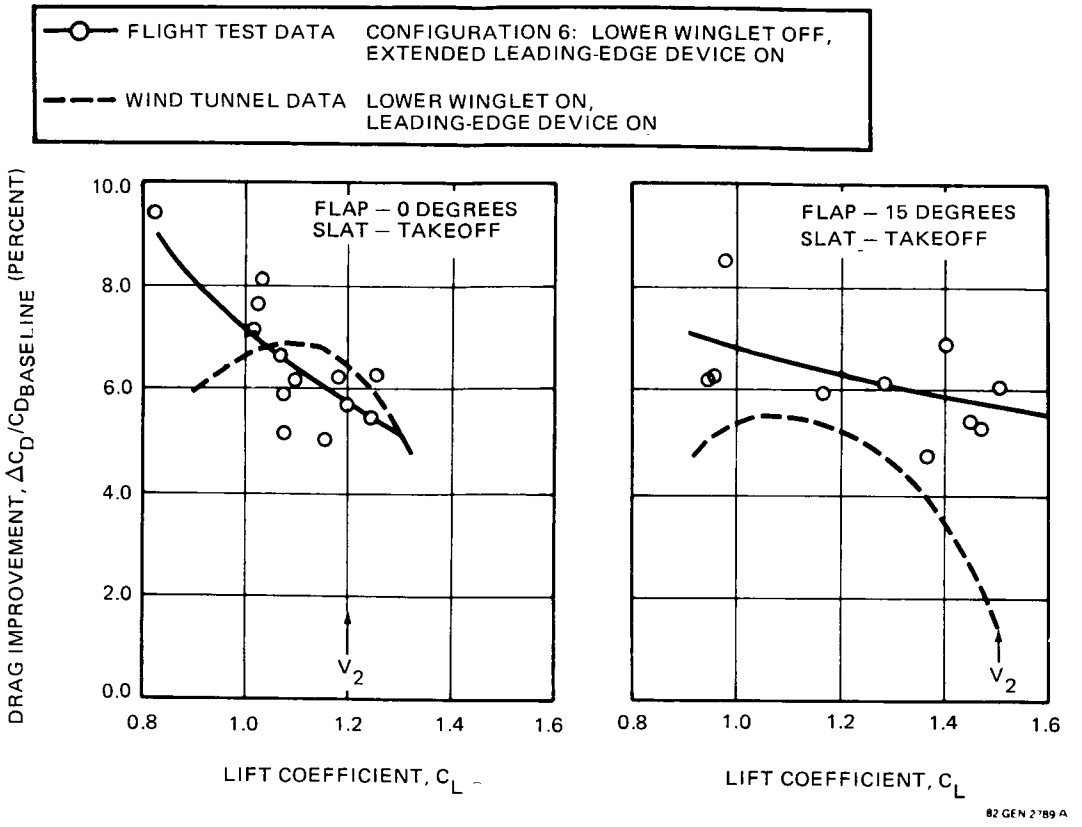

FIGURE 45. LOW-SPEED DRAG IMPROVEMENT – BASIC WINGLET

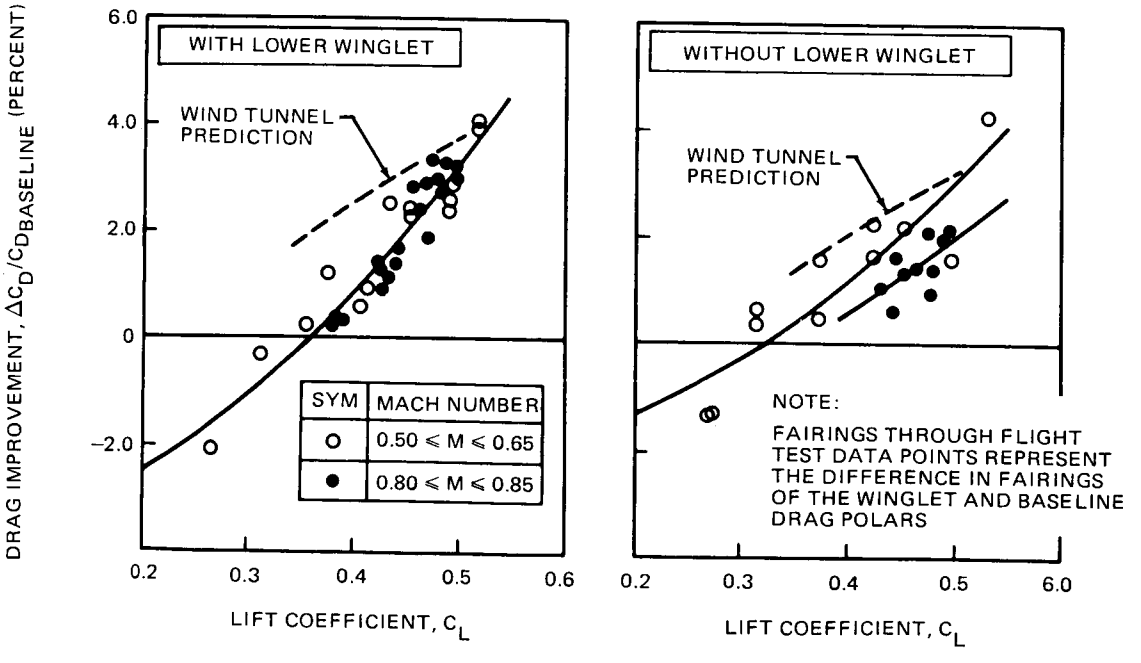

FIGURE 46. CRUISE DRAG IMPROVEMENT – BASIC WINGLET

The flow quality was observed to be excellent. Wing deflection and wing tip loading, which may affect the value of cruise drag reduction due to winglets, was shown to be in agreement with preflight estimates. A significantly strong shock wave was observed on the upper winglet, particularly on the outer span at high-lift coefficient, where the drag reduction was nearest to the predicted value. The stronger shock wave on the outer panel was also evident at the lower lift coefficients. These results suggested that at least part of the performance shortfall might be related to compressibility effects but that the trend with lift coefficients was not. However, the postflight wind tunnel test evaluation, included later in this report, suggests that the more likely explanation was that the winglet was loaded beyond its optimum value.

Stall Speeds and Characteristics, Cruise Buffet, and Stability and Control Characteristics – In all these areas, it was concluded that the effect of winglets was very small or negligible.

Loads Measurement Results – The results indicate that:

- The measured winglet normal force levels were approximately at the expected levels.
- The variation of winglet normal force coefficient with aircraft angle of attack was in agreement with the prediction.
- The effects of aeroelasticity were clearly evident.
- The measured increment of wing bending moment was generally as predicted. The horizontal bending effect resulting from the inboard acting winglet load and wing sweepback was also evident.
- Measured aileron loads were close to the predicted level.

RSWL Test Configurations

All the RSWL configurations tested are shown in Figure 47. As in the BWL phase, a leading edge device was tested at low speed. Configurations without such a device were tested both in the low-speed and high-speed regimes. The features of the configurations in the figure are as follows:

- Configuration 13: Upper Krueger flap extended root to tip, no lower winglet.
- Configuration 14: Upper winglet only.
- Configuration 15: Configuration 14 with lower winglet.
- Configuration 16: Configuration 13 with lower winglet.
- Configuration 17: Configuration 13 with modified (extended chord) lower winglet. This winglet had a chord extension of 80 percent of the local chord of the basic original lower

CONFIGURATION NUMBER	13	14	15	16	17	18	19
PHYSICAL APPEARANCE	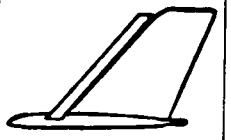	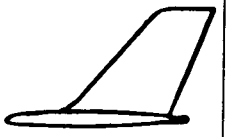	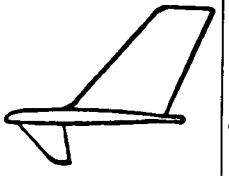	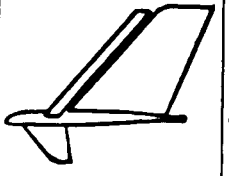	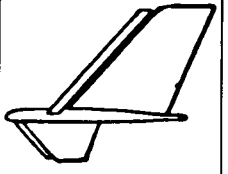	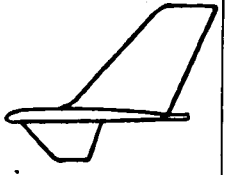	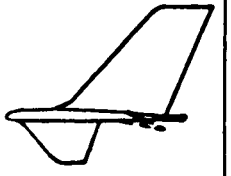
DESCRIPTION	REDUCED-SPAN WINGLET WITH KRUEGER FLAP INSTALLED WITH EXTENSION TO WING TIP. KRUEGER FLAP DEFLECTION WAS 40 DEGREES	REDUCED-SPAN UPPER WINGLET WITHOUT LOWER WINGLET	REDUCED-SPAN UPPER WINGLET WITH BASIC LOWER WINGLET INSTALLED	CONFIGURATION NUMBER 13 WITH BASIC LOWER WINGLET INSTALLED	CONFIGURATION NUMBER 13 WITH 80-PERCENT EXTENDED CHORD LOWER WINGLET INSTALLED. LOWER WINGLET HAD SEALED KRUEGER FLAP INSTALLED	REDUCED-SPAN UPPER WINGLET WITH 80-PERCENT EXTENDED CHORD LOWER WINGLET INSTALLED. (NO LEADING EDGE DEVICES ON UPPER OR LOWER WINGLET)	CONFIGURATION NUMBER 18 WITH OUTBOARD AILERONS DROOPED 3.0 DEGREES

FIGURE 47. CONFIGURATION IDENTIFICATION FOR REDUCED-SPAN WINGLET FLIGHT PROGRAM

winglet. The extension was made aft from the leading edge. The leading edge shape forward of the front spar was retained.

- Configuration 18: Configuration 17 without leading edge devices.
- Configuration 19: Configuration 18 with outboard ailerons drooped 3 degrees (measured in the streamwise direction) from the basic rigged position.

RSWL Results

Low-Speed Buffet – Figure 48 summarizes the low-speed buffet results. Configuration 13, the first tested, was directly related to the most promising BWL configuration. Like this BWL, this configuration exhibited acceptable buffet characteristics. All of the remaining configurations tested (except Configuration 16 which was marginal) were found to be acceptable. It was clear that some combination of the lower aspect ratio of the reduced-span winglet and its structural response to the separated flow was having a significantly favorable effect on buffet characteristics.

Configuration 17, which employed the extended chord lower winglet with a leading edge device, did not prevent flow separation on the lower winglet at V_2 conditions. However, the flow on the leading edge device itself stayed attached, thus providing significant leading edge suction. In addition, the wake from the separated flow did not go over the wing.

Low-Speed Drag – Figure 49 shows the low-speed drag improvement for Configuration 13 (extended upper leading-edge devices, no lower winglet), Configuration 14 (Configuration 13 with no leading-edge devices), and Configuration 17 (Configuration 13 with extended-chord lower winglet and leading-edge devices on both winglets). Removal of the upper winglet leading-edge device resulted in more than a 50-percent loss in performance improvement at V_2 conditions. The low-speed drag improvement at V_2 for the RSWL with the lower winglet was 5.9 percent.

Cruise Performance – The cruise drag benefit of the initial RSWL configurations is shown in Figure 50. With the lower winglet installed (Configuration 15) and at the typical cruise lift coefficient, the improvement was about 2 percent. This is only 0.5 percent less than the BWL while the preflight predicted difference was 1 percent. The slope of the flight-measured improvement with lift coefficient was closer to the prediction than it was for the BWL. The detrimental compressible effect due to removal of the lower winglet was of similar magnitude to the effect of the BWL.

Two major configuration changes were evaluated during this phase, the extended-chord lower winglet (Configuration 18) for low speed and the use of drooped outboard ailerons (Configuration 19) for enhanced cruise drag reduction. The use of drooped outboard ailerons had been studied

FLAP – 15 DEGREES SLAT – TAKEOFF

CONFIGURATION NUMBER / CONFIGURATION DESCRIPTION	13 UPPER WL AND FCK EXT	14 UPPER WL	15 UPPER WL WITH LOWER WL	16 UPPER WL WITH FCK EXT AND LOWER WL	17 UPPER WL WITH FCK EXT AND LOWER EXT WL WITH FCK	18 UPPER WL AND LOWER EXT WL	19 UPPER WL AND LOWER EXT WL AND DROOPED AILERON
BUFFET AT 1.35 V_{MIN}	NONE	NONE	PERCEPTIBLE	LIGHT	NONE	VERY LIGHT	PERCEPTIBLE
BUFFET AT 1.2 V_{MIN}	PERCEPTIBLE	LIGHT	LIGHT	MODERATE	BARELY PERCEPTIBLE	LIGHT	LIGHT
VERTICAL BOUNCE AT 1.2 V_{MIN}	NO	NO	NO	NO	NO	NO	NO
WING FLOW VISUALIZATION WINGLET FLOW VISUALIZATION AT 1.2 V_{MIN}	ATTACHED 	ATTACHED 	NO FLOW VISUALIZATION 	ATTACHED 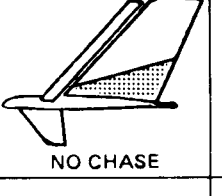 NO CHASE	ATTACHED 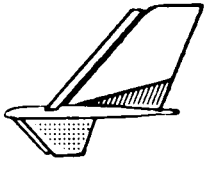	SEPARATED 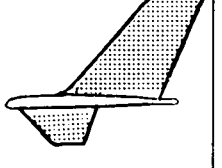	NO FLOW VISUALIZATION 
PILOT SEAT ACCELERATION AT 1.2 V_{MIN} (PEAK-TO-PEAK)	0.03	0.04	0.04	0.07	0.04	0.05	0.06

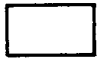
ATTACHED STREAMWISE FLOW


SEPARATED FLOW


SPANWISE FLOW

FLOW VISUALIZATION SHOWN ON THE INBOARD SURFACE OF UPPER WINGLET AND OUTBOARD SURFACE OF LOWER WINGLET

FIGURE 48. SUMMARY OF LOW-SPEED BUFFET CHARACTERISTICS – REDUCED-SPAN WINGLET

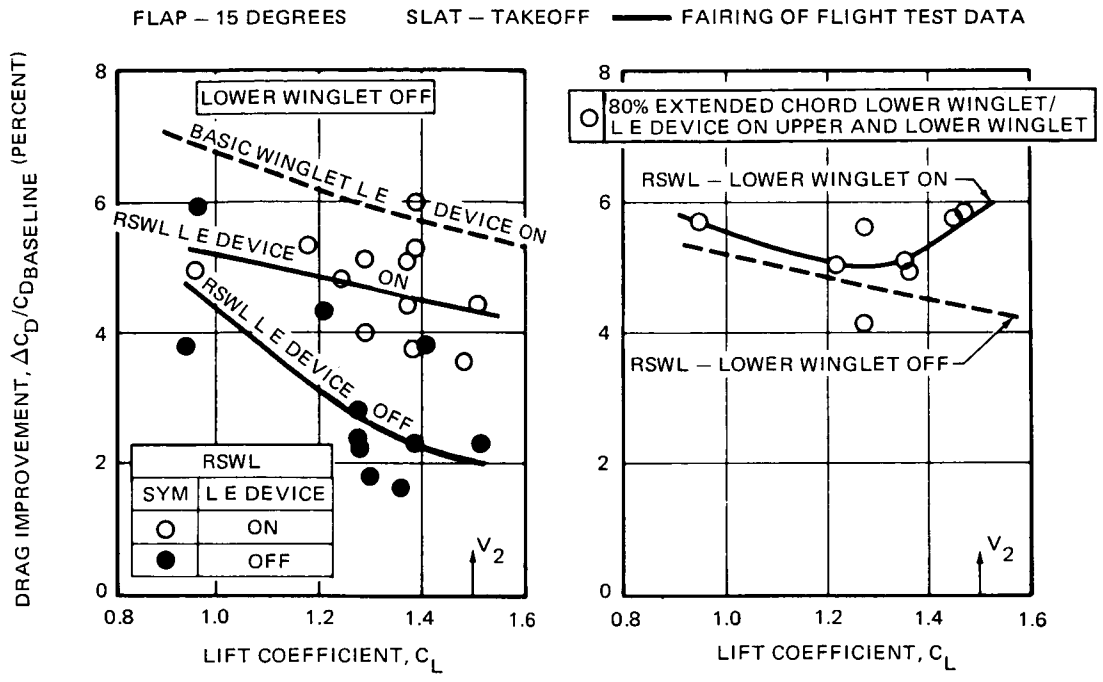

FIGURE 49. LOW-SPEED DRAG IMPROVEMENT – REDUCED-SPAN WINGLET

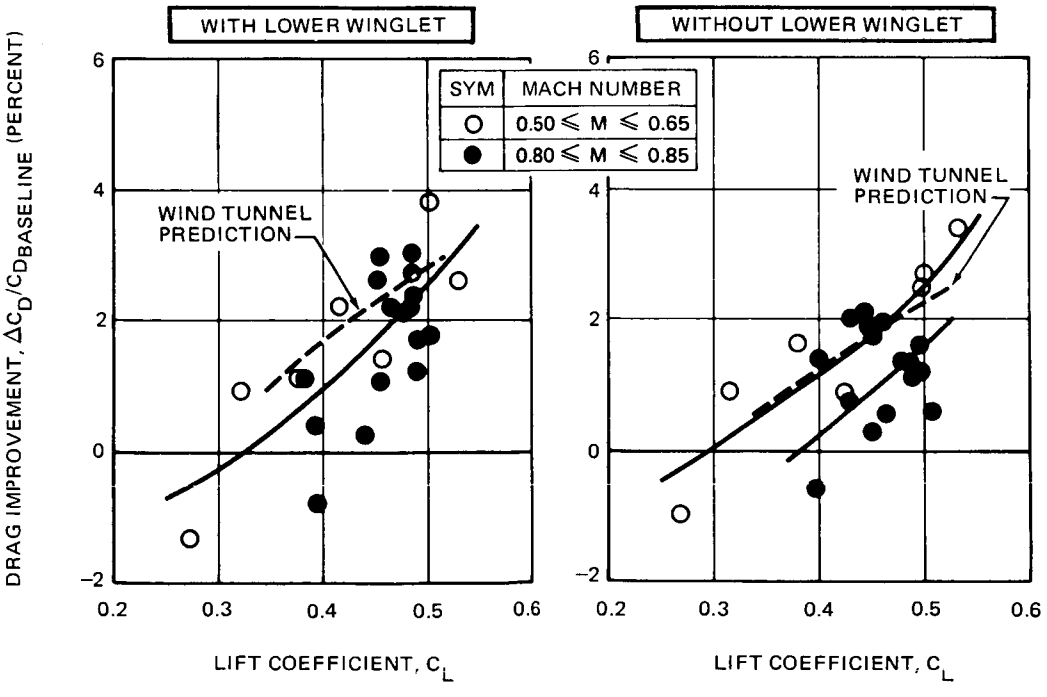

FIGURE 50. CRUISE DRAG IMPROVEMENT – REDUCED-SPAN WINGLET

analytically prior to the flight program. Compared with Configuration 18, an improvement of 1 percent was obtained from drooping the ailerons. This was in agreement with the preflight estimate for this design. Pressure data showed that both the winglet and the wing tip were loaded more with the aileron droop. The benefit arises from these increases in loading. Configuration 19 was the best for improving cruise drag. At $C_L = 0.47$, the measured drag improvement was 2.8 percent. If the extended-chord lower winglet, which showed a small penalty by itself, were replaced with the original lower winglet, a configuration with a nominal cruise drag improvement of about 3 percent would be expected.

Impact of Flight Evaluation Results on Operational Performance

The DC-10 Series 10 used as a basis for the evaluation carries a payload of 26,943 kg (59,400 lb) which represents a full load of 297 passengers and baggage. Its maximum takeoff gross weight is 195,045 kg (430,000 lb), and it is powered by three General Electric CF6-6D engines rated at 177,9 kN (40,000 lb) sea level static thrust.

The winglet configurations used on the derivative version were the BWL, the RSWL, and the RSWL with aileron droop. Each had upper and lower winglets with winglet leading-edge devices deployed for takeoff and landing. The original basic planform without chord extensions was used for the lower winglet. The effects of the winglet installation on aircraft characteristics and performance are summarized in Figure 51.

DRAG AND WEIGHT CHANGES	BASIC WINGLET	REDUCED-SPAN WINGLET	REDUCED-SPAN WINGLET PLUS AILERON DROOP
CRUISE DRAG IMPROVEMENT = PERCENT	2.5	2.0	3.0
OPERATOR EMPTY WEIGHT = kg (LB)	1,340 (2,955)	633 (1,396)	745 (1,643)
LOW SPEED DRAG IMPROVEMENT = PERCENT	6.8	5.8	5.8
AIRCRAFT PERFORMANCE CHANGES			
FUEL BURNED = PERCENT			
AT 3,704 km (2,000 N MI)	−1.8	−1.7	−2.7
AT 6,112 km (3,300 N MI)	−2.1	−2.0	−3.0
RANGE = km (N MI)	−9 (−5)	+59 (+32)	+113 (+61)
TAKEOFF FIELD LENGTH = m (FT) AT MTOGW	−198 (−650)	−162 (−530)	−162 (−530)

FIGURE 51. EFFECT OF WINGLETS ON DC-10 SERIES 10 PERFORMANCE CHARACTERISTICS

The fuel burn improvement estimation, utilizing data from the performance and loads tests, resulted in the same improvement for the basic and reduced-span winglets, nearly 3 percent. While the basic winglet drag improvement was higher than for the reduced-span winglet, the higher increase in empty weight almost negated the added drag benefit.

Conclusions from the Winglet Flight Evaluation

The principal conclusions of the DC-10 winglet flight evaluation are:

1. The drag reduction at typical cruise operating conditions for the BWL was 2.5 percent and 2.0 percent for the RSWL. This was about 75 percent of the level predicted from the preflight wind tunnel test data. Drooping the outboard ailerons 3 degrees resulted in an additional cruise drag reduction of 1 percent (tested only on the reduced-span winglet).
2. Removal of the lower winglet significantly detracted from the cruise performance benefit, reducing it by about 1 percent.
3. Flow separation was experienced on the winglets in the low-speed high-lift configuration, resulting in unacceptable aircraft buffet for some BWL configurations. A winglet leading-edge device and removal of the lower winglet resulted in an acceptable configuration for the BWL. The low-speed drag reduction for this configuration exceeded 5 percent, which was better than expected. For the reduced-span winglet, acceptable low-speed buffet characteristics were achieved with or without the winglet leading-edge devices or the lower winglet. The low-speed drag improvement was nearly 6 percent with the leading-edge devices installed. Removal of the leading-edge devices and the lower winglet reduced the low-speed drag improvement to 2 percent.
4. Stability and control characteristics, minimum stall speeds, and the high-speed buffet boundary were basically unchanged by the winglets.
5. The loads measurements were in good agreement with preflight estimates.
6. The flutter test did not reveal any unforeseen behavior, and the data showed good agreement with ground vibration test and analysis data.
7. Application of the reduced-span winglet with aileron droop to a production DC-10 Series 10 is estimated to yield a 3-percent reduction in fuel burned at maximum range.

WINGLET MODEL TESTING – POSTFLIGHT EVALUATION

Effect of Wing Trailing-Edge Modifications on the High-Speed Stability and Control Characteristics of the DC-10 with Winglets

Configuration and Results – The winglet flight evaluation showed that a significant drag reduction in cruise resulted from a small deflection, or "droop," of the outboard aileron, in the presence of the winglet. Other Douglas studies have indicated that drag may be reduced by drooping the entire outboard-wing trailing edge or by adding a small amount of aft camber. Such modifications cause an increased loading of the outboard wing panel, and therefore concern exists that the aircraft maneuvering stability may be degraded.

In this fourth phase program, the high-speed maneuvering characteristics were evaluated with a 3.25-percent scale DC-10 Series 10 model tested in the NASA Ames Research Center 11-Foot Wind Tunnel. The reduced span winglets of the flight evaluation, together with the basic lower winglets, were used. The trailing-edge modifications include 3 degrees of outboard aileron droop, 3 degrees of outboard wing trailing-edge droop, and several lengths of trailing-edge camber. Trailing-edge droop was applied outboard from the trailing-edge aerodynamic break (Figure 52). The trailing-edge camber was applied over the wing outboard from the

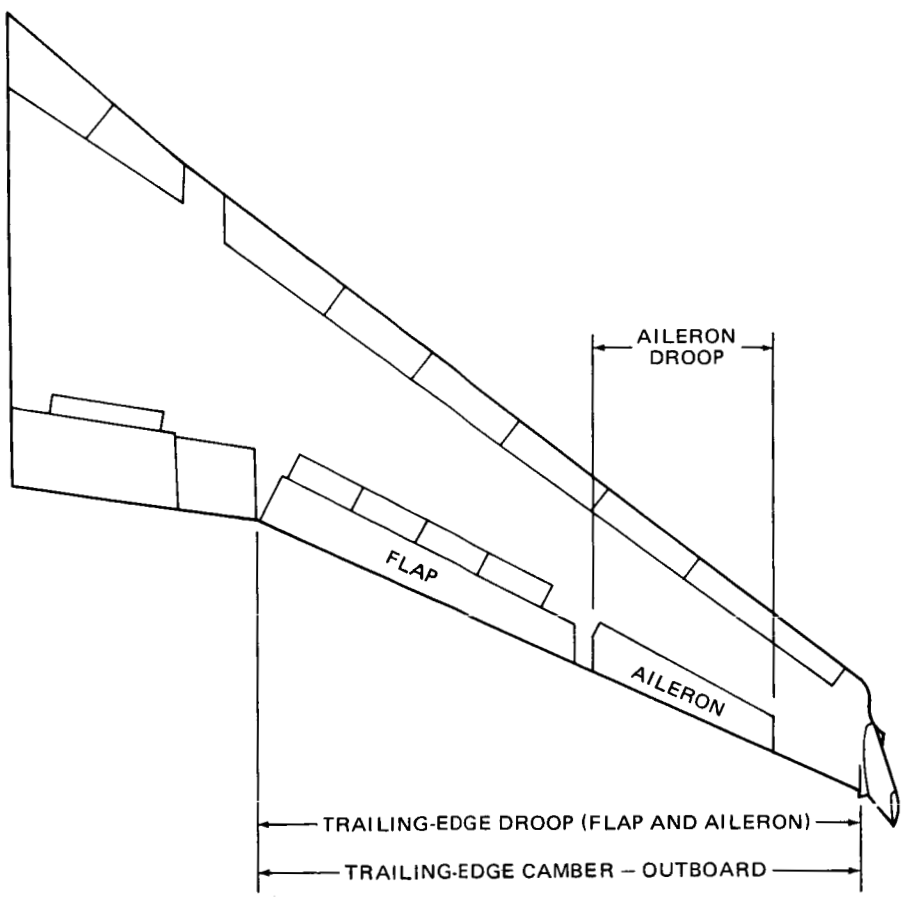

FIGURE 52. WING TRAILING-EDGE TEST CONFIGURATIONS

aerodynamic break over the wing outboard of the midspan of the flap, and over the wing outboard from the flap.

The effect of aileron droop, trailing-edge (flap and aileron) droop, and trailing-edge camber outboard of the planform break is shown in Figure 53. Up to and through buffet onset, the addition of aileron droop had negligible effects on the maneuvering stability, but a mild, positive incremental pitching-moment gradient was exhibited beyond buffet onset. This change can be considered negligible. The addition of trailing-edge droop caused a mild increase in static stability, up to near-buffet onset and a positive incremental pitching-moment gradient beyond buffet onset. This increase can be considered significant. The addition of the trailing-edge camber caused a large increase in static stability up to and through buffet onset and a positive incremental pitching-moment gradient beyond buffet onset. This increase can be considered small. In essence, all modifications improved the maneuvering characteristics of the winglet aircraft in that pitch-up tendencies were postponed to higher load factors than without the modifications. However, beyond buffet onset each modification affected the maneuvering characteristics of the winglet aircraft to some extent, from a negligible change due to the aileron droop to a significant degradation caused by the trailing-edge droop. The results also indicated negligible changes in the dihedral effect (lateral-directional stability) of the aircraft.

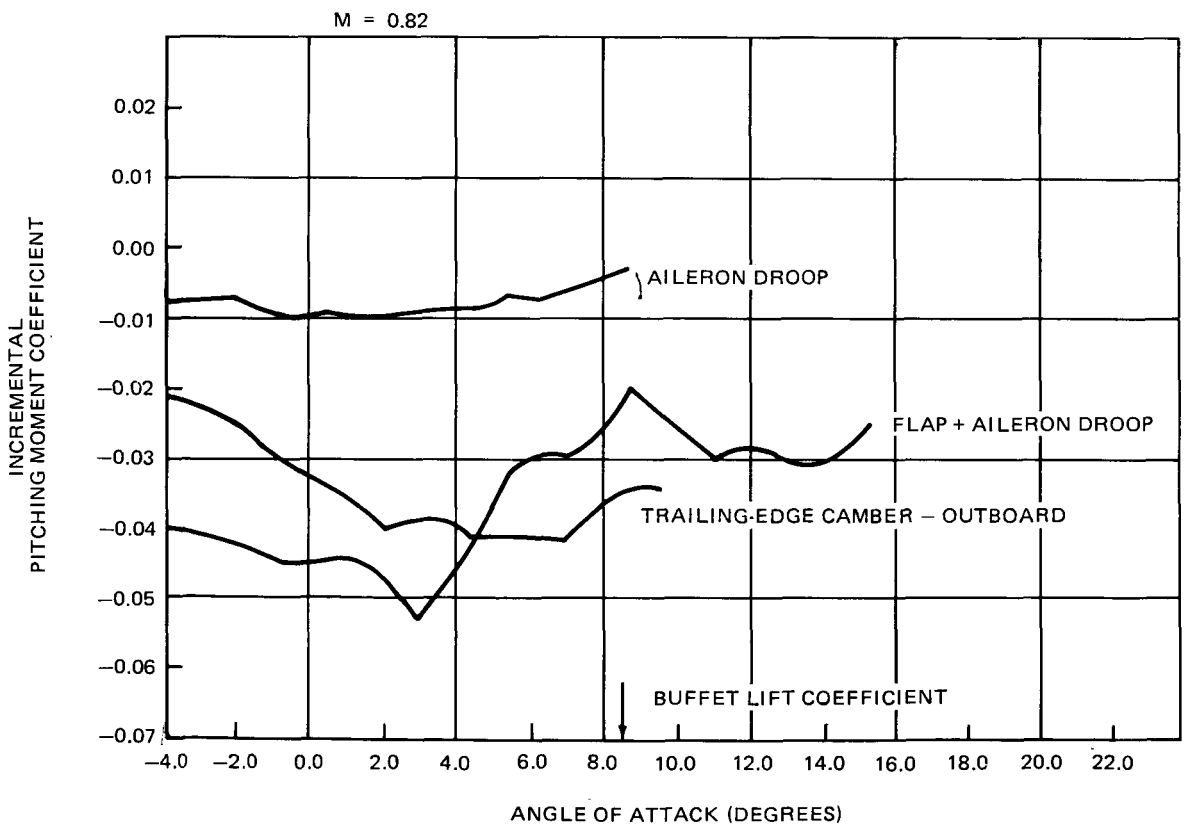

FIGURE 53. EFFECT OF WING TRAILING-EDGE MODIFICATIONS ON PITCHING MOMENT

Low-Speed Tests of the DC-10 Aircraft with Winglet and Wing Modifications

Configuration – The winglet flight evaluation showed that configurations with leading-edge flow separation protection could provide substantially more drag reduction than the basic configuration. However, the Krueger flap simulated in the test was subsequently determined to be difficult to store in the space available. This fourth-phase wind tunnel program was therefore planned to evaluate representations of simple mechanical devices, and also leading-edge modifications with no articulation. This evaluation was preceded by a correlation of model and flight data. Also included in the program was an evaluation of the trailing-edge camber described in the preceding section.

Test configurations were defined through an analytical and design process. (This definition was conducted under Douglas funding.) From flight data, a criterion was established for achieving separation-free flow on the upper winglet. A two-dimensional analysis method for the upper winglet was then established, correlated to flight test data, and used to evaluate candidate upper winglet modifications. A three-dimensional Neumann potential flow model of the aircraft was then used, primarily for evaluation of the lower winglet, since the lack of flight test pressure measurements on this surface prevented the use of a two-dimensional method.

From a consideration of structural and mechanical aspects, a test candidate using articulated leading edges was selected. A sealed Krueger flap was rejected through objections similar to the flight evaluation Krueger. A conventional slat, because of the thinness of the airfoil, was limited to an insufficient deflection angle. Also, it was impractical to install these devices on the lower winglet. The selected design contained a drooped leading edge (DLE) hinged on the lower surface of the winglet at the front spar, actuated by a simple push/pull actuator. The lower winglet could be similarly fitted with a DLE and slaved to the upper winglet actuator.

A leading-edge modification using no articulation was also devised. This modification was based on increasing leading-edge camber and nose radius.

Analysis Method – In general, the flight evaluation pressure data showed that the flow on the upper winglet was always separated from near the leading edge to the trailing edge at V_2 conditions, unless it was protected by the leading-edge Krueger flap, in which case it was always attached. Flow on the lower winglet was always fully separated at V_2 even when provided with leading-edge protection; the lower winglet Krueger flow was, however, attached at the V_2 condition. It was concluded from the flight results that the design which allowed the upper winglet to be attached and well loaded at V_2 would result in significant low-speed drag improvement.

A two-dimensional method for analyzing the upper winglet was developed in order to evaluate a number of alternatives economically. This method used the Halsey code, a Douglas multielement conformal mapping program. Figure 54 compares the predicted performance of the can-

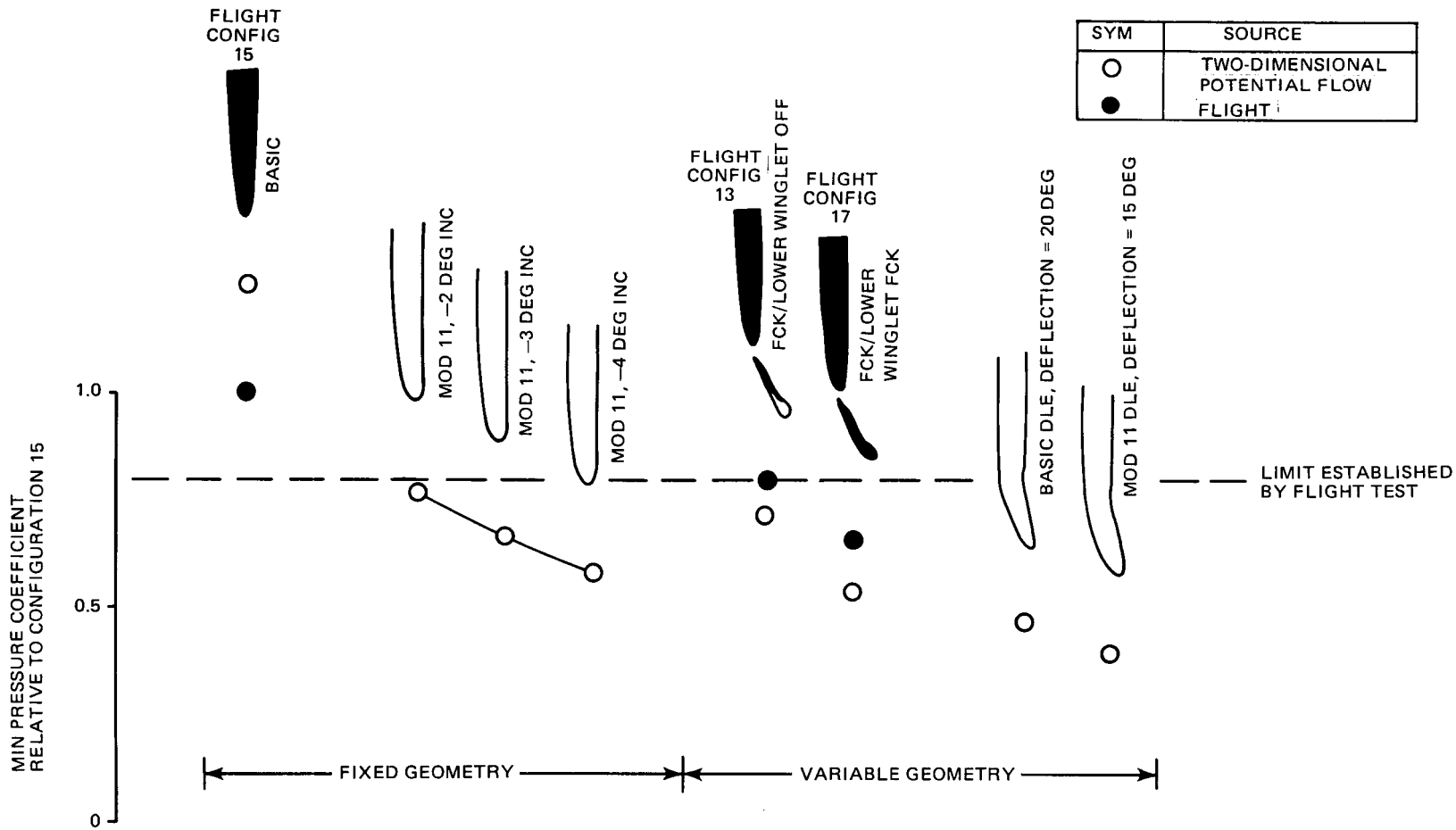

FIGURE 54. WINGLET LEADING-EDGE TWO-DIMENSIONAL STUDY CONFIGURATIONS

didate configurations with flight test data. The aircraft lift coefficient is 1.5 (V_2 for 15-degree flaps). Except as noted in the figure, all configurations included the lower winglet with a clean leading edge. The method resulted in good predictions of the peak pressures for the flight-tested Krueger flap configuration. The selected fixed-geometry design, identified as Mod 11, had the suction peak reduced by slightly more than 20 percent at the nominal winglet incidence. A reduction of incidence further diminished the suction peak. It was established in a separate study that Mod 11 had no compressibility drag penalty in cruise. The DLE variable geometry concept was applied to both the basic and Mod 11 winglet sections. The figure shows the prediction for a DLE with hingeline near the front spar, and a practical deflection of 20 degrees for the basic DLE and 15 degrees for the Mod 11 DLE.

Because no flight test or previous wind tunnel test pressure measurements existed for the lower winglet, and since the use of an analysis method was desirable, a three-dimensional Neumann potential flow geometry of the winglet aircraft was constructed, using the Douglas three-dimensional potential flow program. It was concluded from the analysis that the lower winglet flow attachment by leading-edge modifications of fixed or variable geometry was impractical. This conclusion was consistent with results from the DC-10 flight test program. It was therefore determined that test configurations should be defined to reduce the possibility that the separated wake from the lower winglet could cause premature flow separation on the upper winglet by flowing around the wing tip and into the upper wing/winglet juncture. One alternative moved the lower winglet aft 76 cm (30 inches). The other drooped the nose of the lower winglet to keep the nose region attached. This would create a situation analogous to adding the lower Krueger on the flight test aircraft, which resulted in attached flow on the upper winglet and a significant enhancement of the drag improvement at V_2 conditions.

The selected leading-edge test configurations are shown in Figure 55. The test was conducted in the NASA Ames Research Center 12-foot wind tunnel. A 4.7-percent full-span model of the DC-10 Series 10 aircraft was used.

Results – The trimmed incremental drag coefficient for installing the winglet is plotted against aircraft lift coefficient in Figure 56. Wind tunnel results are compared with flight data for the winglet with no leading-edge device and no lower winglet (Flight Configuration 14), and for the configuration with a leading-edge device on both upper and lower winglets. The model results agree well with the flight data.

Figure 57 compares the wind tunnel and flight visualization for Configuration 14. The correlation is excellent.

Figure 58 summarizes the principal wind tunnel drag improvement results for both the fixed geometry and the simplified variable-geometry configurations. The basic DLE (variable geometry) configurations achieved a performance level approaching that of the unacceptably

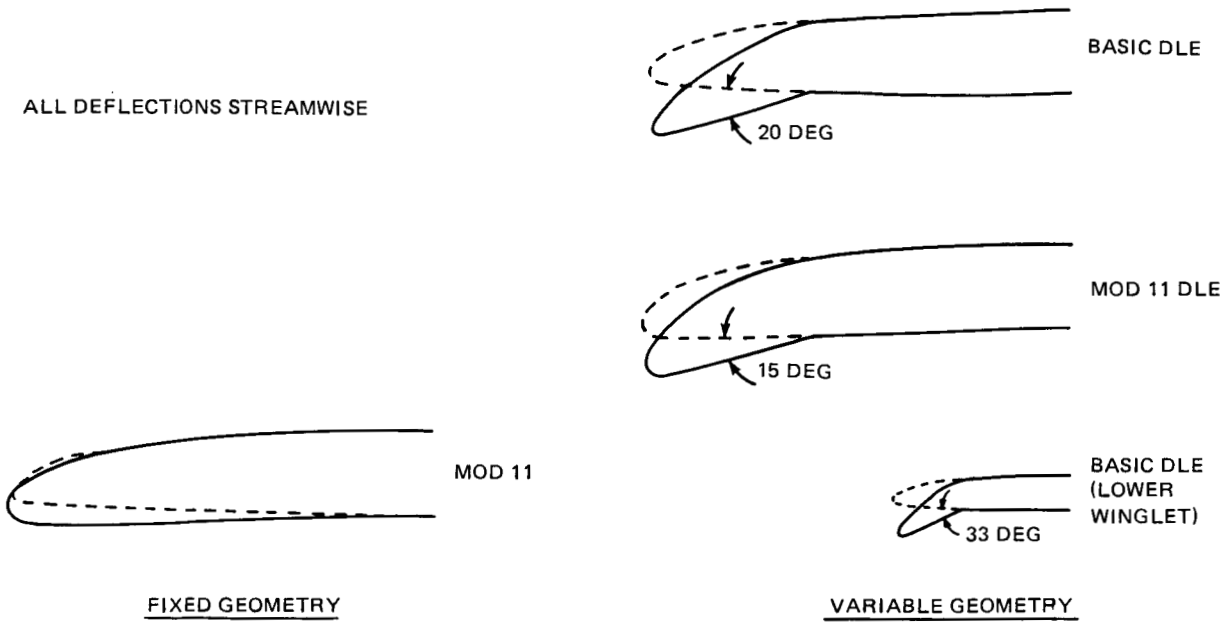

FIGURE 55. WINGLET LEADING-EDGE TEST CONFIGURATIONS

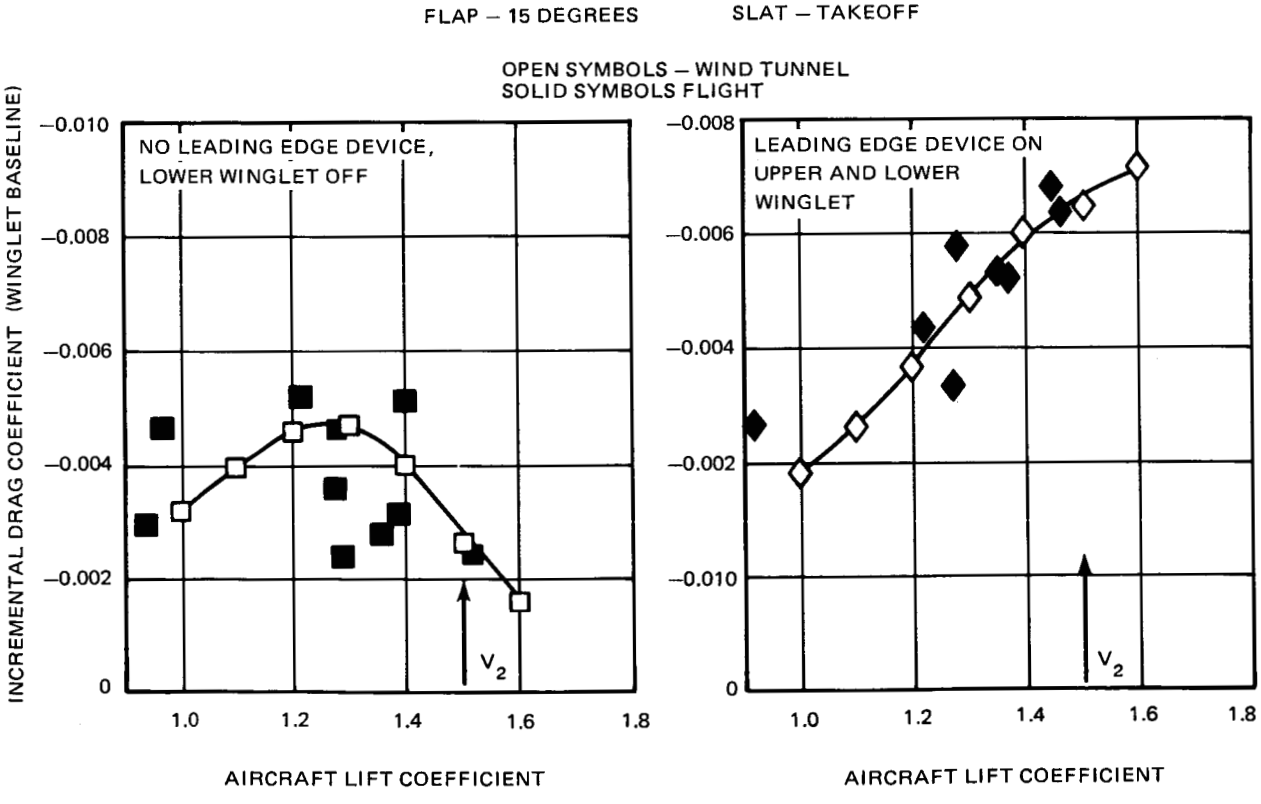

FIGURE 56. CORRELATION OF WINGLET LOW-SPEED DRAG DATA

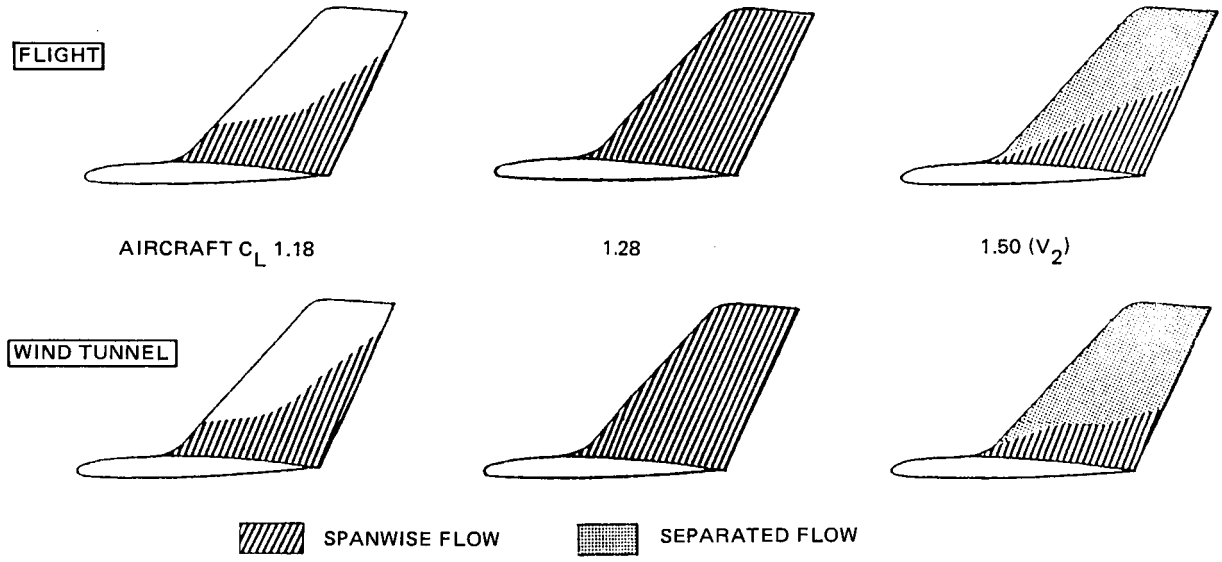

FIGURE 57. FLOW VISUALIZATION – WIND TUNNEL-TO-FLIGHT CORRELATION

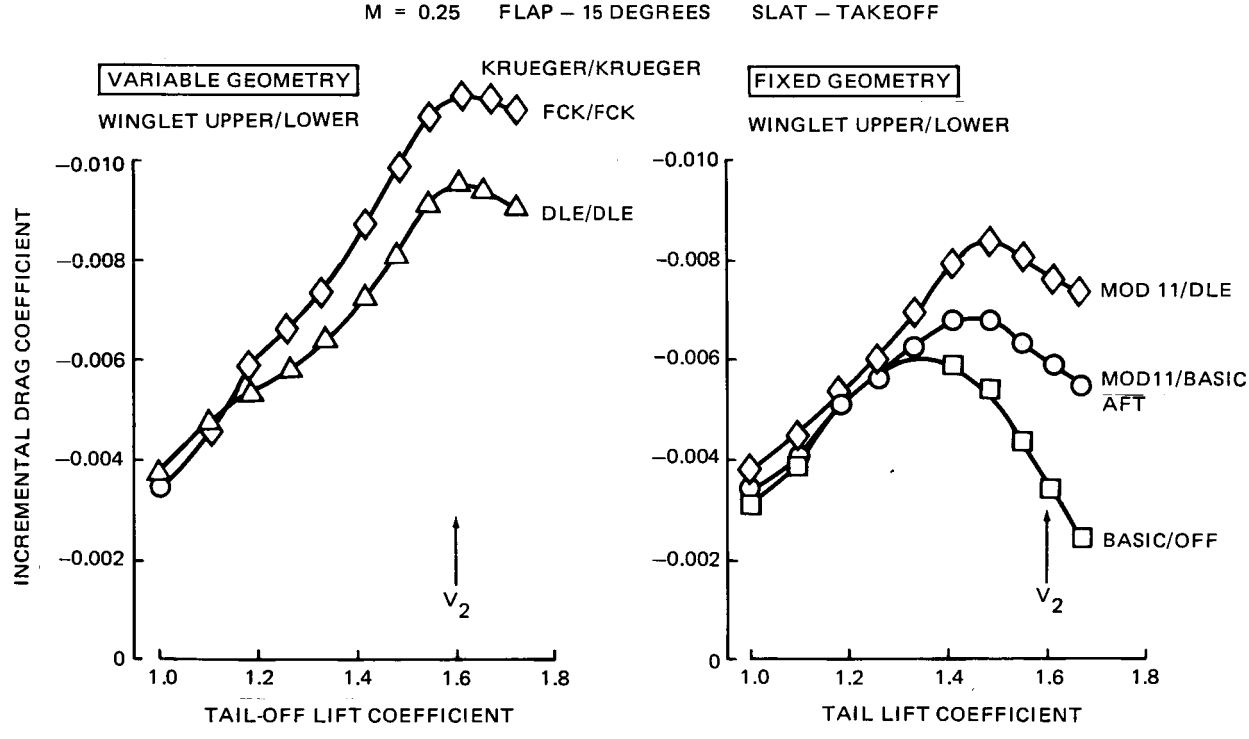

FIGURE 58. WINGLET DRAG IMPROVEMENT SUMMARY

complex Krueger flap. The Mod 11 DLE performance (not shown in the figure) was not as good as that of the basic DLE, possibly because the deflection angle was not as close to optimum. A substantial reduction in performance resulted from removal of the lower winglet DLE (also not shown in the figure). The Mod 11 fixed-geometry configuration, with DLE on the lower winglet, resulted in a drag improvement much superior to the Flight Configuration 14. This improvement was nearly 80 percent of the best DLE variable geometry configuration at V_2. Moving the lower winglet aft reduced this improvement somewhat.

The test program also investigated variations of the angle of incidence of the upper winglet. It was observed that the flight design case of −2 degrees was optimum for drag reduction up to the V_2 limit. The incidence variations did not affect the flow separation characteristics. Investigation of the effects of trailing-edge camber showed that there was a small benefit in drag reduction for takeoff conditions. A somewhat larger benefit for landing conditions was indicated. No undesirable lift or stability characteristics were identified.

High-Speed Test of the DC-10 Aircraft with Winglet and Wing Modifications

Configuration – From the preceding programs, a number of areas were selected for further high-speed wind tunnel investigation. First, there was interest in the result that drooping the outboard aileron yielded 1 percent more cruise drag benefit than with the original setting. This result was in agreement with the analytical estimate. It was speculated that the winglet alone was not achieving its full potential due to either insufficient loading or a viscous problem which the drooped aileron mitigated. Second, the rather large leading-edge suction peaks on the winglet could have contributed to adverse compressibility effects, although these were more pronounced on the basic winglet than for the reduced-span winglet. In each of these areas, it was desired to understand the apparent differences between flight data and preflight estimates and to determine if the basic shortfall of the winglet alone could be improved through redesign. Further, it was desired to evaluate the impact on cruise drag of employing selected fixed-geometry low-speed configurations from those described in the preceding section.

Moreover, because of the advantage shown with the outboard aileron droop, it was considered advisable to examine potential further improvements by changing the wing trailing-edge camber over a greater extent of the span. Analytical calculations had indicated that, in combination with the winglet, induced drag improvements could be effected through span loading changes and that compressibility characteristics could potentially be improved through aft loading of the wing airfoils.

In this program, a high-speed test was conducted in the NASA Ames Research Center 11-foot wind tunnel. A semispan model of the DC-10 Series 10, of 4.7 percent scale, was used.

Test configurations were used directly from the foregoing tests or came from a Douglas-funded related activity. The wing trailing-edge modifications were essentially as used in the postflight stability and control tests previously described. The three configurations from the postflight low-speed test were the drooped leading-edge lower winglet (Figure 55), the upper winglet leading-edge modification, Mod 11 (Figure 55), and the basic lower winglet moved aft 0.76 m (30 in.). The reduced-span upper winglet planform was used. A revised upper winglet (Mod 15), aimed at improved cruise performance, was designed; it is compared with the Mod 11 and flight winglet configurations in Figure 59. The flight test configuration itself was tested with

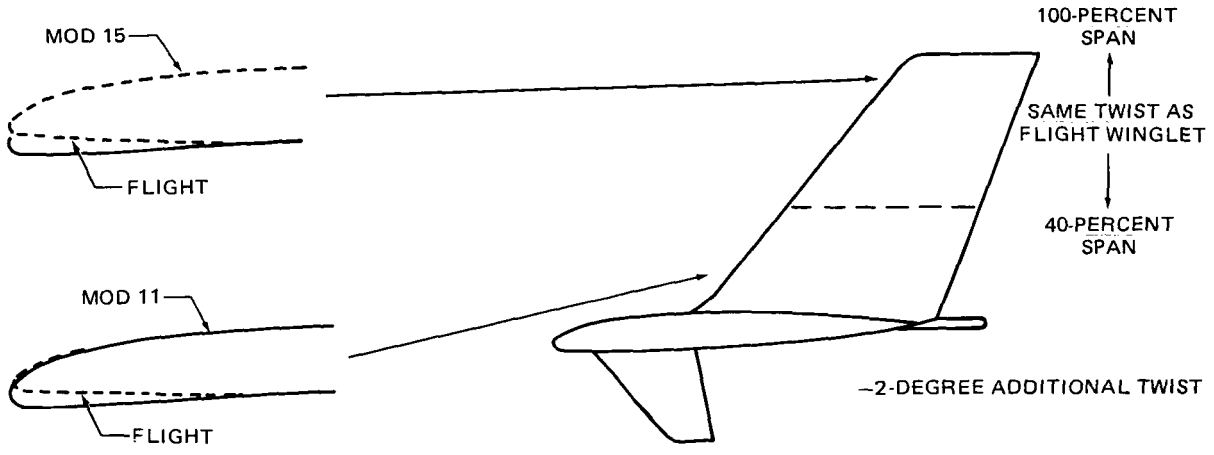

FIGURE 59. MOD 15 WINGLET GEOMETRY COMPARED WITH MOD 11 AND BASIC CONFIGURATIONS

and without the lower winglet to establish correlation of model data. As in the postflight high-speed stability and control test, this configuration had the reduced-span upper winglet with basic lower winglet.

Analysis Method – The assessment that Mod 11 would probably have no effect on compressibility drag was made using a transonic wing code with adaptations. Since these codes commonly cannot evaluate a three-dimensional wing and winglet configuration, the code was arranged to utilize a winglet out-of-a-wall simulation. The winglet was then twisted to match the span load measured in flight. It was found that Mod 11 did not increase the leading-edge suction peaks and therefore would not be expected to affect the compressibility characteristics.

The Mod 15 winglet was designed with a leading-edge modification to reduce the high suction peaks of the basic winglet and potentially improve the winglet drag. An inverse two-dimensional design computer code was used to redesign the cruise pressure distribution of the upper winglet. A three-dimensional analysis was then used to evaluate the incorporation of the Mod 15 airfoil section on the upper winglet. The winglet out-of-a-wall simulation was utilized. The inboard root section utilized the Mod 11 airfoil with −2-degree additional twist to reduce the inboard pressure peaks. The Mod 11 airfoil was then blended into the Mod 15 defining section near the mid-span station which was carried outboard to the winglet tip with the same twist as the flight winglet. The three-dimensional analysis predicted a parasite drag reduction and a reduction in leading-edge pressures across the span.

A three-dimensional vortex lattice analysis was conducted to study the effects of using the trailing-edge camber to change the span load for improved induced drag of the wing and winglet configuration. The transonic flow code was then used to analyze the effects of the camber modifications on the wing-alone compressibility. Both programs predicted reductions in induced drag and compressibility drag.

Results – Excellent correlation between flight and the two previous wind tunnel tests was obtained of wing span load distribution. The drag reduction data from the flight test winglet configuration showed good correlation with the actual flight data. Good correlation was also evident for the drooped outboard aileron effect. The degree of model-to-flight correlation provided a high level of confidence in the subsequent test results for the wing/winglet modifications.

The aft movement of the lower winglet was found to result in only a small penalty in the cruise drag. This penalty at the typical cruise lift coefficient of 0.47 was slightly more than 0.1 percent. This modification, which in the previous low-speed test had resulted in favorable low-speed effects, could therefore be considered an acceptable candidate for a cruise configuration.

The DLE lower winglet, which in the previous low-speed wind tunnel test had offered a significant low-speed drag reduction advantage, resulted in a drag penalty of over 1 percent of aircraft drag at the design cruise speed. This penalty was probably caused by a lower surface separation behind the DLE. The fixed-geometry DLE lower winglet would therefore not be acceptable for cruise conditions.

The drag data for the upper winglets with revised airfoils are shown in Figure 60. The Mod 11 winglet, which had shown merit in the low-speed tests, resulted in a drag penalty at the design cruise lift coefficient. The data suggest a possible compressibility effect, not predicted by analysis. At the typical lift coefficient, the Mod 15 winglet performance was worse than the basic winglet, having a trend of increasing drag penalty with increased winglet loading. Again, compressibility effects are suggested. The design technique had predicted a reduction in leading-edge suction peaks for Mod 15 and no change in the suction peaks for Mod 11. The test results suggest inaccuracy in the technique owing to the inability to simulate the complex flow field generated at the winglet/wing tip interface.

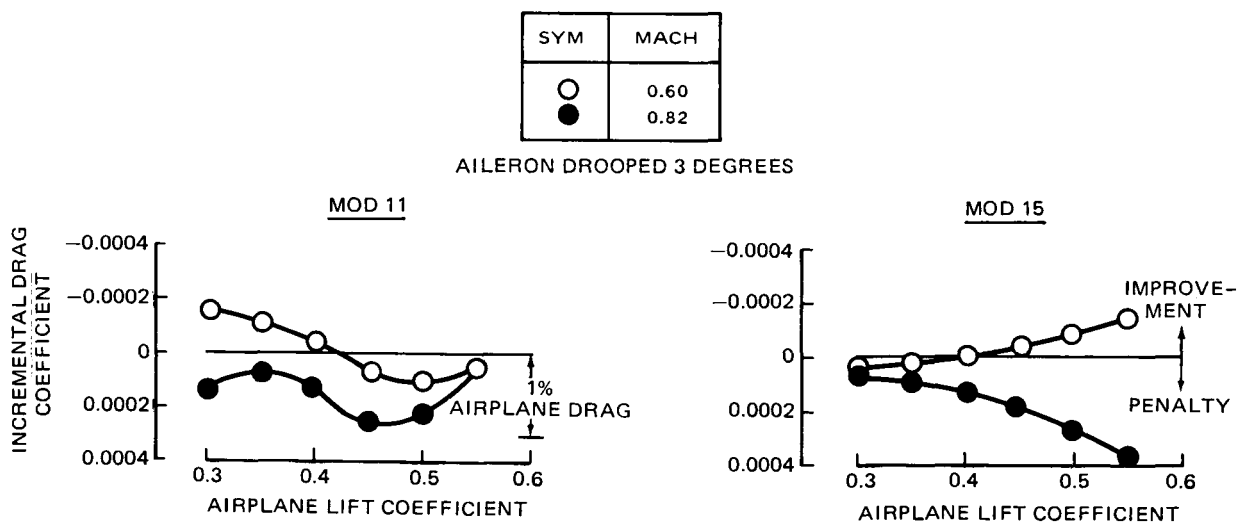

FIGURE 60. DRAG CHANGE FROM FLIGHT WINGLET FOR UPPER WINGLET MODIFICATIONS

The wing trailing-edge modification, adding camber so as to aft load the wing sections, was shown to be effective in contributing to the winglet drag reduction. Application to the aileron area was as effective as to the outboard wing trailing edge as a whole. The camber modification over the aileron span to the wing tip was essentially equal in drag reduction to the drooped aileron. The spanwise wing loading measured was close to the estimate for all the configurations tested. The modification applied from the trailing-edge break to the tip resulted in an increased tail-off drag reduction, but this was offset by increased trim drag. The drag improvement for the camber modifications is shown in Figure 61. This figure also shows the correlation of wing span load increase with the estimate for the outboard wing application. No benefit in compressibility drag resulted from the modifications. No degradation of the maneuvering characteristics was exhibited for the two applications of trailing-edge camber.

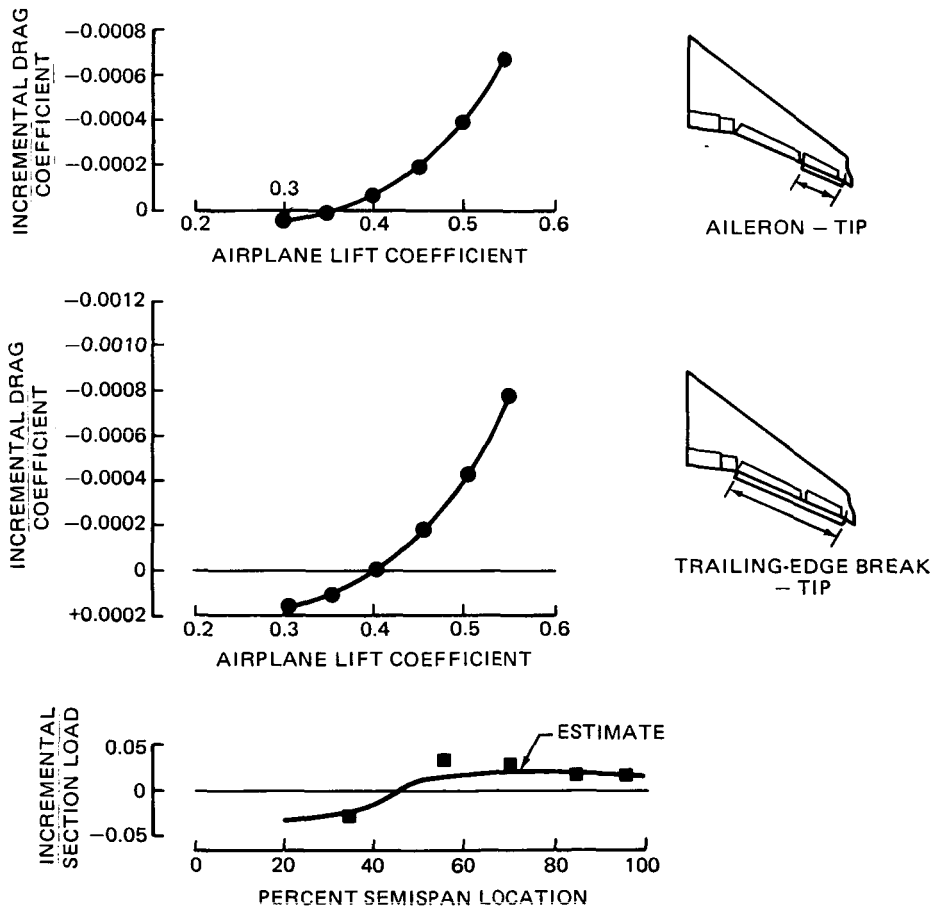

FIGURE 61. DRAG IMPROVEMENT FROM FLIGHT WINGLET LEVEL OF WING TRAILING-EDGE CAMBER

Evaluation of Results Relative to the Analysis – Upon the completion of the winglet program, it is appropriate to evaluate the performance results compared with the potential offered by the inviscid and incompressible analyses. During the flight program, it was concluded that the winglet combined with drooped outboard aileron achieved the full potential. However, the winglet alone achieved only 80 percent of the potential. The postflight model data also substantiate these conclusions.

An attempt to improve the performance of the winglet alone by a change in the winglet airfoil was unsuccessful under test. Further, the flight winglet configuration as a whole (i.e., upper and lower winglets) exhibited no difference in drag reduction between the incompressible and compressible conditions. This result was confirmed in the wind tunnel tests. It can therefore be concluded that the failure of the winglet alone to achieve all of its estimated performance was not related to adverse compressibility effects. More likely, the winglet alone was suffering from slightly non-optimum loading. During analytical design, the benefit of increasing winglet loading was predicted, being achieved by increasing the winglet incidence. However, wind tunnel results showed no improvement. It is not known whether this result was due to a non-optimum increased loading or to related viscous problems. The winglet incidence for the flight program was set by evaluation of the wind tunnel results.

From these results, the inference can be drawn that tailoring the camber of the outboard wing increases the loading on the wing and winglet in a more optimum way and thus allows the winglet to achieve its full potential drag reduction.

Conclusions from the Winglet Postflight Investigation

The principal conclusions of the postflight high-speed tests on the effect of trailing-edge modifications on stability and control characteristics were as follows:

1. Outboard-aileron droop resulted in a negligible effect on maneuvering stability.
2. Trailing-edge droop significantly degraded the maneuvering stability characteristics at the Mach numbers of primary interest.
3. The full trailing-edge camber resulted in a small degradation of maneuvering stability.

The principal conclusions of the postflight low-speed tests of winglet and wing variations were as follows:

1. Correlation with the flight evaluation results was very good.
2. The simpler variable-geometry configuration having drooped leading edges (DLE) on both upper and lower winglets had a performance nearly equal to that of the unacceptably complex flight test Krueger flapped winglet.
3. The fixed-geometry upper winglet Mod 11 with DLE lower winglet yielded a drag reduction that was nearly 80 percent of the best variable-geometry configuration (i.e., the configuration with DLE on upper and lower winglets).
4. A small drag reduction benefit was identified for the wing trailing-edge camber.

The conclusions from the postflight high-speed tests with winglet and wing modifications are as follows:

1. The model-to-flight data correlation provided a confident basis for evaluation of the results for the modifications.
2. Of the three modifications which had been shown to improve low-speed performance, only repositioning the lower winglet aft was found to have negligible adverse impact on cruise performance.
3. The winglet airfoil modification designed to reduce leading-edge suction pressures showed poorer performance characteristics than with the basic airfoil.
4. Modifications to the wing trailing edge to increase the camber resulted in a performance improvement similar to that from drooping the outboard aileron. The modifications did not adversely impact the maneuvering stability characteristics.
5. The winglet, when properly loaded, can achieve its full analytical performance benefit. In the tests, such a winglet loading was approached by tailoring the wing trailing edge near the tip.

CONCLUDING REMARKS

The EET project, together with the related Douglas studies, embarked on a program to build the technology base for selected areas for near-term and far-term application to transport aircraft. Under this contract, which was the predominant activity of the three in the project, the most promising concepts have been taken to readiness for commercial application. These concepts are the high-aspect-ratio supercritical wing and the winglet for second-generation transports. In addition, further work was done on the aerodynamic installation of the long-duct nacelle. The data, together with those of related Douglas investigations on internal mixing of fan and core flows for such a nacelle, were made available to other workers in a related NASA-sponsored project, the Energy Efficient Engine. In the field of active controls, significant progress was made in establishing the capability of simple laws for elastic mode control.

The remarks which follow supplement the conclusions of the sections of this report dealing with the most important parts of the work; namely, the elastic mode control, the high-aspect-ratio supercritical wing, and the winglet. These remarks also indicate some of the current applications of the technology being considered at Douglas.

Elastic Mode Control

The elastic mode control development has demonstrated the feasibility of increasing the flutter speed and reducing gust loads, using simple control laws sensors and operating surfaces. The tests were subject to some limitations, however. In order to advance the technology, further investigations are considered necessary; some of this work has been started at Douglas.

The Douglas investigations since the completion of the contract have extended the effort to the control of more than one flutter mode. In addition to exploring the capability of the concept to handle more complex conditions, insight has been gained into the effect of design parameters. As a basis for this work, the flutter characteristics of the DC-10 Series 10 winglet flight evaluation (in which two modes appeared) were employed. A modification of the simple control law used in the contract work was developed. Actuator characteristics from an actual high band-pass unit were used. With tailoring of the control law, the flutter speed of both modes was increased. Adequate gain margins were obtained. However, further development is needed to obtain satisfactory phase shift margins.

High-Aspect-Ratio Supercritical Wing Technology

A technology basis has been provided for designing wing configurations featuring increased aspect ratio, increased wing thickness, and competitive performance. A comprehensive high-and low-speed data base has been provided for design and for the development and validation of theoretical methods. In particular, performance advances were made in reducing drag creep and

improving cruise buffet boundary. Since the contract work, further improvements have been made, particularly in low- and high-speed maneuvering stability.

The technology base has been applied to several major projects. These include the Douglas C-17A "Airlifter" transport, and studies of advanced commercial aircraft, both new and derivatives of existing models.

Winglet

Building the technology base for application of winglets to a representative second-generation jet transport such as the DC-10 has been accomplished. This objective was reached through comprehensive analysis and development wind tunnel tests, followed by a full-scale flight test evaluation and finally by postflight wind tunnel tests to explore areas for additional improvement. Significant drag reductions in both the cruise and low-speed high-lift flight regimes were achieved, while no adverse effects from the winglets were discovered in the stability and control characteristics, the minimum stall speeds, and on the high-speed buffet boundary. The results from this program indicated that a good correlation between flight and wind tunnel tests can be achieved for aerodynamic data as well as for loads and flutter data.

The cruise speed drag reduction obtained by the winglet alone yielded about 80 percent of the value predicted by analysis. However, by tailoring the outboard wing trailing edge, excellent agreement was reached between the data and the analytical estimate. It can be inferred, however, that better analytical and design tools are needed to handle the complex three-dimensional flaws in the region of nonplanar wing tip surfaces.

The technology base for winglets has been used to apply designs to the C-17A "Airlifter" transport and to the MD-100 commercial program.

REFERENCES

1. Taylor, A. B.: Selected Winglet and Mixed-Flow Long-Duct Nacelle Development for DC-10 Derivative Aircraft – Summary Report. NASA CR-3296, June 1980.
2. The Staff of Douglas Aircraft Company: Selected Advanced Aerodynamic and Active Control Concepts Development – Summary Report. NASA CR-3469, October 1981.
3. Patel, S. P.; and Donelson, J.E.: Long-Duct Nacelle Aerodynamic Development for DC-10 Derivatives. NASA CR-159271, August 1980.
4. The Staff of Douglas Aircraft Company: Experimental Investigation of Elastic Mode Control on a Model of a Transport Aircraft. NASA CR-3472, November 1981.
5. Abel, I.; Newsom, J. R.; and Dunn, J. J.: Application of Two Synthesis Methods for Active Flutter Suppression on an Aeroelastic Wing Tunnel Model. AIAA Paper 79-1633, August 1979.
6. Abel, I.; and Newsom, J. R.: Wing Tunnel Evaluation of NASA-Developed Control Laws for Flutter Suppression on a DC-10 Derivative Wing. AIAA Paper 81-0639, April 1981.
7. Perry, B., III: Qualitative Comparison of Calculated Turbulence Responses with Wind Tunnel Measurements for a DC-10 Derivative Wing with an Active Control System. AIAA Paper 81-0567, April 1981.
8. Steckel, D. K.; Dahlin, J. A.; and Henne, P. A.: Results of Design Studies and Wind Tunnel Tests of High-Aspect-Ratio Supercritical Wings for an Energy Efficient Transport. NASA CR-159332, 1980.
9. Oliver, W. R.: Results of Design Studies and Wind Tunnel Tests of an Advanced High-Lift System for an Energy-Efficient Transport. NASA CR-159389, 1980.
10. Henne, P. A.; Dahlin, J. A.; Peavey, C. C.; and Gerren, D. S.: Configuration Design Studies and Wind Tunnel Tests of an Energy Efficient Transport with a High-Aspect-Ratio Supercritical Wing. NASA CR-3524, May 1982.
11. Allen, J. B.; Oliver, W. R.; and Spacht, L. A.: Wind Tunnel Tests of High-Lift Systems for Advanced Transports Using High-Aspect-Ratio Supercritical Wings. NASA CR-3523, July 1982.
12. Whitcomb, R. T.: A Design Approach and Selected Wing-Tunnel Results at High Subsonic Speeds for Wing-Tip-Mounted Winglets. NASA TN D8260, July 1976.
13. Gilkey, R. D.: Design and Wind Tunnel Tests of Winglets on a DC-10 Wing. NASA CR-3119, April 1979.
14. Shollenberger, C. A.; Humphreys, J. W.; Heilberger, F. S.; and Pearson, R. M.: Results of Winglet Development Studies for DC-10 Derivatives. NASA CR-3677, March 1983.
15. The Staff of Douglas Aircraft Company: DC-10 Winglet Flight Evaluation. NASA CR-3704, June 1983.
16. Taylor, A. B.: DC-10 Winglet Flight Evaluation Summary Report. NASA CR-3748, December 1983.

APPENDIX

WIND TUNNEL TESTING CONDUCTED

Model Designation and Purpose	Scale and Description	Wind Tunnel	Entry Date
(Long-Duct Nacelle)			
LB-245Q	4.7-percent Semispan	Cal-Span 8-foot High-speed	Nov 1979
(Active Control Transport)			
LB-253G	4.5-percent Semispan	Douglas Long Beach Low-speed	Aug 1979, July 1980
LB-253H	4.5-percent Full span	Northrop 7- by 10-foot Low-speed	Sept 1980
(High-Aspect-Ratio Supercritical Wing, High-Speed)			
LB-506A	5.59-percent Full span	NASA Ames 11-foot	May 1980
LB-506B	5.59-percent Full span	NASA Ames 11-foot	April 1981
LB-350E	Two-dimensional	NAE-Canada 15- by 60-inch	Nov 1982
(High-Aspect-Ratio Supercritical Wing, High-Lift)			
LB-486C	4.7-percent Full span	NASA Langley V/STOL Low-speed	Nov 1979
LB-486B	4.7-percent Full span	NASA Ames 12-foot	Jun 1980
LB-507A	5.59-percent Full span	NASA Ames 12-foot	Jan 1981

Model Designation and Purpose	Scale and Description	Wind Tunnel	Entry Date
(Winglet Preflight Evaluation)			
LB-246S	4.7-percent Full span	NASA Ames 12-foot	Aug 1979
LB-244AB	3.25-percent Full span	NASA Ames 11-foot	March 1980
LB-246AD	4.7-percent Full span	NASA Ames 12-foot	March 1981
(Winglet Postflight Evaluation)			
LB-244AG	3.25-percent Full span	NASA Ames 11-foot	Feb 1982
LB-246AF	4.7-percent Full span	NASA Ames 12-foot	Oct 1982
LB-245R	4.7-percent Semispan	NASA Ames 11-foot	June 1983

1. Report No.	2. Government Accession No.	3. Recipient's Catalog No.
NASA CR-3781		

4. Title and Subtitle	5. Report Date
DEVELOPMENT OF SELECTED ADVANCED AERODYNAMICS AND ACTIVE CONTROL CONCEPTS FOR COMMERCIAL TRANSPORT AIRCRAFT	February 1984
	6. Performing Organization Code
7. Author(s)	8. Performing Organization Report No.
A. B. TAYLOR	ACEE-17-FR-3206
	10. Work Unit No.
9. Performing Organization Name and Address	11. Contract or Grant No.
DOUGLAS AIRCRAFT COMPANY MCDONNELL DOUGLAS CORPORATION 3855 LAKEWOOD BOULEVARD LONG BEACH, CA 90846	NAS 1-15327
	13. Type of Report and Period Covered CONTRACTOR REPORT February 1979-December 1983
12. Sponsoring Agency Name and Address	14. Sponsoring Agency Code
NATIONAL AERONAUTICS AND SPACE ADMINISTRATION WASHINGTON, DC 20546	

15. Supplementary Notes

LANGLEY TECHNICAL MONITOR: THOMAS G. GAINER
PROGRAM SUMMARY REPORT

16. Abstract

The report summarizes work done under the Energy Efficient Transport project in the field of advanced aerodynamics and active controls. The project task selections focused on: the investigation of long-duct nacelle shape variation on interference drag; the investigation of the adequacy of a simple control law for controlling the elastic modes of a wing; the development of the aerodynamic technology at cruise and low speed of high-aspect-ratio supercritical wings of high performance; and the development of winglets for a second-generation jet transport.

All the tasks involved analysis and substantial wind tunnel testing. The winglet program also included flight evaluation.

It is considered that the technology base has been built for the application of high-aspect-ratio supercritical wings and for the use of winglets on second-generation transports.

17. Key Words (Suggested by Author(s))	18. Distribution Statement
Propulsion Integration Active Controls Wing Design Winglets Energy Efficient Transport	[redacted] Subject Categories 01, 02, and 05

19. Security Classif. (of this report)	20. Security Classif. (of this page)	21. No. of Pages	22. Price
Unclassified	Unclassified	98	

Available: NASA's Industrial Applications Centers

NASA-Langley, 1984